International Tables for Crystallography (2006). Vol. D, Chapter 1.5, pp. 105–149.

1.5. Magnetic properties

By A. S. Borovik-Romanov† and H. Grimmer

1.5.1. Introduction

In the present chapter, we shall give a short review of the structure and some properties of magnetic substances that depend mainly on the symmetry of these substances. Aspects related to the magnetic symmetry receive the most emphasis. The magnetic symmetry takes into account the fact that it is necessary to consider time inversion in addition to the usual spatial transformations in order to describe the invariance of the thermodynamic equilibrium states of a body.

The symmetry of magnetic materials depends not only on the mean charge density function $\rho(\mathbf{r})$, but also on the mean current density $\mathbf{j}(\mathbf{r})$ and the mean spin density $\mathbf{S}(\mathbf{r})$. The symmetry of the function $\rho(\mathbf{r})$ is called the crystallographic or crystallochemical symmetry of a body. If the current density $\mathbf{j}(\mathbf{r})$ in the crystal is not zero, an orbital magnetic moment is produced. It is obvious that there can be no macroscopic current in a substance which is in thermodynamic equilibrium and the integral $\int \mathbf{j}\,\mathrm{d}\tau$ over the magnetic elementary cell is always equal to zero. The current $\mathbf{j}$, however, may produce a macroscopic nonzero magnetic moment $\mathbf{m}(\mathbf{r})$. We shall consider below the function $\mathbf{m}(\mathbf{r})$, which determines the space distribution of the total (spin and orbital) magnetic moment density. The symmetry of the distribution of the magnetic moment density $\mathbf{m}(\mathbf{r})$ may be considered as the symmetry of the arrangement and orientation of the mean atomic (or ionic) magnetic moments in the crystal (we shall not consider the magnetism of the conduction electrons in this chapter).

The first part of the chapter is devoted to a brief classification of magnetics. If $\mathbf{m}(\mathbf{r}) \equiv 0$ at every point, the substance is a disordered magnetic. There are two types of such magnetics: diamagnets and paramagnets. The most important features of these magnetics are briefly outlined in Section 1.5.1.1.

If $\mathbf{m}(\mathbf{r}) \neq 0$, the substance possesses a magnetic structure. There are two cases to be considered: (1) The integral of $\mathbf{m}(\mathbf{r})$ over the primitive cell is not zero ($\int \mathbf{m}\,\mathrm{d}\tau \neq 0$); such a substance is called ferromagnetic. (2) $\int \mathbf{m}\,\mathrm{d}\tau = 0$; such a substance is called antiferromagnetic. The integration is performed over the magnetic elementary cell, which may differ from the crystallographic one. This crude classification is extended in Section 1.5.1.2.

The classification of ferromagnets according to the type of the magnetic structure is given in Section 1.5.1.2.1. The concept of the magnetic sublattice is introduced and the ferromagnets are divided into two groups: one-sublattice ferromagnets and multisublattice ferro- and ferrimagnets. Collinear and non-collinear ferromagnets are described.

In Section 1.5.1.2.2, the antiferromagnets are classified by the types of their magnetic structures: collinear, weakly non-collinear and strongly non-collinear antiferromagnets.

Incommensurate structures are briefly mentioned in Section 1.5.1.2.3.

The study of ordered magnetics has led to an extension of the theory of crystallographic symmetry. This extension is based on the fact that $\mathbf{m}(\mathbf{r})$ changes sign under a specific transformation R, which is equivalent to time inversion. The invariance of the equation of motion is preserved under R. The symmetry that admits the operation R along with ordinary crystallographic transformations (translations, rotations and reflections) is called the magnetic symmetry. Section 1.5.2 is devoted to magnetic symmetry. Different types of magnetic point (Section 1.5.2.1) and magnetic space (Section 1.5.2.3) groups are defined. The 22 magnetic Bravais lattices are displayed in Section 1.5.2.2. All magnetic groups (both point and space) are categorized into three types: (1) The groups that possess R as an additional element. The crystals which belong to such space groups satisfy $\mathbf{m}(\mathbf{r}) = -\mathbf{m}(\mathbf{r})$ at every point, hence $\mathbf{m}(\mathbf{r}) = 0$. Such crystals are found to be paramagnetic or diamagnetic. Crystals with a point group that possesses R as an additional element may also be antiferromagnetic. This is the case if R appears in the space group multiplied by some translations but not as a separate element. (2) The groups that do not possess R at all. (3) The groups that contain the element R only in combination with some other elements (translations, rotations, reflections). The latter two types of space groups describe ordered magnetics.

The transition from the paramagnetic state into the magnetically ordered state entails a transition from one magnetic group into another. These transitions are considered in Section 1.5.3. Section 1.5.3.1 gives an example of the analysis of such transitions in terms of magnetic symmetry and introduces the concept of ferromagnetic and antiferromagnetic vectors, which characterize the magnetic structures. The phenomenological theory of magnetic transitions is based on the Landau theory of second-order transitions. Section 1.5.3.3 is dedicated to this theory (see also Section 3.1.2). The Landau theory is based on the expansion of the thermodynamic potential into a series of the basic functions of irreducible representations of the space group of the crystal under consideration. It is essential to distinguish the exchange and relativistic terms in the expansion of the thermodynamic potential (see Section 1.5.3.2).

The domain structure of ferromagnets and antiferromagnets is considered in Section 1.5.4, where 180° and T-domains are described. The change from a multidomain structure to a single-domain structure under the action of an applied magnetic field explains the magnetization process in ferro- and ferrimagnets. The existence of 180° domains in antiferromagnets was shown in experiments on piezomagnetism and the linear magnetoelectric effect.

Non-collinear antiferromagnetic structures (weakly ferromagnetic, non-collinear and non-coplanar antiferromagnetic structures) are described in Section 1.5.5. The existence of these structures is directly connected with the magnetic symmetry. Such a structure arises if the irreducible representation responsible for the phase transition into the ordered state is two- or three-dimensional. Correspondingly, the magnetic group allows the coexistence of two or three different ferro- or antiferromagnetic vectors.

Besides the magnetic phase transition from the disordered into the ordered state, there exist transitions from one magnetic structure into another. Those of these that are obtained by a rotation of the ferromagnetic or antiferromagnetic vector relative to the crystallographic axis are called reorientation transitions and are analysed in Section 1.5.6.

Sections 1.5.7 and 1.5.8 are devoted to phenomena that can be (and were) predicted only on the basis of magnetic symmetry. These are piezomagnetism (Section 1.5.7) and the magnetoelectric effect (Section 1.5.8). The reciprocal of the piezomagnetic effect (Section 1.5.7.1) is linear magnetostriction (Section 1.5.7.2). The magnetoelectric effect has been investigated far more than piezomagnetism. In addition to the linear

† The sudden death of Andrey Stanislavovich Borovik-Romanov is deeply regretted. At the age of 77, he died on 31 July 1997 in Cairns, Australia, where he was taking part in the International Conference on Magnetism ICM'97.

magnetoelectric effect (Section 1.5.8.1), effects of higher order (Section 1.5.8.2) have also been observed. In connection with the magnetoelectric effect, ferromagnetic and antiferromagnetic ferroelectrics are also considered (Section 1.5.8.3).

In Section 1.5.9, the magnetostriction in ferromagnets is discussed. Only fundamental points of this problem are considered.

As noted above, only those problems of magnetism that are closely connected with magnetic symmetry are considered in this chapter. However, these problems are only outlined briefly here because of the restrictions on the extent of this volume. For the same reason, it is impossible to give an exhaustive list of references. The references given here include selected publications on magnetic symmetry and those describing the first experimental work devoted to the properties connected with magnetic symmetry.

1.5.1.1. *Disordered magnetics*

A crystal placed in a magnetic field **H** is magnetized. The magnetized state is characterized by two vectors, the magnetization **M** (the magnetic moment per unit volume) and the magnetic induction **B**. The Gaussian system of units is used in this chapter (see Table 1.5.10.1 at the end of the chapter for a list of conversions from Gaussian to SI units). The magnetic induction is given by

$$\mathbf{B} = \mathbf{H} + 4\pi\mathbf{M}. \tag{1.5.1.1}$$

This equation shows that the dimensions of **B**, **H** and **M** are the same in the Gaussian system. The unit for **B**, the gauss (G), and for **H**, the oersted (Oe), also coincide in magnitude, whereas the unit for **M**, usually called emu cm^{-3}, is 4π times larger. These units are related to the corresponding SI units as follows: 1 G $= 10^{-4}$ tesla (T), 1 Oe $= 10^3/(4\pi)$ A m^{-1}, 1 emu cm^{-3} $= 10^3$ A m^{-1}.

In disordered magnetics, the vectors **B** and **M** are linear in the magnetic field. Using a Cartesian coordinate system, this can be expressed as

$$M_i = \chi_{ij}H_j \quad \text{and} \quad B_i = \mu_{ij}H_j, \tag{1.5.1.2}$$

where χ_{ij} is the dimensionless magnetic susceptibility per unit volume and μ_{ij} is the magnetic permeability. The susceptibility is frequently referred to 1 g or to one mole of substance. The mass susceptibility is written as χ_g, the molar susceptibility as χ_{mol}.

All three vectors **H**, **M** and **B** are axial vectors (see Section 1.1.4.5.3), the symmetry of which is ∞/m. Accordingly, the components of these vectors perpendicular to a mirror plane do not change sign on being reflected by this plane, whereas the components parallel to the plane do change sign. Consequently, these three vectors are invariant with respect to inversion. The quantities χ_{ij} and μ_{ij} are components of second-rank polar tensors. In principal axes, the tensors become diagonal and both the magnetic susceptibility and permeability of a crystal are characterized by the three values of the principal susceptibilities and principal permeabilities, respectively.

All disordered magnetics are divided into two types: diamagnets ($\chi < 0$) and paramagnets ($\chi > 0$).

Diamagnetism is a universal property of all materials. It is associated with the tendency of all the electrons to screen the applied external field according to the Lenz law. For materials in which the electron orbits are spherically symmetric, the relation for the diamagnetic susceptibility was calculated by Langevin. For monoatomic substances he obtained

$$\chi = -\frac{Ne^2}{6mc^2}\left(\sum_{i=1}^{i=Z}\overline{r_i^2}\right), \tag{1.5.1.3}$$

where N is the number of atoms per unit volume, Z is the number of electrons per atom, e and m are the charge and the mass of the electron, respectively, and $\overline{r_i^2}$ are the mean squares of the radii of the electron orbits. In polyatomic substances, the summation must be done over all types of atoms. In most chemical compounds, the orbits are not spherical and the calculation of the diamagnetic susceptibility becomes more complicated. In metals, the conduction electrons contribute significantly to the diamagnetic susceptibility. The diamagnetic susceptibility of most substances is very small ($\chi \sim 10^{-6}$) and isotropic. Rare exceptions are bismuth and some organic compounds, in which the diamagnetism is strongly anisotropic.

Most paramagnetic materials contain ions (or free atoms) with a partly filled inner electronic shell. Examples are the transition metals and the rare-earth and actinide elements. Atoms, molecules and point defects possessing an odd number of electrons are also paramagnetic. Ions with a partly filled inner electronic shell possess orbital **L** and spin **S** angular momenta, which determine the total angular momentum **J** if the spin–orbit interaction is strong compared with the crystal field.

The magnetic susceptibility of paramagnets follows the Curie–Weiss law in low magnetic fields ($\mu_B B \ll k_B T$):

$$\chi = \frac{Np^2\mu_B^2}{3k_B(T-\Delta)}, \tag{1.5.1.4}$$

where N is the number of magnetic ions (or atoms) per cm^3, μ_B is the Bohr magneton, p is the effective number of Bohr magnetons, k_B is the Boltzmann factor and Δ is the Weiss constant. The Weiss constant is related to the interaction between the magnetic moments (mostly exchange interaction) and to the effect of the splitting of electron levels of the paramagnetic ion in the crystalline electric field. Many paramagnets that obey the Curie–Weiss law transform into ordered magnetics at a temperature T_c, which is of the order of $|\Delta|$. The sign of Δ depends on the sign of the exchange constant J [see relation (1.5.1.7)]. For the substances that at low temperatures become ferromagnets, we have $\Delta > 0$, for antiferromagnets $\Delta < 0$, and for ferrimagnets the temperature dependence of χ is more complicated (see Fig. 1.5.1.1). For those paramagnets that do not go over into an ordered state, Δ is close to zero and equation (1.5.1.4) changes to the Curie law.

The value of the effective number of Bohr magnetons p depends strongly on the type of the magnetic ions and their environment. For most rare-earth compounds at room temperature, the number p has the same value as for free ions:

$$p = g[J(J+1)]^{1/2}, \tag{1.5.1.5}$$

where g is the Landé g-factor or the spectroscopic splitting factor ($1 \le g \le 2$). In this case, the paramagnetic susceptibility is practically isotropic. Some anisotropy can arise from the anisotropy of the Weiss constant Δ.

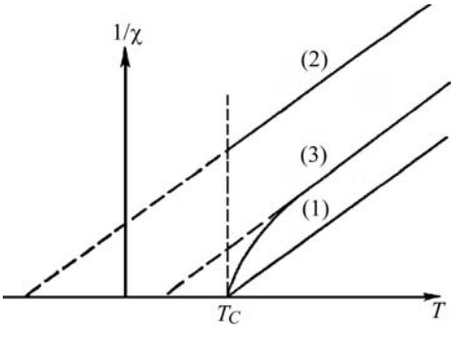

Fig. 1.5.1.1. Temperature dependence of $1/\chi$ at high temperatures for different types of magnetics: (1) ferromagnet; (2) antiferromagnet; (3) ferrimagnet.

The behaviour of the transition-metal ions is very different. In contrast to the rare-earth ions, the electrons of the partly filled shell in transition metals interact strongly with the electric field of the crystal. As a result, their energy levels are split and the orbital moments can be 'quenched'. This means that relation (1.5.1.5) transforms to

$$p_{ij} = (g_{\rm eff})_{ij}[S(S+1)]^{1/2}. \qquad (1.5.1.6)$$

Here the value of the effective spin S represents the degeneration of the lowest electronic energy level produced by the splitting in the crystalline field; $(g_{\rm eff})_{ij}$ differs from the usual Landé g-factor. The values of its components lie between 0 and 10–20. The tensor $(g_{\rm eff})_{ij}$ becomes diagonal in the principal axes. According to relation (1.5.1.6), the magnetic susceptibility also becomes a tensor. The anisotropy of $(g_{\rm eff})_{ij}$ can be studied using electron paramagnetic resonance (EPR) techniques.

The Curie–Weiss law describes the behaviour of those paramagnets in which the magnetization results from the competition of two forces. One is connected with the reduction of the magnetic energy by orientation of the magnetic moments of ions in the applied magnetic field; the other arises from thermal fluctuations, which resist the tendency of the field to orient these moments. At low temperatures and in strong magnetic fields, the linear dependence of the magnetization *versus* magnetic field breaks down and the magnetization can be saturated in a sufficiently strong magnetic field. Most of the paramagnetic substances that obey the Curie–Weiss law ultimately transform to an ordered magnetic as the temperature is decreased.

The conduction electrons in metals possess paramagnetism in addition to diamagnetism. The paramagnetic susceptibility of the conduction electrons is small (of the same order of magnitude as the diamagnetic susceptibility) and does not depend on temperature. This is due to the fact that the conduction electrons are governed by the laws of Fermi–Dirac statistics.

1.5.1.2. *Ordered magnetics*

1.5.1.2.1. *Ferromagnets (including ferrimagnets)*

As stated above, all ordered magnetics that possess a spontaneous magnetization $\mathbf{M}_s$ different from zero (a magnetization even in zero magnetic field) are called ferromagnets. The simplest type of ferromagnet is shown in Fig. 1.5.1.2(*a*). This type possesses only one kind of magnetic ion or atom. All their magnetic moments are aligned parallel to each other in the same direction. This magnetic structure is characterized by one vector **M**. It turns out that there are very few ferromagnets of this type in which only atoms or ions are responsible for the ferromagnetic magnetization ($CrBr_3$, EuO *etc.*). The overwhelming majority of ferromagnets of this simplest type are metals, in which the magnetization is the sum of the magnetic moments of the localized ions and of the conduction electrons, which are partly polarized.

More complicated is the type of ferromagnet which is called a ferrimagnet. This name is derived from the name of the oxides of the elements of the iron group. As an example, Fig. 1.5.1.2(*b*) schematically represents the magnetic structure of magnetite (Fe_3O_4). It contains two types of magnetic ions and the number of Fe^{3+} ions ($\boldsymbol{\mu}_1$ and $\boldsymbol{\mu}_2$) is twice the number of Fe^{2+} ions ($\boldsymbol{\mu}_3$). The values of the magnetic moments of these two types of ions differ. The magnetic moments of all Fe^{2+} ions are aligned in one direction. The Fe^{3+} ions are divided into two parts: the magnetic moments of one half of these ions are aligned parallel to the magnetic moments of Fe^{2+} and the magnetic moments of the other half are aligned antiparallel. The array of all magnetic moments of identical ions oriented in one direction is called a magnetic sublattice. The magnetization vector of a given sublattice will be denoted by $\mathbf{M}_i$. Hence the magnetic structure of Fe_3O_4 consists of three magnetic sublattices. The magnetizations of two of them are aligned in one direction, the magnetization of the third one is oriented in the opposite direction. The net ferromagnetic magnetization is $M_s = M_1 - M_2 + M_3 = M_3$.

The special feature of ferrimagnets, as well as of many antiferromagnets, is that they consist of sublattices aligned antiparallel to each other. Such a structure is governed by the nature of the main interaction responsible for the formation of the ordered magnetic structures, the exchange interaction. The energy of the exchange interaction does not depend on the direction of the interacting magnetic moments (or spins **S**) rela-

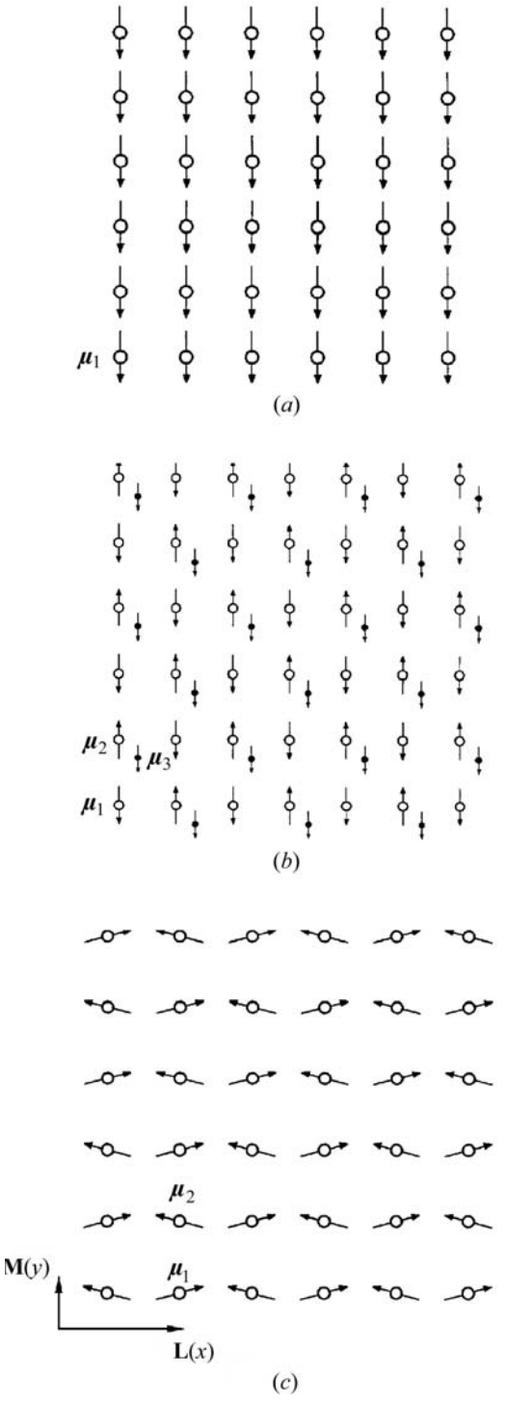

Fig. 1.5.1.2. Ordered arrangements of magnetic moments $\boldsymbol{\mu}_i$ in: (*a*) an ordinary ferromagnet $\mathbf{M}_s = N\boldsymbol{\mu}_1$; (*b*) a ferrimagnet $\mathbf{M}_s = (N/3)(\boldsymbol{\mu}_1 + \boldsymbol{\mu}_2 + \boldsymbol{\mu}_3)$; (*c*) a weak ferromagnet $\mathbf{M} = \mathbf{M}_D = (N/2)(\boldsymbol{\mu}_1 + \boldsymbol{\mu}_2)$, $\mathbf{L} = (N/2)(\boldsymbol{\mu}_1 - \boldsymbol{\mu}_2)$, ($L_x \gg M_y$; $M_x = M_z = L_y = L_z = 0$). ($N$ is the number of magnetic ions per cm^3.)

tive to the crystallographic axes and is represented by the following relation:

$$U_{\rm ex} = -\sum_{m,n} J_{mn}\mathbf{S}_m\mathbf{S}_n. \qquad (1.5.1.7)$$

Here $\mathbf{S}_m$, $\mathbf{S}_n$ are the spins of magnetic atoms (ions) and J_{mn} is the exchange constant, which usually decreases fast when the distance between the atoms rises. Therefore, usually only the nearest neighbour interaction needs to be taken into account. Hence, according to (1.5.1.7), the exchange energy is a minimum for the state in which neighbouring spins are parallel (if $J > 0$) or antiparallel (if $J < 0$). If the nearest neighbour exchange interaction were the only interaction responsible for the magnetic ordering, only collinear magnetic structures would exist (except in triangle lattices). Together with the exchange interaction, there is also a magnetic dipole interaction between the magnetic moments of the atoms as well as an interaction of the atomic magnetic electrons with the crystalline electric field. These interactions are much smaller than the exchange interaction. They are often called relativistic interactions. The relativistic interactions and the exchange interaction between next-nearest atoms bring about the formation of non-collinear magnetic structures.

A simple non-collinear structure is the magnetic structure of a weak ferromagnet. It contains identical magnetic ions divided in equal amounts between an even number of sublattices. In the first approximation, the magnetizations of these sublattices are antiparallel, as in usual antiferromagnets. In fact, the magnetizations are not strictly antiparallel but are slightly canted, *i.e.* non-collinear, as shown in Fig. 1.5.1.2(*c*). There results a ferromagnetic moment M_D, which is small compared with the sublattice magnetization M_i. The magnetic properties of weak ferromagnets combine the properties of both ferromagnets and antiferromagnets. They will be discussed in detail in Section 1.5.5.1.

1.5.1.2.2. *Antiferromagnets*

As discussed above, the exchange interaction, which is of prime importance in the formation of magnetic order, can lead to a parallel alignment of the neighbouring magnetic moments as well as to an antiparallel one. In the latter case, the simplest magnetic structure is the collinear antiferromagnet, schematically shown in Fig. 1.5.1.3(*a*). Such an antiferromagnet consists of one or several pairs of magnetic sublattices of identical magnetic ions located in equivalent crystallographic positions. The magnetizations of the sublattices are oriented opposite to each other.

Fig. 1.5.1.3(*b*) shows a weakly non-collinear antiferromagnet, in which the vectors of magnetization of four equivalent sublattices form a cross with a small tilting angle 2α. Such a structure can be considered as an admixture of 'weak antiferromagnetism' $\mathbf{L}_1$ with easy axis Ox to an ordinary antiferromagnet $\mathbf{L}_2$ with easy axis Oy. This weak antiferromagnetism is of the same origin as weak ferromagnetism. Its nature will be discussed in detail in Section 1.5.5.2.

The minimum of the exchange interaction energy of three spins located at the corners of a triangle corresponds to a structure in which the angles between two adjacent spins are 120°. Correspondingly, many hexagonal crystals possess a triangular antiferromagnetic structure like the one shown in Fig. 1.5.1.3(*c*). The sum of the magnetizations of the three sublattices in this structure equals zero. In tetragonal crystals, there is a possibility of the existence of a 90° antiferromagnetic structure, which consists of four equivalent sublattices with magnetizations oriented along the positive and negative directions of the x and y axes.

Finally, it is worth noting that in addition to the electronic magnetically ordered substances, there exist nuclear ferro- and antiferromagnets (below 1 mK for some insulators and below 1 μK for metals).

1.5.1.2.3. *Helical and sinusoidal magnetics*

There are many more complicated non-collinear magnetic structures. Fig. 1.5.1.4(*a*) shows an antiferromagnetic helical structure. It consists of planes perpendicular to the z axis in which all the magnetic moments are parallel to each other and are perpendicular to **z**. The polar angle of the direction of the moments changes from plane to plane by some constant δ. Thus the magnetization vectors describe a spiral along the axis of the crystal. Such structures were observed in hexagonal rare-earth metals. A specific feature is that they often are incommensurate structures. This means that $2\pi/\delta$ is not a rational number and that the period of the magnetic spiral is not a multiple of the period of the lattice.

Similar to the antiferromagnetic helix, ferromagnetic helical or spiral structures exist [see Fig. 1.5.1.4(*b*)] in which the magnetizations of the layers are tilted to the axis at an angle θ. As a result,

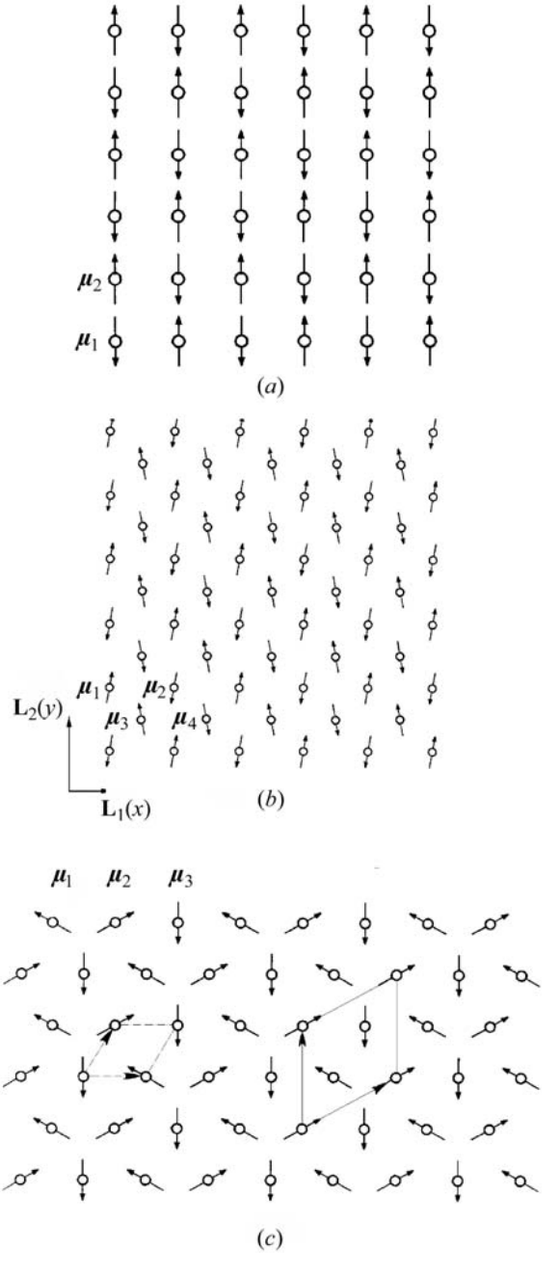

Fig. 1.5.1.3. Ordered arrangements of magnetic moments $\boldsymbol{\mu}_i$ in: (*a*) an ordinary two-sublattice antiferromagnet $\mathbf{L} = (N/2)(\boldsymbol{\mu}_1 - \boldsymbol{\mu}_2)$; (*b*) a weakly non-collinear four-sublattice antiferromagnet $\mathbf{L}_1(x) = (N/4)(\boldsymbol{\mu}_1 - \boldsymbol{\mu}_2 - \boldsymbol{\mu}_3 + \boldsymbol{\mu}_4)$, $\mathbf{L}_2(y) = (N/4)(\boldsymbol{\mu}_1 - \boldsymbol{\mu}_2 + \boldsymbol{\mu}_3 - \boldsymbol{\mu}_4)$; (*c*) a strongly non-collinear three-sublattice antiferromagnet $\mathbf{L}_1 = (N/3)(3)^{1/2}(\boldsymbol{\mu}_2 - \boldsymbol{\mu}_1)$, $\mathbf{L}_2 = (N/3)(\boldsymbol{\mu}_1 + \boldsymbol{\mu}_2 - \boldsymbol{\mu}_3)$. The broken lines show the crystallographic primitive cell and the solid lines show the magnetic primitive cell.

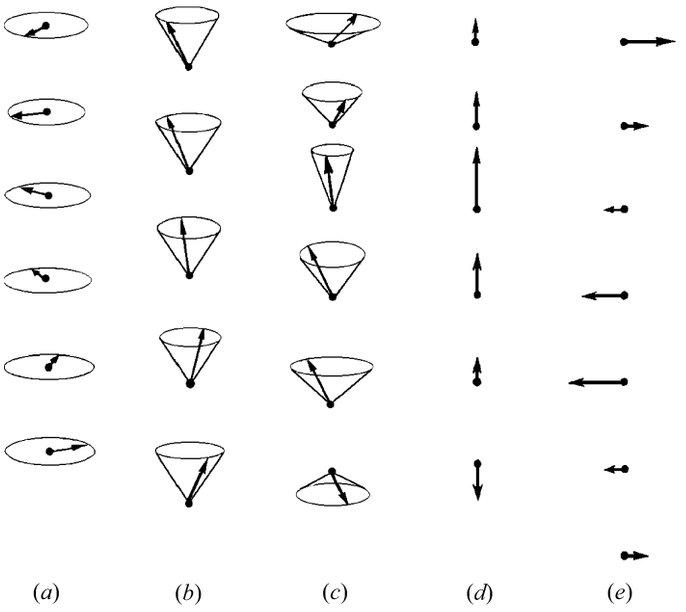

Fig. 1.5.1.4. Helical and sinusoidal magnetic structures. (*a*) An antiferromagnetic helix; (*b*) a cone spiral; (*c*) a cycloidal spiral; (*d*) a longitudinal spin-density wave; (*e*) a transverse spin-density wave.

the vectors of the magnetization of the layers are arranged on the surface of a cone. The ferromagnetic magnetization is aligned along the z axis. This structure is called a ferromagnetic helix. It usually belongs to the incommensurate magnetic structures.

More complicated antiferromagnetic structures also exist: sinusoidal structures, which also consist of layers in which all the magnetic moments are parallel to each other. Fig. 1.5.1.4(*c*) displays the cycloidal spiral and Figs. 1.5.1.4(*d*) and (*e*) display longitudinal and transverse spin density waves, respectively.

1.5.2. Magnetic symmetry

As discussed in Section 1.5.1, in studies of the symmetry of magnetics one should take into account not only the crystallographic elements of symmetry (rotations, reflections and translations) but also the time-inversion element, which causes the reversal of the magnetic moment density vector $\mathbf{m}(\mathbf{r})$. Following Landau & Lifshitz (1957), we shall denote this element by R. If combined with any crystallographic symmetry element G we get a product RG, which some authors call the space-time symmetry operator. We shall not use this terminology in the following.

To describe the symmetry properties of magnetics, one should use magnetic point and space groups instead of crystallographic ones. (See also Section 1.2.5.)

By investigating the 'four-dimensional groups of three-dimensional space', Heesch (1930) found not only the 122 groups that now are known as magnetic point groups but also the seven triclinic and 91 monoclinic magnetic space groups. He also recognized that these groups can be used to describe the symmetry of spin arrangements. The present interest in magnetic symmetry was much stimulated by Shubnikov (1951), who considered the symmetry groups of figures with black and white faces, which he called antisymmetry groups. The change of colour of the faces in antisymmetry (black–white symmetry, see also Section 3.3.5) corresponds to the element R. These antisymmetry classes were derived as magnetic symmetry point groups by Tavger & Zaitsev (1956). Beside antisymmetry, the concept of colour (or generalized) symmetry also was developed, in which the number of colours is not 2 but 3, 4 or 6 (see Belov *et al.*, 1964; Koptsik & Kuzhukeev, 1972). A different generalization to more than two colours was proposed by van der Waerden & Burckhardt (1961). The various approaches have been compared by Schwarzenberger (1984).

Table 1.5.2.1. *Comparison of different symbols for magnetic point groups*

Schoenflies	Hermann–Mauguin	Shubnikov	
$\boldsymbol{D}_{4R}$	$4221'$	$4{:}21'$	$4{:}2\underline{1}$
$\boldsymbol{D}_4$	422	4:2	4:2
$\boldsymbol{D}_4(\boldsymbol{C}_4)$	$42'2'$	$4{:}2'$	$4{:}\underline{2}$
$\boldsymbol{D}_4(\boldsymbol{D}_2)$	$4'22'$	$4'{:}2$	$\underline{4}{:}2$

As the theories of antisymmetry and of magnetic symmetry evolved often independently, different authors denote the operation of time inversion (black–white exchange) by different symbols. Of the four frequently used symbols ($R = E' = \underline{1} = 1'$) we shall use in this article only two: R and $1'$.

1.5.2.1. *Magnetic point groups*

Magnetic point groups may contain rotations, reflections, the element R and their combinations. A set of such elements that satisfies the group properties is called a magnetic point group. It is obvious that there are 32 trivial magnetic point groups; these are the ordinary crystallographic point groups supplemented by the element R. Each of these point groups contains all the elements of the ordinary point group $\mathcal{P}$ and also all the elements of this group $\mathcal{P}$ multiplied by R. This type of magnetic point group $\mathcal{M}_{P1}$ can be represented by

$$\mathcal{M}_{P1} = \mathcal{P} + R\mathcal{P}. \qquad (1.5.2.1)$$

These groups are sometimes called 'grey' magnetic point groups. As pointed out above, all dia- and paramagnets belong to this type of point group. To this type belong also antiferromagnets with a magnetic space group that contains translations multiplied by R (space groups of type III^b).

The second type of magnetic point group, which is also trivial in some sense, contains all the 32 crystallographic point groups without the element R in any form. For this type $\mathcal{M}_{P2} = \mathcal{P}$. Thirteen of these point groups allow ferromagnetic spontaneous magnetization (ferromagnetism, ferrimagnetism, weak ferromagnetism). They are listed in Table 1.5.2.4. The remaining 19 point groups describe antiferromagnets. The groups $\mathcal{M}_{P2}$ are often called 'white' magnetic point groups.

The third type of magnetic point group $\mathcal{M}_{P3}$, 'black and white' groups (which are the only nontrivial ones), contains those point groups in which R enters only in combination with rotations or reflections. There are 58 point groups of this type. Eighteen of them describe different types of ferromagnetism (see Table 1.5.2.4) and the others represent antiferromagnets.

Replacing R by the identity element E in the magnetic point groups of the third type does not change the number of elements in the point group. Thus each group of the third type $\mathcal{M}_{P3}$ is isomorphic to a group $\mathcal{P}$ of the second type.

The method of derivation of the nontrivial magnetic groups given below was proposed by Indenbom (1959). Let $\mathcal{H}$ denote the set of those elements of the group $\mathcal{P}$ which enter into the asso-

Table 1.5.2.2. *Comparison of different symbols for the elements of magnetic point groups*

Magnetic point group	Elements	
	Schoenflies	Hermann–Mauguin
$\boldsymbol{D}_{4R} = 4221'$	$E, C_2, 2C_4, 2U_2, 2U_2^a,$ $R, RC_2, 2RC_4, 2RU_2, 2RU_2^a$	$1, 2_x, 2_y, 2_z, 2_{xy}, 2_{-xy}, \pm 4_z,$ $1', 2'_x, 2'_y, 2'_z, 2'_{xy}, 2'_{-xy}, \pm 4'_z$
$\boldsymbol{D}_4 = 422$	$E, C_2, 2C_4, 2U_2, 2U_2^a$	$1, 2_x, 2_y, 2_z, 2_{xy}, 2_{-xy}, \pm 4_z$
$\boldsymbol{D}_4(\boldsymbol{C}_4) = 42'2'$	$E, C_2, 2C_4, 2RU_2, 2RU_2^a$	$1, 2_z, \pm 4_z, 2'_x, 2'_y, 2'_{xy}, 2'_{-xy}$
$\boldsymbol{D}_4(\boldsymbol{D}_2) = 4'22'$	$E, C_2^z, C_2^y, C_2^x, 2RU_2^a, 2RC_4$	$1, 2_x, 2_y, 2_z, 2'_{xy}, 2'_{-xy}, \pm 4'_z$

Table 1.5.2.3. *The 90 magnetic point groups of types 2 and 3*

1	2	3	4	5	6
	Symbol of magnetic point group $\mathcal{M}$				
			Hermann–Mauguin		
System	Schoenflies	Shubnikov	Short	Full	Symmetry operators of group $\mathcal{M}$
Triclinic	$\boldsymbol{C}_1$	1	1	1	1
	$\boldsymbol{C}_i$	$\underline{2}$	$\bar{1}$	$\bar{1}$	$1, \bar{1}$
	$\boldsymbol{C}_i(\boldsymbol{C}_1)$	$\underline{2}$	$\bar{1}'$	$\bar{1}'$	$1, \bar{1}'$
Monoclinic	$\boldsymbol{C}_2$	2	2	121	$1, 2_y$
	$\boldsymbol{C}_2(\boldsymbol{C}_1)$	$\underline{2}$	$2'$	$12'1$	$1, 2'_y$
	$\boldsymbol{C}_s$	m	m	$1m1$	$1, m_y$
	$\boldsymbol{C}_s(\boldsymbol{C}_1)$	$\underline{m}$	m'	$1m'1$	$1, m'_y$
	$\boldsymbol{C}_{2h}$	$2:m$	$2/m$	$1\frac{2}{m}1$	$1, \bar{1}, 2_y, m_y$
	$\boldsymbol{C}_{2h}(\boldsymbol{C}_i)$	$\underline{2}:\underline{m}$	$2'/m'$	$1\frac{2'}{m'}1$	$1, \bar{1}, 2'_y, m'_y$
	$\boldsymbol{C}_{2h}(\boldsymbol{C}_2)$	$2:\underline{m}$	$2/m'$	$1\frac{2}{m'}1$	$1, 2_y, \bar{1}', m'_y$
	$\boldsymbol{C}_{2h}(\boldsymbol{C}_s)$	$\underline{2}:m$	$2'/m$	$1\frac{2'}{m}1$	$1, m_y, \bar{1}', 2'_y$
Orthorhombic	$\boldsymbol{D}_2$	$2:2$	222	222	$1, 2_x, 2_y, 2_z$
	$\boldsymbol{D}_2(\boldsymbol{C}_2)$	$2:\underline{2}$	$2'2'2$	$2'2'2$	$1, 2_z, 2'_x, 2'_y$
	$\boldsymbol{C}_{2v}$	$2{\cdot}m$	$mm2$	$mm2$	$1, 2_z, m_x, m_y$
	$\boldsymbol{C}_{2v}(\boldsymbol{C}_2)$	$2{\cdot}\underline{m}$	$m'm'2$	$m'm'2$	$1, 2_z, m'_x, m'_y$
	$\boldsymbol{C}_{2v}(\boldsymbol{C}_s)$	$\underline{2}{\cdot}m$	$2'm'm$	$2'm'm$	$1, m_z, 2'_x, m'_y$
	$\boldsymbol{D}_{2h}$	$m{\cdot}2:m$	mmm	$\frac{2}{m}\frac{2}{m}\frac{2}{m}$	$1, \bar{1}, 2_x, 2_y, 2_z, m_x, m_y, m_z$
	$\boldsymbol{D}_{2h}(\boldsymbol{C}_{2h})$	$\underline{m}{\cdot}2:m$	$mm'm'$	$\frac{2}{m}\frac{2'}{m'}\frac{2'}{m'}$	$1, \bar{1}, 2_x, m_x, 2'_y, 2'_z, m'_y, m'_z$
	$\boldsymbol{D}_{2h}(\boldsymbol{D}_2)$	$\underline{m}{\cdot}2:\underline{m}$	$m'm'm'$	$\frac{2'}{m'}\frac{2}{m'}\frac{2}{m'}$	$1, 2_x, 2_y, 2_z, \bar{1}', m'_x, m'_y, m'_z$
	$\boldsymbol{D}_{2h}(\boldsymbol{C}_{2v})$	$m{\cdot}2:\underline{m}$	mmm'	$\frac{2'}{m}\frac{2'}{m}\frac{2}{m'}$	$1, 2_z, m_x, m_y, \bar{1}', 2'_x, 2'_y, m'_z$
Tetragonal	$\boldsymbol{C}_4$	4	4	4	$1, 2_z, \pm 4_z$
	$\boldsymbol{C}_4(\boldsymbol{C}_2)$	$\underline{4}$	$4'$	$4'$	$1, 2_z, \pm 4'_z$
	$\boldsymbol{S}_4$	$\bar{4}$	$\bar{4}$	$\bar{4}$	$1, 2_z, \pm \bar{4}_z$
	$\boldsymbol{S}_4(\boldsymbol{C}_2)$	$\underline{\bar{4}}$	$\bar{4}'$	$\bar{4}'$	$1, 2_z, \pm \bar{4}'_z$
	$\boldsymbol{C}_{4h}$	$4:m$	$4/m$	$\frac{4}{m}$	$1, \bar{1}, 2_z, m_z, \pm 4_z, \pm \bar{4}_z$
	$\boldsymbol{C}_{4h}(\boldsymbol{C}_{2h})$	$\underline{4}:m$	$4'/m$	$\frac{4'}{m}$	$1, \bar{1}, 2_z, m_z, \pm 4'_z, \pm \bar{4}'_z$
	$\boldsymbol{C}_{4h}(\boldsymbol{C}_4)$	$4:\underline{m}$	$4/m'$	$\frac{4}{m'}$	$1, 2_z, \pm 4_z, \bar{1}', m'_z, \pm \bar{4}'_z$
	$\boldsymbol{C}_{4h}(\boldsymbol{S}_4)$	$\underline{4}:\underline{m}$	$4'/m'$	$\frac{4'}{m'}$	$1, 2_z, \pm \bar{4}_z, \bar{1}', m'_z, \pm 4'_z$
	$\boldsymbol{D}_4$	$4:2$	422	422	$1, 2_x, 2_y, 2_z, 2_{xy}, 2_{-xy}, \pm 4_z$
	$\boldsymbol{D}_4(\boldsymbol{D}_2)$	$\underline{4}:2$	$4'22'$	$4'22'$	$1, 2_x, 2_y, 2_z, 2'_{xy}, 2'_{-xy}, \pm 4'_z$
	$\boldsymbol{D}_4(\boldsymbol{C}_4)$	$4:\underline{2}$	$42'2'$	$42'2'$	$1, 2_z, \pm 4_z, 2'_x, 2'_y, 2'_{xy}, 2'_{-xy}$
	$\boldsymbol{C}_{4v}$	$4{\cdot}m$	$4mm$	$4mm$	$1, 2_z, m_x, m_y, m_{xy}, m_{-xy}, \pm 4_z$
	$\boldsymbol{C}_{4v}(\boldsymbol{C}_{2v})$	$\underline{4}{\cdot}m$	$4'mm'$	$4'mm'$	$1, 2_z, m_x, m_y, m'_{xy}, m'_{-xy}, \pm 4'_z$
	$\boldsymbol{C}_{4v}(\boldsymbol{C}_4)$	$4{\cdot}\underline{m}$	$4m'm'$	$4m'm'$	$1, 2_z, \pm 4_z, m'_x, m'_y, m'_{xy}, m'_{-xy}$
	$\boldsymbol{D}_{2d}$	$\bar{4}{\cdot}m$	$\bar{4}2m$	$\bar{4}2m$	$1, 2_x, 2_y, 2_z, m_{xy}, m_{-xy}, \pm \bar{4}_z$
	$\boldsymbol{D}_{2d}(\boldsymbol{D}_2)$	$\underline{\bar{4}}{\cdot}\underline{m}$	$\bar{4}'2m'$	$\bar{4}'2m'$	$1, 2_x, 2_y, 2_z, m'_{xy}, m'_{-xy}, \pm \bar{4}'_z$
	$\boldsymbol{D}_{2d}(\boldsymbol{C}_{2v})$	$\underline{\bar{4}}{\cdot}m$	$\bar{4}'m2'$	$\bar{4}'m2'$	$1, 2_z, m_x, m_y, 2'_{xy}, 2'_{-xy}, \pm \bar{4}'_z$
	$\boldsymbol{D}_{2d}(\boldsymbol{S}_4)$	$\bar{4}{\cdot}\underline{m}$	$\bar{4}2'm'$	$\bar{4}2'm'$	$1, 2_z, \pm \bar{4}_z, 2'_x, 2'_y, m'_{xy}, m'_{-xy}$
	$\boldsymbol{D}_{4h}$	$m{\cdot}4:m$	$4/mmm$	$\frac{4}{m}\frac{2}{m}\frac{2}{m}$	$1, \bar{1}, 2_x, 2_y, 2_z, 2_{xy}, 2_{-xy}, m_x, m_y, m_z, m_{xy}, m_{-xy}, \pm 4_z, \pm \bar{4}_z$
	$\boldsymbol{D}_{4h}(\boldsymbol{D}_{2h})$	$m{\cdot}\underline{4}:m$	$4'/mmm'$	$\frac{4'}{m}\frac{2}{m}\frac{2'}{m'}$	$1, \bar{1}, 2_x, 2_y, 2_z, m_x, m_y, m_z, 2'_{xy}, 2'_{-xy}, m'_{xy}, m'_{-xy}, \pm 4'_z, \pm \bar{4}'_z$
	$\boldsymbol{D}_{4h}(\boldsymbol{C}_{4h})$	$\underline{m}{\cdot}4:m$	$4/mm'm'$	$\frac{4}{m}\frac{2'}{m'}\frac{2'}{m'}$	$1, \bar{1}, 2_z, m_z, \pm 4_z, \pm \bar{4}_z, 2'_x, 2'_y, 2'_{xy}, 2'_{-xy}, m'_x, m'_y, m'_{xy}, m'_{-xy}$
	$\boldsymbol{D}_{4h}(\boldsymbol{D}_4)$	$\underline{m}{\cdot}4:\underline{m}$	$4/m'm'm'$	$\frac{4}{m'}\frac{2}{m'}\frac{2}{m'}$	$1, 2_x, 2_y, 2_z, 2_{xy}, 2_{-xy}, \pm 4_z, \bar{1}', m'_x, m'_y, m'_z, m'_{xy}, m'_{-xy}, \pm \bar{4}'_z$
	$\boldsymbol{D}_{4h}(\boldsymbol{C}_{4v})$	$m{\cdot}4:\underline{m}$	$4/m'mm$	$\frac{4}{m'}\frac{2'}{m}\frac{2'}{m}$	$1, 2_z, m_x, m_y, m_{xy}, m_{-xy}, \pm 4_z, \bar{1}', 2'_x, 2'_y, 2'_{xy}, 2'_{-xy}, m'_z, \pm \bar{4}'_z$
	$\boldsymbol{D}_{4h}(\boldsymbol{D}_{2d})$	$m{\cdot}\underline{4}:\underline{m}$	$4'/m'm'm$	$\frac{4'}{m'}\frac{2}{m'}\frac{2'}{m}$	$1, 2_x, 2_y, 2_z, m_{xy}, m_{-xy}, \pm \bar{4}_z, \bar{1}', 2'_{xy}, 2'_{-xy}, m'_x, m'_y, m'_z, \pm 4'_z$

ciated magnetic group $\mathcal{M}_{P3}$ not multiplied by R. The set $\mathcal{H}$ contains the identity element E, for each element H also its inverse H^{-1}, and for each pair H_1, H_2 also its products H_1H_2 and H_2H_1. Thus the set $\mathcal{H}$ forms a group. It is a subgroup of the crystallographic group $\mathcal{P}$. Let P_i denote an element of $(\mathcal{P}-\mathcal{H})$. All these elements enter $\mathcal{M}_{P3}$ in the form of products RP_i because $RP_i = P_iR$ and $R^2 = 1$. Multiplying the elements of $\mathcal{M}_{P3}$ by a fixed element RP_1 corresponds to a permutation of the elements of $\mathcal{M}_{P3}$. This permutation maps each element of the subgroup $\mathcal{H}$ on an element of $\mathcal{M}_{P3}$ that does not belong to $\mathcal{H}$ and *vice versa*. It follows that one half of the elements of $\mathcal{M}_{P3}$ are elements of $(\mathcal{P}-\mathcal{H})$ multiplied by R and the other half belong to $\mathcal{H}$. The relation for the magnetic point groups of the third type may therefore be written as

$$\mathcal{M}_{P3} = \mathcal{H} + R(\mathcal{P}-\mathcal{H}) = \mathcal{H} + RP_1\mathcal{H}. \qquad (1.5.2.2)$$

$\mathcal{H}$ is therefore a subgroup of index 2 of $\mathcal{P}$. The subgroups of index 2 of $\mathcal{P}$ can easily be found using the tables of irreducible representations of the point groups. Every real non-unit one-dimensional representation of $\mathcal{P}$ contains equal numbers of characters $+1$ and -1. In the corresponding magnetic point group $\mathcal{M}_{P3}$, the elements of $\mathcal{P}$ with character -1 are multiplied by R and those with character $+1$ remain unchanged. The latter form the subgroup $\mathcal{H}$. This rule can be stated as a theorem: every real non-unit one-dimensional representation τ of a point group of symmetry $\mathcal{P}$ produces an isomorphic mapping of this group upon a magnetic group $\mathcal{M}_{P3}$ (Indenbom, 1959). This concept will be developed in Section 1.5.3.

Using the Schoenflies symbols and the method described above, the point groups of magnetic symmetry (magnetic point groups) can be denoted by $\mathcal{P}(\mathcal{H})$, where $\mathcal{P}$ is the symbol of the original crystallographic point group and $\mathcal{H}$ is the symbol of that

Table 1.5.2.3 (*cont.*)

1	2	3	4	5	6
	Symbol of magnetic point group $\mathcal{M}$				
			Hermann–Mauguin		
System	Schoenflies	Shubnikov	Short	Full	Symmetry operators of group $\mathcal{M}$
Trigonal	$\boldsymbol{C}_3$	3	3	3	$1, \pm 3_z$
	$\boldsymbol{S}_6$	$\bar{6}$	$\bar{3}$	$\bar{3}$	$1, \bar{1}, \pm 3_z, \pm\bar{3}_z$
	$\boldsymbol{S}_6(\boldsymbol{C}_3)$	$\underline{\bar{6}}$	$\bar{3}'$	$\bar{3}'$	$1, \pm 3_z, \bar{1}', \pm\bar{3}'_z$
	$\boldsymbol{D}_3$	$3:2$	32	321	$1, 3(2_\perp), \pm 3_z$
	$\boldsymbol{D}_3(\boldsymbol{C}_3)$	$3:\underline{2}$	$32'$	$32'1$	$1, \pm 3_z, 3(2'_\perp)$
	$\boldsymbol{C}_{3v}$	$3\cdot m$	$3m$	$3m1$	$1, 3(m_\perp), \pm 3_z$
	$\boldsymbol{C}_{3v}(\boldsymbol{C}_3)$	$3\cdot\underline{m}$	$3m'$	$3m'1$	$1, \pm 3_z, 3(m'_\perp)$
	$\boldsymbol{D}_{3d}$	$\bar{6}\cdot m$	$\bar{3}m$	$\bar{3}\frac{2}{m}1$	$1, \bar{1}, 3(2_\perp), 3(m_\perp), \pm 3_z, \pm\bar{3}_z$
	$\boldsymbol{D}_{3d}(\boldsymbol{S}_6)$	$\bar{6}\cdot\underline{m}$	$\bar{3}m'$	$\bar{3}\frac{2'}{m'}1$	$1, \bar{1}, \pm 3_z, \pm\bar{3}_z, 3(2'_\perp), 3(m'_\perp)$
	$\boldsymbol{D}_{3d}(\boldsymbol{D}_3)$	$\underline{\bar{6}}\cdot\underline{m}$	$\bar{3}'m'$	$\bar{3}'\frac{2}{m'}1$	$1, 3(2_\perp), \pm 3_z, \bar{1}', 3(m'_\perp), \pm\bar{3}'_z$
	$\boldsymbol{D}_{3d}(\boldsymbol{C}_{3v})$	$\underline{\bar{6}}\cdot m$	$\bar{3}'m$	$\bar{3}'\frac{2'}{m}1$	$1, 3(m_\perp), \pm 3_z, \bar{1}', 3(2'_\perp), \pm\bar{3}'_z$
Hexagonal	$\boldsymbol{C}_6$	6	6	6	$1, 2_z, \pm 3_z, \pm 6_z$
	$\boldsymbol{C}_6(\boldsymbol{C}_3)$	$\underline{6}$	$6'$	$6'$	$1, \pm 3_z, 2'_z, \pm 6'_z$
	$\boldsymbol{C}_{3h}$	$3:m$	$\bar{6}$	$\bar{6}$	$1, m_z, \pm 3_z, \pm\bar{6}_z$
	$\boldsymbol{C}_{3h}(\boldsymbol{C}_3)$	$3:\underline{m}$	$\bar{6}'$	$\bar{6}'$	$1, \pm 3_z, m'_z, \pm\bar{6}'_z$
	$\boldsymbol{C}_{6h}$	$6:m$	$6/m$	$\frac{6}{m}$	$1, \bar{1}, 2_z, m_z, \pm 3_z, \pm\bar{3}_z, \pm 6_z, \pm\bar{6}_z$
	$\boldsymbol{C}_{6h}(\boldsymbol{S}_6)$	$\underline{6}:\underline{m}$	$6'/m'$	$\frac{6'}{m'}$	$1, \bar{1}, \pm 3_z, \pm\bar{3}_z, 2'_z, m'_z, \pm 6'_z, \pm\bar{6}'_z$
	$\boldsymbol{C}_{6h}(\boldsymbol{C}_6)$	$6:\underline{m}$	$6/m'$	$\frac{6}{m'}$	$1, 2_z, \pm 3_z, \pm 6_z, \bar{1}', m'_z, \pm\bar{3}'_z, \pm\bar{6}'_z$
	$\boldsymbol{C}_{6h}(\boldsymbol{C}_{3h})$	$\underline{6}:m$	$6'/m$	$\frac{6'}{m}$	$1, m_z, \pm 3_z, \pm\bar{6}_z, \bar{1}', 2'_z, \pm\bar{3}'_z, \pm 6'_z$
	$\boldsymbol{D}_6$	$6:2$	622	622	$1, 6(2_\perp), 2_z, \pm 3_z, \pm 6_z$
	$\boldsymbol{D}_6(\boldsymbol{D}_3)$	$\underline{6}:2$	$6'22'$	$6'22'$	$1, 3(2_\perp), \pm 3_z, 3(2'_\perp), 2'_z, \pm 6'_z$
	$\boldsymbol{D}_6(\boldsymbol{C}_6)$	$6:\underline{2}$	$62'2'$	$62'2'$	$1, 2_z, \pm 3_z, \pm 6_z, 6(2'_\perp)$
	$\boldsymbol{C}_{6v}$	$6\cdot m$	$6mm$	$6mm$	$1, 2_z, 6(m_\perp), \pm 3_z, \pm 6_z$
	$\boldsymbol{C}_{6v}(\boldsymbol{C}_{3v})$	$\underline{6}\cdot m$	$6'mm'$	$6'mm'$	$1, 3(m_\perp), \pm 3_z, 2'_z, 3(m'_\perp), \pm 6'_z$
	$\boldsymbol{C}_{6v}(\boldsymbol{C}_6)$	$6\cdot\underline{m}$	$6m'm'$	$6m'm'$	$1, 2_z, \pm 3_z, \pm 6_z, 6(m'_\perp)$
	$\boldsymbol{D}_{3h}$	$m\cdot 3:m$	$\bar{6}m2$	$\bar{6}m2$	$1, 3(2_\perp), 3(m_\perp), m_z, \pm 3_z, \pm\bar{6}_z$
	$\boldsymbol{D}_{3h}(\boldsymbol{D}_3)$	$\underline{m}\cdot 3:\underline{m}$	$\bar{6}'2m'$	$\bar{6}'2m'$	$1, 3(2_\perp), \pm 3_z, 3(m'_\perp), m'_z, \pm\bar{6}'_z$
	$\boldsymbol{D}_{3h}(\boldsymbol{C}_{3v})$	$m\cdot 3:\underline{m}$	$\bar{6}'m2'$	$\bar{6}'m2'$	$1, 3(m_\perp), \pm 3_z, 3(2'_\perp), m'_z, \pm\bar{6}'_z$
	$\boldsymbol{D}_{3h}(\boldsymbol{C}_{3h})$	$\underline{m}\cdot 3:m$	$\bar{6}m'2'$	$\bar{6}m'2'$	$1, m_z, \pm 3_z, \pm\bar{6}_z, 3(2'_\perp), 3(m'_\perp)$
	$\boldsymbol{D}_{6h}$	$m\cdot 6:m$	$6/mmm$	$\frac{6}{m}\frac{2}{m}\frac{2}{m}$	$1, \bar{1}, 6(2_\perp), 2_z, 6(m_\perp), m_z, \pm 3_z, \pm\bar{3}_z, \pm 6_z, \pm\bar{6}_z$
	$\boldsymbol{D}_{6h}(\boldsymbol{D}_{3d})$	$m\cdot\underline{6}:\underline{m}$	$6'/m'mm'$	$\frac{6'}{m'}\frac{2}{m}\frac{2'}{m'}$	$1, \bar{1}, 3(2_\perp), 3(m_\perp), \pm 3_z, \pm\bar{3}_z, 3(2'_\perp), 2'_z, 3(m'_\perp), m'_z, \pm 6'_z, \pm\bar{6}'_z$
	$\boldsymbol{D}_{6h}(\boldsymbol{C}_{6h})$	$\underline{m}\cdot 6:m$	$6/mm'm'$	$\frac{6}{m}\frac{2'}{m'}\frac{2'}{m'}$	$1, \bar{1}, 2_z, m_z, \pm 3_z, \pm\bar{3}_z, \pm 6_z, \pm\bar{6}_z, 6(2'_\perp), 6(m'_\perp)$
	$\boldsymbol{D}_{6h}(\boldsymbol{D}_6)$	$\underline{m}\cdot 6:\underline{m}$	$6/m'm'm'$	$\frac{6}{m'}\frac{2}{m'}\frac{2}{m'}$	$1, 6(2_\perp), 2_z, \pm 3_z, \pm 6_z, \bar{1}', 6(m'_\perp), m'_z, \pm\bar{3}'_z, \pm\bar{6}'_z$
	$\boldsymbol{D}_{6h}(\boldsymbol{C}_{6v})$	$m\cdot 6:\underline{m}$	$6/m'mm$	$\frac{6}{m'}\frac{2'}{m}\frac{2'}{m}$	$1, 2_z, 6(m_\perp), \pm 3_z, \pm 6_z, \bar{1}', 6(2'_\perp), m'_z, \pm\bar{3}'_z, \pm\bar{6}'_z$
	$\boldsymbol{D}_{6h}(\boldsymbol{D}_{3h})$	$m\cdot\underline{6}:m$	$6'/mmm'$	$\frac{6'}{m}\frac{2'}{m}\frac{2}{m'}$	$1, 3(2_\perp), 3(m_\perp), m_z, \pm 3_z, \pm\bar{6}_z, \bar{1}', 3(2'_\perp), 2'_z, 3(m'_\perp), \pm\bar{3}'_z, \pm 6'_z$
Cubic	$\boldsymbol{T}$	$3/2$	23	23	$1, 3(2), 4(\pm 3)$
	$\boldsymbol{T}_h$	$\bar{6}/2$	$m\bar{3}$	$\frac{2}{m}\bar{3}$	$1, \bar{1}, 3(2), 3(m), 4(\pm 3), 4(\pm\bar{3})$
	$\boldsymbol{T}_h(\boldsymbol{T})$	$\underline{\bar{6}}/2$	$m'\bar{3}'$	$\frac{2}{m'}\bar{3}'$	$1, 3(2), 4(\pm 3), \bar{1}', 3(m'), 4(\pm\bar{3}')$
	$\boldsymbol{O}$	$3/4$	432	432	$1, 9(2), 4(\pm 3), 3(\pm 4)$
	$\boldsymbol{O}(\boldsymbol{T})$	$3/\underline{4}$	$4'32'$	$4'32'$	$1, 3(2), 4(\pm 3), 6(2'), 3(\pm 4')$
	$\boldsymbol{T}_d$	$3/\bar{4}$	$\bar{4}3m$	$\bar{4}3m$	$1, 3(2), 6(m), 4(\pm 3), 3(\pm\bar{4})$
	$\boldsymbol{T}_d(\boldsymbol{T})$	$3/\underline{\bar{4}}$	$\bar{4}'3m'$	$\bar{4}'3m'$	$1, 3(2), 4(\pm 3), 6(m'), 3(\pm\bar{4}')$
	$\boldsymbol{O}_h$	$\bar{6}/4$	$m\bar{3}m$	$\frac{4}{m}\bar{3}\frac{2}{m}$	$1, \bar{1}, 9(2), 9(m), 4(\pm 3), 4(\pm\bar{3}), 3(\pm 4), 3(\pm\bar{4})$
	$\boldsymbol{O}_h(\boldsymbol{T}_h)$	$\bar{6}/\underline{4}$	$m\bar{3}m'$	$\frac{4'}{m}\bar{3}\frac{2'}{m'}$	$1, \bar{1}, 3(2), 3(m), 4(\pm 3), 4(\pm\bar{3}), 6(2'), 6(m'), 3(\pm 4'), 3(\pm\bar{4}')$
	$\boldsymbol{O}_h(\boldsymbol{O})$	$\underline{\bar{6}}/4$	$m'\bar{3}'m'$	$\frac{4}{m'}\bar{3}'\frac{2}{m'}$	$1, 9(2), 4(\pm 3), 3(\pm 4), \bar{1}', 9(m'), 4(\pm\bar{3}'), 3(\pm\bar{4}')$
	$\boldsymbol{O}_h(\boldsymbol{T}_d)$	$\underline{\bar{6}}/\underline{4}$	$m'\bar{3}'m$	$\frac{4'}{m'}\bar{3}'\frac{2'}{m}$	$1, 3(2), 6(m), 4(\pm 3), 3(\pm\bar{4}), \bar{1}', 6(2'), 3(m'), 4(\pm\bar{3}'), 3(\pm 4')$

subgroup the elements of which are not multiplied by R. This notation is often used in the physics literature. In the crystallographic literature, the magnetic groups are defined by Hermann–Mauguin or Shubnikov symbols. In this type of designation, the symbols of elements multiplied by R are primed or underlined. The primed symbols are used in most of the recent publications. The Hermann–Mauguin and Shubnikov definitions differ slightly, as in the case of crystallographic groups. In Table 1.5.2.1, different symbols of magnetic point groups (trivial and nontrivial ones) are compared. This is done for the family that belongs to the crystallographic point group $\boldsymbol{D}_4 = 422$. The symbols of the symmetry elements of these four magnetic point groups are compared in Table 1.5.2.2.

Table 1.5.2.3 gives a list of the 90 magnetic point groups belonging to types 2 and 3. The Schoenflies, Shubnikov and Hermann–Mauguin symbols of the point groups are given in the table. The entries in the Hermann–Mauguin symbol refer to symmetry directions, as explained in Section 2.2.4 of *International Tables for Crystallography*, Vol. A (2002). The elements of symmetry of each point group are displayed using the Hermann–Mauguin symbols. The symbol $N(2_\perp)$ denotes N 180° rotations with axes perpendicular to the principal symmetry axis; $N(m_\perp)$ denotes N mirror planes with normals perpendicular to the principal symmetry axis. Similar definitions hold for the primed symbols $N(2'_\perp)$ and $N(m'_\perp)$. The point groups are arranged in families. The part of the Schoenflies symbol before the bracket is

Table 1.5.2.4. *List of the magnetic classes in which ferromagnetism is admitted*

(*a*) Triclinic

Symbol of symmetry class		Allowed direction of $\mathbf{M}_s$
Schoenflies	Hermann–Mauguin	
$\boldsymbol{C}_1$	1	Any
$\boldsymbol{C}_i$	$\bar{1}$	Any

(*b*) Monoclinic

Symbol of symmetry class		Allowed direction of $\mathbf{M}_s$
Schoenflies	Hermann–Mauguin	
$\boldsymbol{C}_2$	2	$\parallel 2$
$\boldsymbol{C}_2(\boldsymbol{C}_1)$	$2'$	$\perp 2'$
$\boldsymbol{C}_s = \boldsymbol{C}_{1h}$	m	$\perp m$
$\boldsymbol{C}_s(\boldsymbol{C}_1)$	m'	$\parallel m'$
$\boldsymbol{C}_{2h}$	$2/m$	$\parallel 2$
$\boldsymbol{C}_{2h}(\boldsymbol{C}_i)$	$2'/m'$	$\parallel m'$

(*c*) Orthorhombic

Symbol of symmetry class		Allowed direction of $\mathbf{M}_s$
Schoenflies	Hermann–Mauguin	
$\boldsymbol{D}_2(\boldsymbol{C}_2)$	$22'2'$	$\parallel 2$
$\boldsymbol{C}_{2v}(\boldsymbol{C}_2)$	$m'm'2$	$\parallel 2$
$\boldsymbol{C}_{2v}(\boldsymbol{C}_s)$	$m'm2'$	$\perp m$
$\boldsymbol{D}_{2h}(\boldsymbol{C}_{2h})$	$mm'm'$	$\perp m$

(*d*) Tetragonal

Symbol of symmetry class		Allowed direction of $\mathbf{M}_s$
Schoenflies	Hermann–Mauguin	
$\boldsymbol{C}_4$	4	$\parallel 4$
$\boldsymbol{S}_4$	$\bar{4}$	$\parallel \bar{4}$
$\boldsymbol{C}_{4h}$	$4/m$	$\parallel 4$
$\boldsymbol{D}_4(\boldsymbol{C}_4)$	$42'2'$	$\parallel 4$
$\boldsymbol{C}_{4v}(\boldsymbol{C}_4)$	$4m'm'$	$\parallel 4$
$\boldsymbol{D}_{2d}(\boldsymbol{S}_4)$	$\bar{4}2'm'$	$\parallel \bar{4}$
$\boldsymbol{D}_{4h}(\boldsymbol{C}_{4h})$	$4/mm'm'$	$\parallel 4$

(*e*) Trigonal

Symbol of symmetry class		Allowed direction of $\mathbf{M}_s$
Schoenflies	Hermann–Mauguin	
$\boldsymbol{C}_3$	3	$\parallel 3$
$\boldsymbol{S}_6$	$\bar{3}$	$\parallel 3$
$\boldsymbol{D}_3(\boldsymbol{C}_3)$	$32'$	$\parallel 3$
$\boldsymbol{C}_{3v}(\boldsymbol{C}_3)$	$3m'$	$\parallel 3$
$\boldsymbol{D}_{3d}(\boldsymbol{S}_6)$	$\bar{3}m'$	$\parallel 3$

(*f*) Hexagonal

Symbol of symmetry class		Allowed direction of $\mathbf{M}_s$
Schoenflies	Hermann–Mauguin	
$\boldsymbol{C}_6$	6	$\parallel 6$
$\boldsymbol{C}_{3h}$	$\bar{6}$	$\parallel \bar{6}$
$\boldsymbol{C}_{6h}$	$6/m$	$\parallel 6$
$\boldsymbol{D}_6(\boldsymbol{C}_6)$	$62'2'$	$\parallel 6$
$\boldsymbol{C}_{6v}(\boldsymbol{C}_6)$	$6m'm'$	$\parallel 6$
$\boldsymbol{D}_{3h}(\boldsymbol{C}_{3h})$	$\bar{6}m'2'$	$\parallel \bar{6}$
$\boldsymbol{D}_{6h}(\boldsymbol{C}_{6h})$	$6/mm'm'$	$\parallel 6$

the same for each member of a family. Each family begins with a trivial magnetic point group. It contains the same elements as the corresponding crystallographic point group; its Schoenflies symbol contains no brackets. For each nontrivial point group, the list of the elements of symmetry begins with the non-primed elements, which belong to a subgroup $\mathcal{H}$ of the head of the family $\mathcal{G}$. The number of the primed elements is equal to the number of non-primed ones and the total number of the elements is the same for all point groups of one family.

The overall number of the magnetic point groups of all three types is 122. There are two general statements concerning the magnetic point groups. The element $RC_3 = 3'$ does not appear in any of the magnetic point groups of type 3. Only trivial magnetic point groups (of both first and second type) belong to the families containing the point groups $\boldsymbol{C}_1 = 1$, $\boldsymbol{C}_3 = 3$ and $\boldsymbol{T} = 23$.

Only 31 magnetic point groups allow ferromagnetism. The different types of ferromagnetism (one-sublattice ferromagnet, ferrimagnet, weak ferromagnet, any magnetic order with nonzero magnetization) cannot be distinguished by their magnetic symmetry. Ferromagnetism is not admitted in any point group of type 1. For the magnetic point groups of the second type, ferromagnetism is not allowed if the point group contains more than one symmetry axis, more than one mirror plane or a mirror plane that is parallel to the axis. The same restrictions are valid for the point groups of type 3 (if the corresponding elements are not multiplied by R). If the point group contains $\bar{1}'$, ferromagnetic order is also forbidden. There are the following rules for the orientation of the axial vector of ferromagnetic magnetization $\mathbf{M}$: $\mathbf{M} \parallel N, \mathbf{M} \perp 2', \mathbf{M} \perp m, \mathbf{M} \parallel m'$. Table 1.5.2.4 lists those magnetic point groups that admit ferromagnetic order (Tavger, 1958). The allowed direction of the magnetization vector is given for every point group. Ferromagnetic order is allowed in 13 point groups of the second type and 18 point groups of the third type.

All 31 point groups of magnetic symmetry allowing ferromagnetism are subgroups of the infinite noncrystallographic group

$$\boldsymbol{D}_{\infty h}(\boldsymbol{C}_{\infty h}) = \frac{\infty}{m}\frac{2'}{m'}.$$

The transition from a paramagnetic to a ferromagnetic state is always accompanied by a change of the magnetic symmetry.

1.5.2.2. *Magnetic lattices*

If the point group of symmetry describes the macroscopic properties of a crystal, its microscopic structure is determined by the space group, which contains the group of translations $\mathcal{T}$ as a subgroup. The elements $\mathbf{t}$ of $\mathcal{T}$ are defined by the following relation:

$$\mathbf{t} = n_1\mathbf{a}_1 + n_2\mathbf{a}_2 + n_3\mathbf{a}_3, \qquad (1.5.2.3)$$

where $\mathbf{a}_1$, $\mathbf{a}_2$, $\mathbf{a}_3$ are basic primitive translation vectors and n_1, n_2, n_3 are arbitrary integers. The set of points $\mathbf{r}'$ obtained by applying all the translations of the group $\mathcal{T}$ to any point $\mathbf{r}$ defines a lattice. All sites of the crystallographic lattice are equivalent.

The structure of the ordered magnetics is described by the magnetic lattices and corresponding magnetic translation groups $\mathcal{M}_T$. In the magnetic translation groups $\mathcal{M}_T$, some of the elements $\mathbf{t}$ may be multiplied by R (we shall call them primed translations). The magnetic lattices then have two types of sites, which are not equivalent. One set is obtained by non-primed translations and the other set by the primed ones. The magnetic translation group $\mathcal{M}_T$ is isometric to the crystallographic one $\mathcal{G}_0$ that is obtained by replacing R by E in $\mathcal{M}_T$.

There are trivial magnetic translation groups, in which none of the translation elements is multiplied by R. The magnetic lattices of these groups coincide with crystallographic lattices.

Nontrivial magnetic translation groups can be constructed in analogy to relation (1.5.2.2). Zamorzaev (1957) showed that every translation group $\mathcal{T}$ has seven subgroups of index 2. If the basic primitive translations of the group $\mathcal{T}$ are $\mathbf{a}_1$, $\mathbf{a}_2$, $\mathbf{a}_3$, then the basic primitive translations of the seven subgroups $\mathcal{H}$ can be chosen as follows (see also Opechowski & Guccione, 1965)

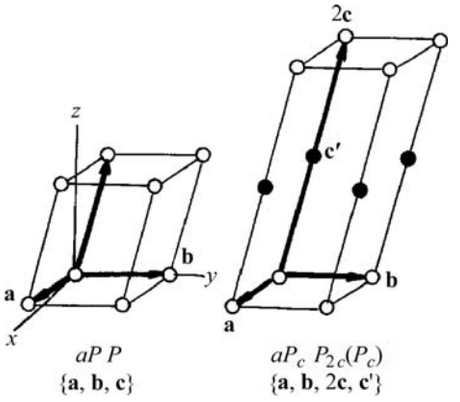

Fig. 1.5.2.1. Magnetic lattices of the triclinic system.

$$\mathcal{H}_1 : 2\mathbf{a}_1, \mathbf{a}_2, \mathbf{a}_3 \quad (1.5.2.4)$$
$$\mathcal{H}_2 : \mathbf{a}_1, 2\mathbf{a}_2, \mathbf{a}_3 \quad (1.5.2.5)$$
$$\mathcal{H}_3 : \mathbf{a}_1, \mathbf{a}_2, 2\mathbf{a}_3 \quad (1.5.2.6)$$
$$\mathcal{H}_4 : 2\mathbf{a}_1, \mathbf{a}_1 + \mathbf{a}_2, \mathbf{a}_3 \quad (1.5.2.7)$$
$$\mathcal{H}_5 : 2\mathbf{a}_2, \mathbf{a}_2 + \mathbf{a}_3, \mathbf{a}_1 \quad (1.5.2.8)$$
$$\mathcal{H}_6 : 2\mathbf{a}_3, \mathbf{a}_3 + \mathbf{a}_1, \mathbf{a}_2 \quad (1.5.2.9)$$
$$\mathcal{H}_7 : 2\mathbf{a}_1, \mathbf{a}_1 + \mathbf{a}_2, \mathbf{a}_1 + \mathbf{a}_3. \quad (1.5.2.10)$$

As an example, let us consider the case (1.5.2.5). In this case, the subgroup $\mathcal{H}$ consists of the following translations:

$$\mathbf{t}(\mathcal{H}) = n_1\mathbf{a}_1 + 2n_2\mathbf{a}_2 + n_3\mathbf{a}_3. \quad (1.5.2.11)$$

Therefore the elements G_i of $(\mathcal{T} - \mathcal{H})$ [which corresponds to $(\mathcal{P} - \mathcal{H})$ in relation (1.5.2.2)] must have the following form:

$$\mathbf{t}(G_i) = n_1\mathbf{a}_1 + (2n_2 + 1)\mathbf{a}_2 + n_3\mathbf{a}_3. \quad (1.5.2.12)$$

The corresponding magnetic translation group consists of the elements (1.5.2.12) multiplied by R and the elements (1.5.2.11).

The crystallographic lattices are classified into Bravais types or Bravais lattices. The magnetic lattices are classified into Bravais types of magnetic lattices. It turns out that there are 22 nontrivial magnetic Bravais types. Together with the trivial ones, there are 36 magnetic Bravais lattices.

Two types of smallest translation-invariant cells are in common use for the description of magnetically ordered structures: the crystallographic cell obtained if the magnetic order is neglected and the magnetic cell, which takes the magnetic order into account. The list of the basic translations of all the magnetic Bravais lattices was given by Zamorzaev (1957). The diagrams of the magnetic unit cells were obtained by Belov *et al.* (1957).

In Figs. 1.5.2.1–1.5.2.7, the diagrams of the magnetic unit cells of all 36 Bravais types are sketched in such a way that it is clear to which family the given cell belongs. All the cells of one family are displayed in one row. Such a row begins with the cell of the trivial magnetic lattice. All nontrivial cells of a family change into the trivial one of this family if R is replaced by E (to draw these diagrams we used those published by Opechowski & Guccione, 1965). Open and full circles are used to show the primed and unprimed translations. A line connecting two circles of the same type is an unprimed translation; a line connecting two circles of different types is a primed translation. The arrows in the trivial magnetic cell represent the primitive (primed or unprimed) translations for all the magnetic lattices of the family. The arrows in the nontrivial cells are primitive translations of the magnetic unit cell. The magnetic unit cell of a nontrivial magnetic lattice is generated by unprimed translations only. Its volume is twice the volume of the smallest cell generated by all (primed and unprimed) translations. The reason for this is that one of the primitive translations of the magnetic cell is twice a primitive primed translation. The crystallographic cell of many simple collinear or weakly non-collinear structures coincides with the smallest cell generated by the primed and unprimed translations. However, there are also magnetic structures with more complicated transformations from the crystallographic to the magnetic unit cell. The second line after each part of Figs. 1.5.2.1–1.5.2.7 gives, between braces, an extended vector basis of the magnetic translation group (Shubnikov & Koptsik, 1972). The first line

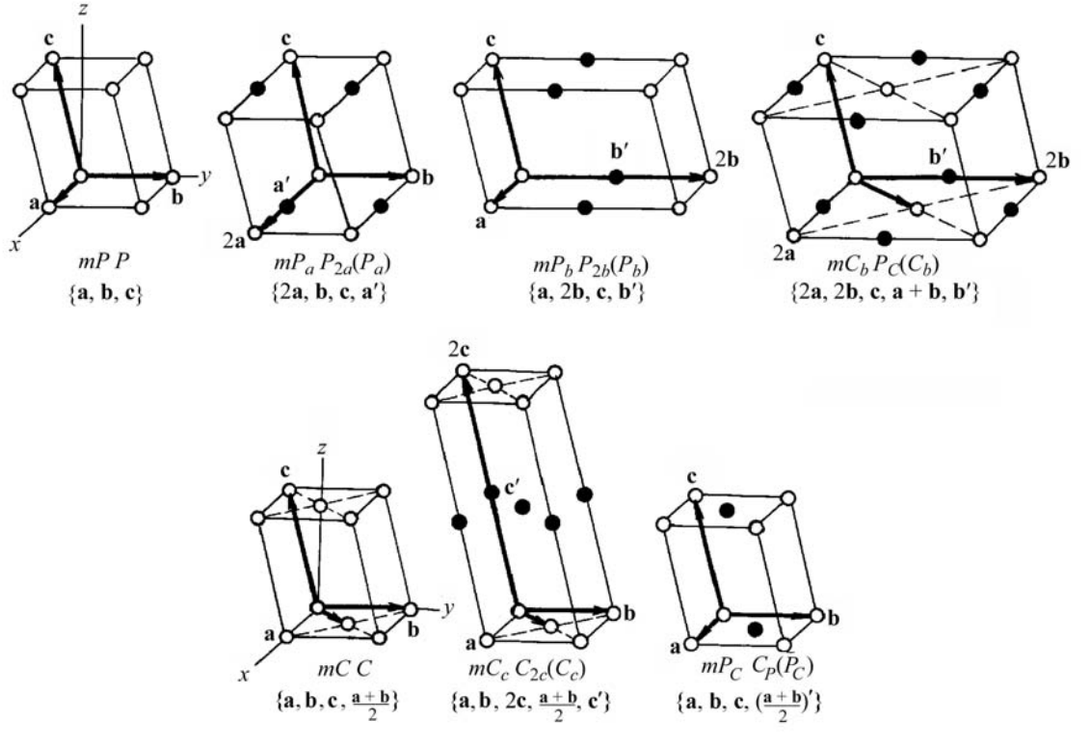

Fig. 1.5.2.2. Magnetic lattices of the monoclinic system (the y axis is the twofold axis).

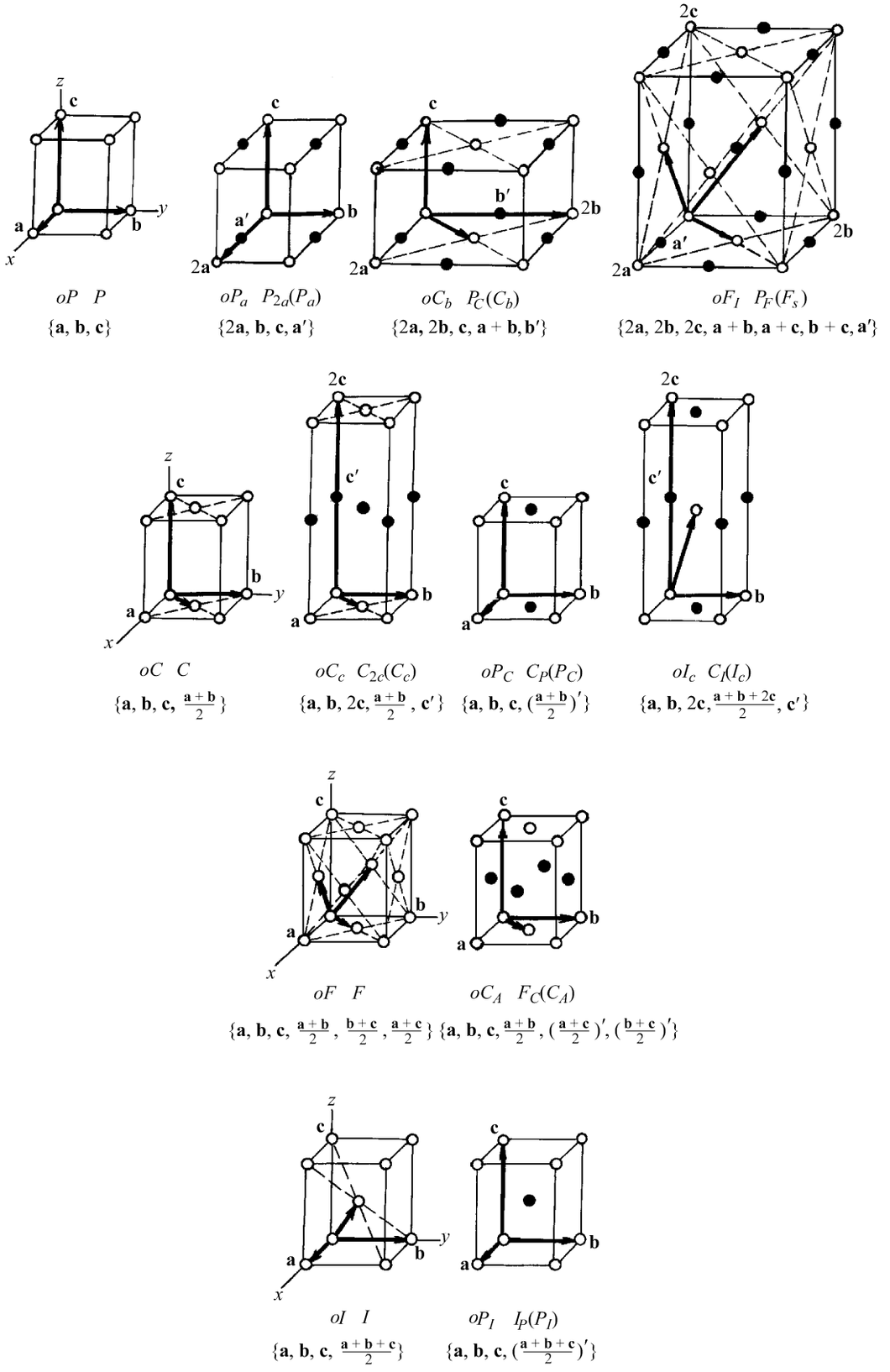

Fig. 1.5.2.3. Magnetic lattices of the orthorhombic system.

gives two symbols for each Bravais type: the symbol to the right was introduced by Opechowski & Guccione (1965). The symbol to the left starts with a lower-case letter giving the crystal system followed by a capital letter giving the centring type of the cell defined by the unprimed translations (*P*: primitive; *C*, *A*, *B*: *C*-, *A*-, *B*-centred; *I*: body-centred; *F*: all-face-centred). The subscript, which appears for the nontrivial Bravais types, indicates the translations that are multiplied by time inversion *R*.

Ferromagnetism is allowed only in trivial magnetic Bravais lattices. All nontrivial magnetic lattices represent antiferromagnetic order. There are only two magnetic sublattices in the simplest antiferromagnetic structures; one sublattice consists

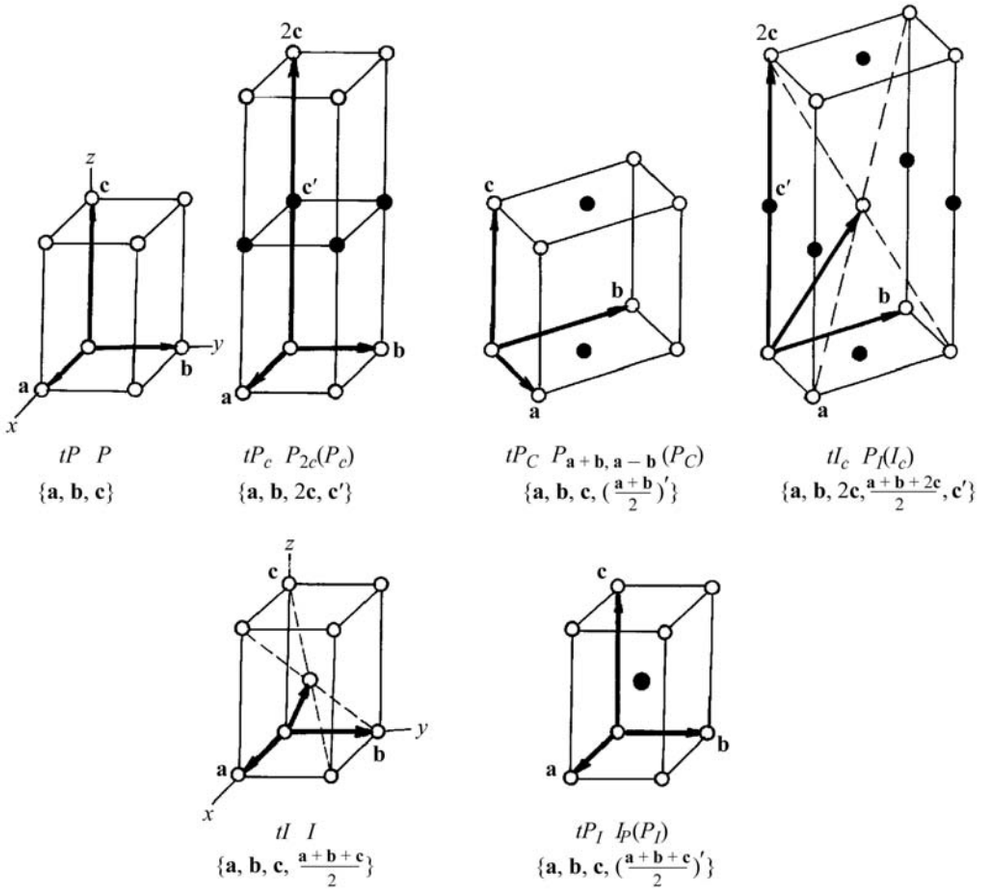

Fig. 1.5.2.4. Magnetic lattices of the tetragonal system.

of the magnetic ions located in the black sites and the other of the ions located in the white sites. All the magnetic moments of one sublattice are oriented in one direction and those of the other sublattice in the opposite direction. However, antiferromagnetism is allowed also in trivial lattices if the (trivial) magnetic cell contains more than one magnetic ion. The magnetic point group must be nontrivial in this case. The situation is more complicated in case of strongly non-collinear structures. In such structures (triangle, 90° *etc.*), the magnetic lattice can differ from the crystallographic one despite the fact that none of the translations is multiplied by *R*. The magnetic elementary cell will possess three or four magnetic ions although the crystallographic cell possesses only one. An example of such a situation is shown in Fig. 1.5.1.3(*c*). More complicated structures in which the magnetic lattice is incommensurate with the crystallographic one also exist. We shall not discuss the problems of such systems in this chapter.

1.5.2.3. *Magnetic space groups*

There are 1651 magnetic space groups $\mathcal{M}_G$, which can be divided into three types. Type I, $\mathcal{M}_{G1}$, consists of the 230 crystallographic space groups to which *R* is added. Crystals belonging to these trivial magnetic space groups show no magnetic order; they are para- or diamagnetic.

Type II, $\mathcal{M}_{G2}$, consists of the same 230 crystallographic groups which do not include *R* in any form. In the ordered magnetics, which belong to the magnetic space groups of this type, the

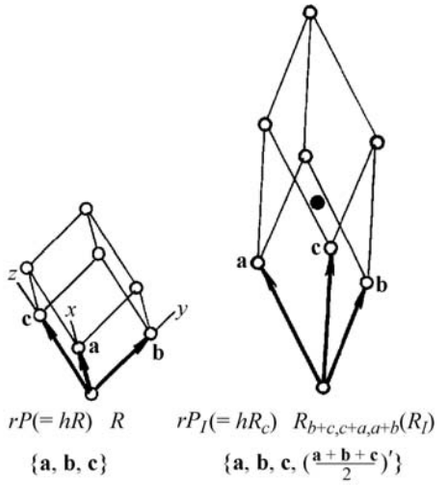

Fig. 1.5.2.5. Magnetic lattices of the rhombohedral system.

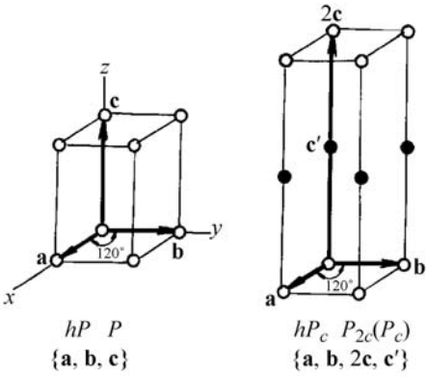

Fig. 1.5.2.6. Magnetic lattices of the hexagonal system.

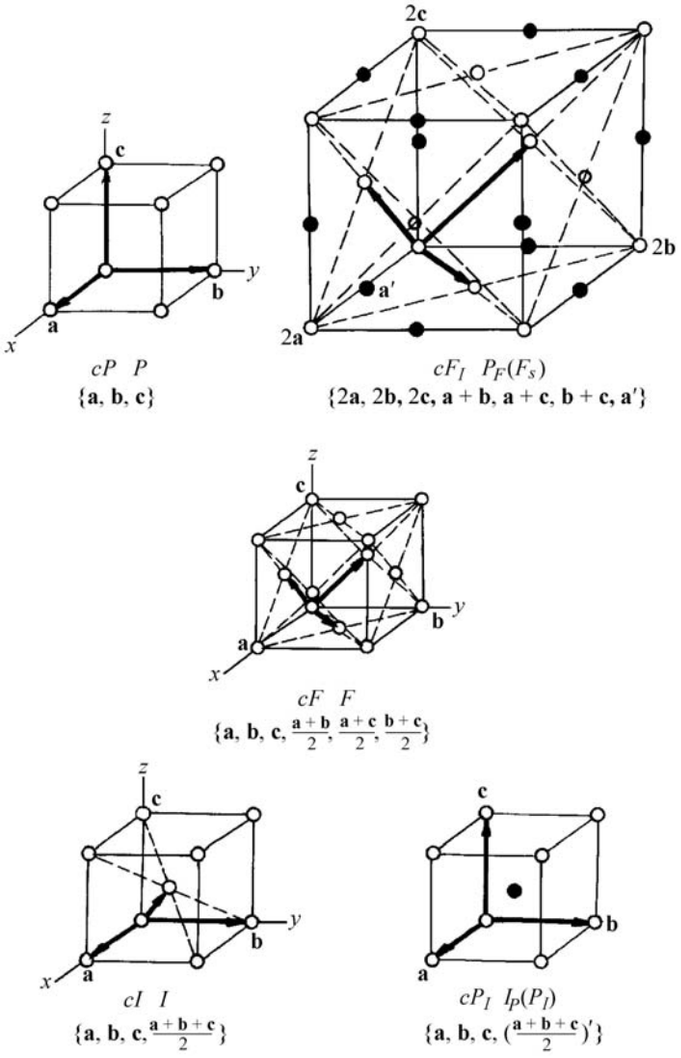

Fig. 1.5.2.7. Magnetic lattices of the cubic system.

magnetic unit cell coincides with the classical one. Forty-four groups of type II describe different ferromagnetic crystals; the remaining antiferromagnets.

The nontrivial magnetic space groups belong to type III, $\mathcal{M}_{G3}$. This consists of 1191 groups, in which R enters only in combination with rotations, reflections or translations. These groups have the structure described by relation (1.5.2.2). The magnetic space groups of this type are divided into two subtypes.

Subtype III^a contains those magnetic space groups $\mathcal{M}_{G3}$ in which R is not combined with translations. In these groups, the magnetic translation group is trivial. To these space groups correspond magnetic point groups of type $\mathcal{M}_{P3}$. There are 674 magnetic space groups of subtype III^a; 231 of them admit ferromagnetism, the remaining 443 describe antiferromagnets.

In the magnetic space groups of the subtype III^b, R is combined with translations and the corresponding point groups are of type $\mathcal{M}_{P1}$. They have a nontrivial magnetic Bravais lattice. There are 517 magnetic space groups of this subtype; they describe antiferromagnets.

In summary, the 230 magnetic space groups that describe dia- and paramagnets are of type I, the 275 that admit spontaneous magnetization are of types II and III^a; the remaining 1146 magnetic space groups (types II, III^a and III^b) describe antiferromagnets.

1.5.2.4. *Exchange symmetry*

The classification of magnetic structures on the basis of the magnetic (point and space) groups is an exact classification. However, it neglects the fundamental role of the exchange energy, which is responsible for the magnetic order (see Sections 1.5.1.2 and 1.5.3.2). To describe the symmetry of the magnetically ordered crystals only by the magnetic space groups means the loss of significant information concerning those properties of these materials that are connected with the higher symmetry of the exchange forces. Andreev & Marchenko (1976, 1980) have introduced the concept of exchange symmetry.

The exchange forces do not depend on the directions of the spins (magnetic moments) of the ions relative to the crystallographic axes and planes. They depend only on the relative directions of the spins. Thus the exchange group $\mathcal{G}_{\rm ex}$ contains an infinite number of rotations U of spin space, *i.e.* rotations of all the spins (magnetic moments) through the same angle about the same axis. The components of the magnetic moment density $\mathbf{m}(\mathbf{r})$ transform like scalars under all rotations of spin space. The exchange symmetry group $\mathcal{G}_{\rm ex}$ contains those combinations of the space transformation elements, the rotations U of spin space and the element R with respect to which the values $m(\mathbf{r})$ are invariant. Setting all the elements U and R equal to the identity transformation, we obtain one of the ordinary crystallographic space groups $\mathcal{G}$. This space group defines the symmetry of the charge density $\rho(\mathbf{r})$ and of all the magnetic scalars in the crystal. However, the vectors $\mathbf{m}(\mathbf{r})$ may not be invariant with respect to $\mathcal{G}$.

The concept of exchange symmetry makes it possible to classify all the magnetic structures (including the incommensurate ones) with the help of not more than three orthogonal magnetic vectors. We shall discuss this in more detail in Section 1.5.3.3.

More information about magnetic symmetry can be found in Birss (1964), Cracknell (1975), Joshua (1991), Koptsik (1966), Landau & Lifshitz (1957), Opechowski & Guccione (1965), and in Sirotin & Shaskol'skaya (1979).

1.5.3. Phase transitions into a magnetically ordered state

Most transitions from a paramagnetic into an ordered magnetic state are second-order phase transitions. A crystal with a given crystallographic symmetry can undergo transitions to different ordered states with different magnetic symmetry. In Section 1.5.3.3, we shall give a short review of the theory of magnetic second-order phase transitions. As was shown by Landau (1937), such a transition causes a change in the magnetic symmetry. The magnetic symmetry group of the ordered state is a subgroup of the magnetic group of the material in the paramagnetic state. But first we shall give a simple qualitative analysis of such transitions.

To find out what ordered magnetic structures may be obtained in a given material and to which magnetic group they belong, one has to start by considering the crystallographic space group $\mathcal{G}$ of the crystal under consideration. It is obvious that a crystal in which the unit cell contains only one magnetic ion can change only into a ferromagnetic state if the magnetic unit cell of the ordered state coincides with the crystallographic one. If a transition into an antiferromagnetic state occurs, then the magnetic cell in the ordered state will be larger than the crystallographic one if the latter contains only one magnetic ion. Such antiferromagnets usually belong to the subtype III^b described in Section 1.5.2.3. In Section 1.5.3.1, we shall consider crystals that transform into an antiferromagnetic state without change of the unit cell. This is possible only if the unit cell possesses two or more magnetic ions. To find the possible magnetic structures in this case, one has to consider those elements of symmetry which interchange the positions of the ions inside the unit cell (especially glide planes and rotation axes). Some of these elements displace the magnetic ion without changing its magnetic moment, and others change the moment of the ion. It is also essential to know the positions of all these elements in the unit cell. All this information is contained in the space group $\mathcal{G}$. If the magnetic ordering occurs without change of the unit cell, the translation

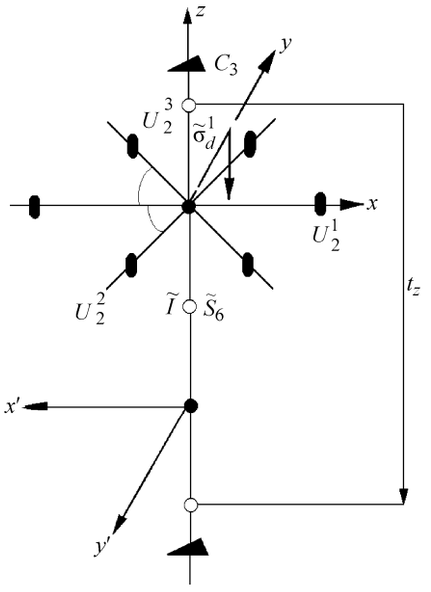

Fig. 1.5.3.1. Arrangement of the symmetry elements of the group $\widetilde{\boldsymbol{D}}^6_{3d}$.

group $\mathcal{T}$ in the ordered state does not contain primed elements. Therefore, there is no need to consider the whole crystal space group $\mathcal{G}$. It will suffice to consider the cosets of $\mathcal{T}$ in $\mathcal{G}$. Such a coset consists of all elements of $\mathcal{G}$ that differ only by a translation. From each coset, a representative with minimum translative component is chosen. We denote a set of such representatives by $\widetilde{\mathcal{G}}$; it can be made into a group by defining AB $(A, B \in \widetilde{\mathcal{G}})$ as the representative of the coset that contains AB. Obviously, $\widetilde{\mathcal{G}}$ is then isomorphic to the factor group $\mathcal{G}/\mathcal{T}$ and therefore to the point group $\mathcal{P}$ of $\mathcal{G}$.

Once more, we should like to stress that to construct the magnetic structures and the magnetic groups of a given crystal it is not enough to consider only the point group of the crystal, but it is necessary to perform the analysis with the help of its space group in the paramagnetic state or the corresponding group of coset representatives. An example of such an analysis will be given in the following section.

1.5.3.1. *Magnetic structures in rhombohedral crystals*

Following Dzyaloshinskii (1957*a*), we consider crystals belonging to the crystallographic space group $\boldsymbol{D}^6_{3d} = R\bar{3}c$. To this group belong α-Fe_2O_3 and the carbonates of Mn^{2+}, Co^{2+} and Ni^{2+}. Weak ferromagnetism was first observed in these materials.

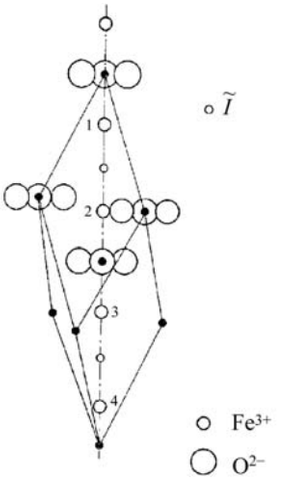

Fig. 1.5.3.2. Crystallographic structure of transition-metal oxides of the type α-Fe_2O_3.

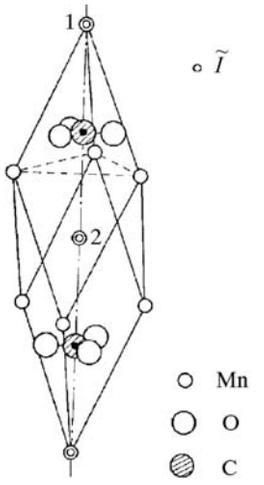

Fig. 1.5.3.3. Crystallographic structure of transition-metal carbonates of the type $MnCO_3$.

Cr_2O_3, in which the magnetoelectric effect was discovered, also belongs to this group. The magnetic ordering in these materials occurs without change of the unit cell.

The representatives of the cosets $\boldsymbol{D}^6_{3d}/\mathcal{T}$ form the group $\widetilde{\boldsymbol{D}}^6_{3d}$. Its symmetry operations are shown in Fig. 1.5.3.1. Directed along the z axis is the threefold axis C_3 and the sixfold roto-inversion axis $\tilde{S}_6$. Three twofold axes U_2 run through the points • at right angles to the z axis. One of these axes is directed along the x axis. Arranged normal to each of the U_2 axes are three glide planes $\tilde{\sigma}_d$. The y axis is directed along one of these planes. The centre of inversion $\tilde{I}$ is located at the point ○, lying on the z axis halfway between two points •. The sign ˜ means that the corresponding operation is accompanied by a translation along the z axis through half the period of the crystal ($\tilde{I}$ means that the inversion centre is shifted from the point • to the point ○). In Fig. 1.5.3.1, the elementary period of translation along the z axis is marked by t_z. Thus the crystallographic group $\widetilde{\boldsymbol{D}}^6_{3d}$ has the following elements:

$$E, 2C_3, 3U_2, \tilde{I}, 3\tilde{\sigma}_d, 2\tilde{S}_6 \quad \{1, \pm 3_z, 3(2_\perp), \tilde{\bar{1}}, 3(c = \tilde{m}), \pm\tilde{\bar{3}}_z\}. \tag{1.5.3.1}$$

In two types of crystals, considered below, the magnetic ions are arranged on the z axis. If we place the magnetic ion at point 1 located between points ○ and • (see Fig. 1.5.3.2), then using symmetry operations (1.5.3.1) we obtain three additional positions for other magnetic ions (points 2, 3, 4). Thus, the elementary cell will contain four magnetic ions. This is the structure of oxides of trivalent ions of iron and chromium (Fe_2O_3, Cr_2O_3). The structure of these oxides is shown in Fig. 1.5.3.2. If the positions of the magnetic ions coincide with the positions of the inversion centre ○, we obtain the structure of the carbonates of the transition metals ($MnCO_3$, $CoCO_3$, $NiCO_3$, $FeCO_3$), which is shown in Fig. 1.5.3.3.

Evidently, the formation of a magnetic structure in the crystal does not result in the appearance of new elements of symmetry. The magnetic groups of magnetically ordered crystals may lack some elements contained in the crystallographic group and some of the remaining elements may happen to be multiplied by R (primed). Let us find the groups of symmetry that correspond to all possible collinear magnetic structures in rhombohedral crystals with four magnetic ions in the elementary cell. We shall assume that the magnetic moments are located at the points of the ion positions 1–4; they will be marked $\boldsymbol{\mu}_\alpha$. The symmetry transformations cannot change the length of the vectors of the magnetic moments but they can change the direction of these vectors and interchange the positions of the sites $1 \leftrightarrow 2$, $3 \leftrightarrow 4$

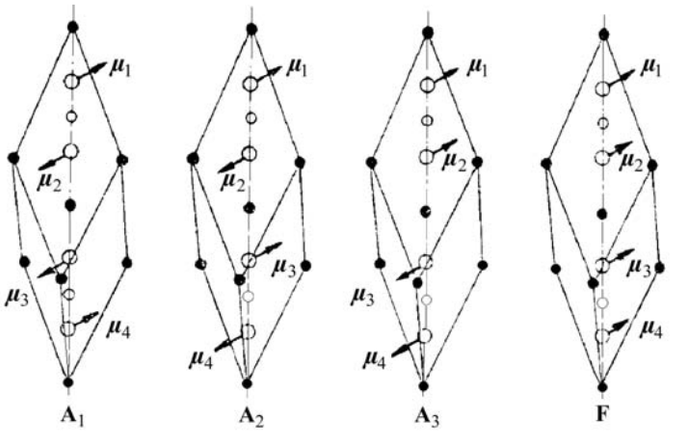

Fig. 1.5.3.4. Four types of magnetic structures of rhombohedral oxides of transition metals. The direction of $\boldsymbol{\mu}_\alpha$ is shown conventionally.

and $1 \leftrightarrow 3$, $2 \leftrightarrow 4$. This interchange of the vectors $\boldsymbol{\mu}_1, \boldsymbol{\mu}_2, \boldsymbol{\mu}_3, \boldsymbol{\mu}_4$ means that these vectors form a basis of a reducible representation of the group $\widetilde{\boldsymbol{D}}^6_{3d}$. The following linear combinations of $\boldsymbol{\mu}_\alpha$ form irreducible representations[1] of $\widetilde{\boldsymbol{D}}^6_{3d}$:

$$\begin{aligned}
\mathbf{l}_1 &= \boldsymbol{\mu}_1 - \boldsymbol{\mu}_2 - \boldsymbol{\mu}_3 + \boldsymbol{\mu}_4 \\
\mathbf{l}_2 &= \boldsymbol{\mu}_1 - \boldsymbol{\mu}_2 + \boldsymbol{\mu}_3 - \boldsymbol{\mu}_4 \\
\mathbf{l}_3 &= \boldsymbol{\mu}_1 + \boldsymbol{\mu}_2 - \boldsymbol{\mu}_3 - \boldsymbol{\mu}_4 \\
\mathbf{m} &= \boldsymbol{\mu}_1 + \boldsymbol{\mu}_2 + \boldsymbol{\mu}_3 + \boldsymbol{\mu}_4. \qquad (1.5.3.2)
\end{aligned}$$

Vectors $\mathbf{l}_\alpha$ characterize the antiferromagnetic states and are called antiferromagnetic vectors. The ferromagnetic vector $\mathbf{m}$ gives the total magnetic moment of the elementary cell. These vectors describe the four possible collinear magnetic structures. Three are antiferromagnetic structures: $\boldsymbol{A}_1$ ($\mathbf{l}_1 \neq 0$, $\mathbf{l}_2 = \mathbf{l}_3 = \mathbf{m} = 0$), $\boldsymbol{A}_2$ ($\mathbf{l}_2 \neq 0$, $\mathbf{l}_3 = \mathbf{l}_1 = \mathbf{m} = 0$), $\boldsymbol{A}_3$ ($\mathbf{l}_3 \neq 0$, $\mathbf{l}_1 = \mathbf{l}_2 = \mathbf{m} = 0$) and one is a ferromagnetic structure, $\boldsymbol{F}$ ($\mathbf{l}_1 = \mathbf{l}_2 = \mathbf{l}_3 = 0$). All these types are presented schematically in Fig. 1.5.3.4.

In the description of the structures of orthoferrites, other symbols were introduced to define the linear combinations of $\boldsymbol{\mu}_\alpha$ and to denote the antiferromagnetic structures under consideration (see Bertaut, 1963). The two types of symbols are compared in Table 1.5.3.1.

It should be borne in mind that in each of these types of magnetic ordering the respective vectors $\mathbf{l}_\alpha$ and $\mathbf{m}$ may be directed along any direction. There are 12 types of such structures in which $\mathbf{l}_\alpha$ or $\mathbf{m}$ are directed along one of the axes or planes of symmetry. To find out to which group of magnetic symmetry each of these structures belongs, one needs to investigate how each element of the crystallographic symmetry transforms the Cartesian components of the four vectors. This is shown in Table 1.5.3.2 for the group $\widetilde{\boldsymbol{D}}^6_{3d}$. If the component keeps its direction, it is marked by the + sign; the − sign corresponds to reversal of the component direction. In some cases, the transformation results in a change of the direction of the components $l_{\alpha i}$ or m_i through an angle other than 0 or π. This is marked by 0. With the help of Table 1.5.3.2, we can easily describe all the elements of symmetry of the magnetic group that corresponds to each structure ($\boldsymbol{A}_{\alpha i}$ or $\boldsymbol{F}_i$) with the aid of the following rule. All the elements that yield the + sign are included in the magnetic group as they stand, while the elements yielding the − sign must be multiplied by R; the elements which are marked by the sign 0 are not included in the magnetic group.[2] With the aid of this rule, Table 1.5.3.3 of the elements of the magnetic groups for the structures under consideration was compiled. In Table 1.5.3.4, the symbols of the magnetic point groups of all the 12 magnetic structures considered are listed. The crystals with two ions in the elementary cell have only two sublattices and their antiferromagnetic structures belong to the same groups as the structures $\boldsymbol{A}_{3i} = \boldsymbol{C}_i$.

Table 1.5.3.1. *Two types of symbols for collinear antiferromagnetic and ferromagnetic structures*

Symbol	Alternative symbol
$\boldsymbol{A}_1$	$\boldsymbol{A}$
$\boldsymbol{A}_2$	$\boldsymbol{G}$
$\boldsymbol{A}_3$	$\boldsymbol{C}$
$\boldsymbol{F}$	$\boldsymbol{F}$

One can see from Tables 1.5.3.3 and 1.5.3.4 that, in accordance with general theory, the magnetic point groups of the crystals under consideration are subgroups of the trivial magnetic point group $\boldsymbol{D}_{3dR} = \bar{3}m1'$ to which they belong in the paramagnetic state. In the example considered, the translation group does not change in going from the paramagnetic to the ordered state. Thus the same statement made for the point groups is also true for the space groups. Putting $R = E$ gives a subgroup of the crystallographic group of the crystal. For the magnetic structures with the ferromagnetic or antiferromagnetic vector directed along the z axis, it turns out that the magnetic group is isomorphic to the crystallographic group. This rule is obeyed by all (optically) uniaxial crystals if the transition occurs without change of the elementary cell. (Optically uniaxial are the non-cubic crystals with a point group possessing a threefold, fourfold or sixfold axis.)

Tables 1.5.3.3 and 1.5.3.4 show that different types of collinear structures may belong to the same point group (and also to the same space group). For the antiferromagnetic structure $\boldsymbol{A}_{3y}$ and the ferromagnetic $\boldsymbol{F}_x$ the group is $2/m$, and for the structures $\boldsymbol{A}_{3x}$ and $\boldsymbol{F}_y$ it is $2'/m'$. Thus the symmetry allows a phase to be simultaneously ferromagnetic and antiferromagnetic. That is not ferrimagnetic order because all the ions in the four sublattices are identical and their numbers are equal. The ferromagnetic vector $\mathbf{m}$ and the antiferromagnetic one $\mathbf{l}_3$ are perpendicular and $|\mathbf{m}| \ll |\mathbf{l}_3|$. This phenomenon is called weak ferromagnetism and will be discussed in detail in Section 1.5.5.1. Like weak ferromagnetism, the symmetry also allows the coexistence of two orthogonal antiferromagnetic structures $\boldsymbol{A}_1$ and $\boldsymbol{A}_2$. This gives rise to weakly non-collinear antiferromagnetic structures.

The strongly non-collinear structures are described by another set of basis vectors for the irreducible representations of the group $\tilde{\mathcal{G}}$. If the magnetic ions $\boldsymbol{\mu}_\alpha$ in the crystal form triangular planes one gets instead of (1.5.3.2) the relations for the basis vectors:

$$\begin{aligned}
\mathbf{l}_1 &= \sqrt{3}(\boldsymbol{\mu}_1 - \boldsymbol{\mu}_2) \\
\mathbf{l}_2 &= \boldsymbol{\mu}_1 + \boldsymbol{\mu}_2 - \boldsymbol{\mu}_3 \qquad (1.5.3.3) \\
\mathbf{m} &= \boldsymbol{\mu}_1 + \boldsymbol{\mu}_2 + \boldsymbol{\mu}_3.
\end{aligned}$$

1.5.3.2. *Exchange and magnetic anisotropy energies*

It is pertinent to compare the different kinds of interactions that are responsible for magnetic ordering. In general, all these interactions are much smaller than the electrostatic interactions between the atoms that determine the chemical bonds in the material. Therefore, if a crystal undergoes a transition into a magnetically ordered state, the deformations of the crystal that

[1] By omitting its translative part, each element of $\widetilde{\boldsymbol{D}}^6_{3d}$ is mapped on the corresponding element of the point group $\boldsymbol{D}_{3d} = \bar{3}m$. This mapping also establishes a one-to-one correspondence between the representations of $\widetilde{\boldsymbol{D}}^6_{3d}$ and those of $\boldsymbol{D}_{3d} = \bar{3}m$.

[2] In Section 1.5.3.3, we shall show that this rule corresponds in the Landau theory of phase transitions to the general law that the magnetically ordered state is described by $L_{\alpha i}$ or M_i, which form the basis of one of the irreducible representations of the paramagnetic space group of the crystal.

Table 1.5.3.2. *Sign variation of the components of antiferromagnetic and ferromagnetic vectors during transformations of the group $\widetilde{\boldsymbol{D}}^6_{3d}$ in rhombohedral crystals with four magnetic ions*

Vector components	Elements of symmetry									
	E	$2C_3$	U_2^1	U_2^2	U_2^3	$\tilde{I}$	$\tilde{\sigma}_d^1$	$\tilde{\sigma}_d^2$	$\tilde{\sigma}_d^3$	$2\tilde{S}_6$
	1	$\pm 3_z$	2_x	$2_\perp^{(2)}$	$2_\perp^{(3)}$	$\tilde{\bar{1}}$	c_x	$c_\perp^{(2)}$	$c_\perp^{(3)}$	$\pm\tilde{\bar{3}}$
l_{1x}	+	0	+	0	0	−	−	0	0	0
l_{1y}	+	0	−	0	0	−	+	0	0	0
l_{1z}	+	+	−	−	−	−	+	+	+	−
l_{2x}	+	0	−	0	0	−	+	0	0	0
l_{2y}	+	0	+	0	0	−	−	0	0	0
l_{2z}	+	+	+	+	+	−	−	−	−	−
l_{3x}	+	0	−	0	0	+	−	0	0	0
l_{3y}	+	0	+	0	0	+	+	0	0	0
l_{3z}	+	+	+	+	+	+	+	+	+	+
m_x	+	0	+	0	0	+	+	0	0	0
m_y	+	0	−	0	0	+	−	0	0	0
m_z	+	+	−	−	−	+	−	−	−	+

give rise to the change of its crystallographic symmetry are comparatively small. It means that most of the non-magnetic properties do not change drastically. As an example, the anisotropic deformation of the crystal that accompanies the transition into the ordered state (see Section 1.5.9.1) is mostly not larger than 10^{-4}.

The formation of the ordered magnetic structures is due mainly to the exchange interaction between the spins $\mathbf{S}_\alpha$ (and corresponding magnetic moments $\boldsymbol{\mu}$ of the atoms or ions). The expression for the exchange energy can contain the following terms [see formula (1.5.1.7)]:

$$\mathbf{S}_\alpha\mathbf{S}_\beta,\ \ \mathbf{S}_\alpha[\mathbf{S}_\beta\mathbf{S}_\gamma]. \tag{1.5.3.4}$$

The exchange interaction decreases rapidly as the distance between the atoms rises. Thus, it is usually sufficient to consider the interaction only between nearest neighbours. The exchange interaction depends only on the relative alignment of the spin moments and does not depend on their alignment relative to the crystal lattice. Therefore, being responsible for the magnetic ordering in the crystal, it cannot define the direction of the spontaneous magnetization in ferromagnets or of the antiferromagnetic vector. This direction is determined by the spin–orbit and magnetic spin–spin interactions, which are often called relativistic interactions as they are small, of the order of v^2/c^2, where v is the velocity of atomic electrons and c is the speed of light. The relativistic interactions are responsible for the magnetic anisotropy energy, which depends on the direction of the magnetic moments of the ions with regard to the crystal lattice. The value of the exchange energy can be represented by the effective exchange field H_e. For an ordered magnetic with a transition temperature of 100 K, $H_e \simeq 1000$ kOe. Thus the external magnetic field hardly changes the value of the magnetization **M** or of the antiferromagnetic vector **L**; they are conserved quantities to a good approximation. The effective anisotropy field H_a in cubic crystals is very small: 1–10 Oe. In most non-cubic materials, H_a is not larger than 1–10 kOe. This means that by applying an external magnetic field we can change only the direction of **M**, or sometimes of **L**, but not their magnitudes.

The magnetic anisotropy energy U_a can be represented as an expansion in the powers of the components of the vectors **M** or **L**. The dependence of U_a on the direction of the magnetization is essential. Therefore, one usually considers the expansion of the spontaneous magnetization or antiferromagnetic vector in powers of the unit vector **n**. The anisotropy energy is invariant under time reversal. Therefore, the general expression for this energy has the form

$$U_a = K_{ij}n_in_j + K_{ijk\ell}n_in_jn_kn_\ell + K_{ijk\ell mn}n_in_jn_kn_\ell n_mn_n, \tag{1.5.3.5}$$

where K_{ij}, $K_{ijk\ell}$, $K_{ijk\ell mn}$ are tensors, the components of which have the dimension of an energy density. The forms of the tensors depend on the symmetry of the crystal. There are at most two independent components in K_{ij}. For a uniaxial crystal, the second-order term in the anisotropy energy expansion is determined by one anisotropy constant, K. Instead of using the components of the unit vector **n**, its direction can be described by two angles: polar θ and azimuthal φ. Correspondingly, the anisotropy energy for a uniaxial crystal can be written as

$$U_a = K(n_x^2 + n_y^2) = K\sin^2\theta. \tag{1.5.3.6}$$

This relation is equivalent to

$$U_a = K(1 - n_z^2) = K - K\cos^2\theta. \tag{1.5.3.7}$$

The direction of the magnetization vector **M** in a ferromagnet or of the antiferromagnetic vector **L** in an antiferromagnet is called the direction or the axis of easy magnetization. The crystals in which this axis is aligned with a threefold, fourfold or sixfold axis of the magnetic point group are called easy-axis magnetics. The magnetic crystals with the main axis higher than twofold in the paramagnetic state in which, in the ordered state, **L** (or **M**) is perpendicular to this axis are often called easy-plane magnetics. The anisotropy in this plane is usually extremely small. In this case, the crystal possesses more then one axis of easy magnetization and the crystal is usually in a multidomain state (see Section 1.5.4).

If the anisotropy constant K is positive, then the vector **n** is aligned along the z axis, and such a magnetic is an easy-axis one.

Table 1.5.3.3. *Magnetic groups of symmetry in rhombohedral oxides of trivalent transition-metal ions*

Type of magnetic structure	Magnetic moments are directed along the axis		
	x	y	z
$\boldsymbol{A}_1 = \boldsymbol{A}$	E; U_2; $\tilde{I}R$; $\tilde{\sigma}_dR$	E; U_2R; $\tilde{I}R$; $\tilde{\sigma}_d$	E; $2C_3$; $3U_2R$; $\tilde{I}R$; $3\tilde{\sigma}_d$; $2\tilde{S}_6R$
$\boldsymbol{A}_2 = \boldsymbol{G}$	E; U_2R; $\tilde{I}R$; $\tilde{\sigma}_d$	E; U_2; $\tilde{I}R$; $\tilde{\sigma}_dR$	E; $2C_3$; $3U_2$; $\tilde{I}R$; $3\tilde{\sigma}_dR$; $2\tilde{S}_6R$
$\boldsymbol{A}_3 = \boldsymbol{C}$	E; U_2R; $\tilde{I}$; $\tilde{\sigma}_dR$	E; U_2; $\tilde{I}$; $\tilde{\sigma}_d$	E; $2C_3$; $3U_2$; $\tilde{I}$; $3\tilde{\sigma}_d$; $2\tilde{S}_6$
$\boldsymbol{F} = \boldsymbol{F}$	E; U_2; $\tilde{I}$; $\tilde{\sigma}_d$	E; U_2R; $\tilde{I}$; $\tilde{\sigma}_dR$	E; $2C_3$; $3U_2R$; $\tilde{I}$; $3\tilde{\sigma}_dR$; $2\tilde{S}_6$

Table 1.5.3.4. *Magnetic point groups in rhombohedral oxides of transition metals*

Type of magnetic structure	Magnetic moments are directed along the axis		
	x	y	z
$\boldsymbol{A}_1 = \boldsymbol{A}$	$\boldsymbol{C}_{2h}(\boldsymbol{C}_2) = 2/m'$	$\boldsymbol{C}_{2h}(\boldsymbol{C}_s) = 2'/m$	$\boldsymbol{D}_{3d}(\boldsymbol{C}_{3v}) = \bar{3}'m$
$\boldsymbol{A}_2 = \boldsymbol{G}$	$\boldsymbol{C}_{2h}(\boldsymbol{C}_s) = 2'/m$	$\boldsymbol{C}_{2h}(\boldsymbol{C}_2) = 2/m'$	$\boldsymbol{D}_{3d}(\boldsymbol{D}_3) = \bar{3}'m'$
$\boldsymbol{A}_3 = \boldsymbol{C}$	$\boldsymbol{C}_{2h}(\boldsymbol{C}_i) = 2'/m'$	$\boldsymbol{C}_{2h} = 2/m$	$\boldsymbol{D}_{3d} = \bar{3}m$
$\boldsymbol{F} = \boldsymbol{F}$	$\boldsymbol{C}_{2h} = 2/m$	$\boldsymbol{C}_{2h}(\boldsymbol{C}_i) = 2'/m'$	$\boldsymbol{D}_{3d}(\boldsymbol{S}_6) = \bar{3}m'$

For an easy-plane magnetic, K is negative. It is convenient to use equation (1.5.3.6) for easy-axis magnetics and equation (1.5.3.7) for easy-plane magnetics. In the latter case, the quantity K is included in the isotropic part of the thermodynamic potential Φ, and (1.5.3.7) becomes $U_a = -K\cos^2\theta$. Instead we shall write $U_a = K\cos^2\theta$ in the following, so that K becomes positive for easy-plane ferromagnetics as well.

Apart from the second-order term, terms of higher order must be taken into account. For tetragonal crystals, the symmetry allows the following invariant terms in the anisotropy energy:

$$\begin{aligned} U_a(4) &= K_1(n_x^2 + n_y^2) + K_2(n_x^2 + n_y^2)^2 + K_{xxyy}n_x^2 n_y^2 \\ &= K_1\sin^2\theta + K_2\sin^4\theta + K_\perp\sin^4\theta\sin^2 2\varphi; \end{aligned} \tag{1.5.3.8}$$

the azimuthal angle φ is measured from the twofold axis x in the basal plane and the constant $K_\perp$ determines the anisotropy in the basal plane.

Trigonal symmetry also allows second- and fourth-order invariants:

$$\begin{aligned} U_a(3) &= K_1(n_x^2 + n_y^2) + K_2(n_x^2 + n_y^2)^2 \\ &\quad + K'_\perp \tfrac{1}{2} n_z[(n_x + in_y)^3 + (n_x - in_y)^3] \\ &= K_1\sin^2\theta + K_2\sin^4\theta + K'_\perp\cos\theta\sin^3\theta\cos 3\varphi, \end{aligned} \tag{1.5.3.9}$$

where φ is measured from the x axis, which is chosen parallel to one of the twofold axes. For easy-plane magnetics and $K'_\perp > 0$, the vector **n** is directed along one of the twofold axes in the basal plane. If $K'_\perp$ is negative, then **n** lies in a vertical mirror plane directed at a small angle to the basal plane. For the complete solution of this problem, the sixth-order term must be taken into account. This term is similar to the one that characterizes the anisotropy of hexagonal crystals. The expression for the latter is of the following form:

$$\begin{aligned} U_a(6) &= K_1(n_x^2 + n_y^2) + K_2(n_x^2 + n_y^2)^2 \\ &\quad + K''_\perp \tfrac{1}{2}[(n_x + in_y)^6 + (n_x - in_y)^6] \\ &= K_1\sin^2\theta + K_2\sin^4\theta + K''_\perp\sin^6\theta\cos 6\varphi, \end{aligned} \tag{1.5.3.10}$$

where x and φ have the same meaning as in (1.5.3.9).

The symmetry of cubic crystals does not allow any second-order terms in the expansion of the anisotropy energy. The expression for the anisotropy energy of cubic crystals contains the following invariants:

$$U_a(\text{cub}) = K_1(n_x^2 n_y^2 + n_x^2 n_z^2 + n_y^2 n_z^2) + K_2 n_x^2 n_y^2 n_z^2. \tag{1.5.3.11}$$

In considering the anisotropy energy, one has to take into account spontaneous magnetostriction and magnetoelastic energy (see Section 1.5.9). This is especially important in cubic crystals. Any collinear cubic magnetic (being brought into a single domain state) ceases to possess cubic crystallochemical symmetry as a result of spontaneous magnetostriction. If K_1 is positive, the easy axis is aligned along one of the edges of the cube and the crystal becomes tetragonal (like Fe). If K_1 is negative, the crystal becomes rhombohedral and can be an easy-axis magnetic with vector **n** parallel to one of the spatial diagonals (like Ni) or an easy-plane magnetic with **n** perpendicular to a spatial diagonal. We shall discuss this topic in more detail in Section 1.5.9.3.

The considerations presented above can be applied to all crystals belonging in the paramagnetic state to the tetragonal, trigonal or hexagonal system that become easy-plane magnetics in the ordered state. All of them, including the cubic crystals, may possess more than one allowed direction of easy magnetization. In the example considered in the previous section, these directions can be aligned along the three twofold axes for the structures A_1^x, A_2^x, A_3^x, F^x and can be parallel to the three mirror planes for A_1^y, A_2^y, A_3^y, F^y.

It is worth noting that in some applications it is more convenient to use an expansion of the anisotropy energy in terms of surface spherical harmonics. This problem has been considered in detail by Birss (1964).

1.5.3.3. *The thermodynamic theory of transitions into a magnetically ordered state*

According to Landau (1937) (see also Landau & Lifshitz, 1951), a phase transition of the second kind can be described by an order parameter η, which varies smoothly in the neighbourhood of the transition temperature T_c. The order parameter $\eta = 0$ when $T \geq T_c$ and rises continuously as the temperature is decreased below T_c, but the symmetry of the crystal changes suddenly. The order parameter can be a scalar, a vector or a tensor.

Consider a crystal with known space group in the paramagnetic state. In this section, we show how the Landau theory allows us to determine the magnetic space groups that are possible after a second-kind phase transition into an ordered state. The application of the Landau theory to the magnetic transitions into different types of antiferromagnets was made by Dzyaloshinskii (1957*a*,*c*; 1964). In these cases, the order parameter is the magnetic moment density $\mathbf{m}(\mathbf{r})$. To determine the equilibrium form of this function, it is necessary to find the minimum of the thermodynamic potential Φ, which is a functional of $\mathbf{m}(\mathbf{r})$. Since the transition is continuous and $\mathbf{m}(\mathbf{r}) = 0$ for $T \geq T_c$, the value of $\mathbf{m}(\mathbf{r})$ must be very small in the neighbourhood below the transition point. In this region, the thermodynamic potential Φ will be expanded into a power series of $\mathbf{m}(\mathbf{r})$. To find the proper form of this expansion, it is convenient to represent $\mathbf{m}(\mathbf{r})$ as a linear combination of functions that form bases of the irreducible representations of the space group of the paramagnetic phase $\mathcal{M}_\mathcal{G}$:

$$m^i(\mathbf{r}) = \sum_{n,\alpha} M^i_{n,\alpha}\varphi_{n,\alpha}(\mathbf{r}), \tag{1.5.3.12}$$

where $\varphi_{n,\alpha}(\mathbf{r})$ are functions that transform under the representation n (α is the number of the function in the representation) and $i = x, y, z$. In this expansion, the quantities $M^i_{n,\alpha}$ are independent of $\mathbf{r}$ and transform with respect to i as the components of an axial vector. The functions $\varphi_{n,\alpha}(\mathbf{r})$ are transformed into combinations of one another by the elements of the group $\mathcal{M}_\mathcal{G}$. Instead, these elements can be regarded as transforming the coefficients $M^i_{n,\alpha}$ and leaving the functions $\varphi_{n,\alpha}$ invariant. In this case, the quantities $M^i_{n,\alpha}$ transform according to the direct product of the representation n of $\mathcal{M}_\mathcal{G}$ and the representation formed by the components of the pseudovector. This representation is reducible in the general case. Irreducible representations $p, q, \ldots$ can be obtained by forming linear combinations of the $M^i_{n,\alpha}$. Let us denote these combinations by $c_{p,\alpha}, c_{q,\alpha}, \ldots$. These variables can be considered as components of the order parameter, and the thermodynamic potential can be expanded into a power series of $c_{p,\alpha}$. The terms of this expansion must be invariant under the transformations of the magnetic space group of the crystal in the paramagnetic state $\mathcal{M}_\mathcal{G}$. This group possesses R as a separate element. Therefore the expansion can contain only even terms. For each irreducible representation, there is only one invariant of second order – the sum of the squares. Consequently, retaining only the square terms, the expansion of the thermodynamic potential Φ has the form:

$$\Phi(T) = \Phi_0(T) + \sum_p A_p(T)\sum_\alpha c^2_{p,\alpha}. \tag{1.5.3.13}$$

To minimize Φ, it is necessary to add the terms of the fourth power. All the coefficients $A_p(T)$ in the relation (1.5.3.13) depend on the temperature. At $T \geq T_c$ all $c_{p,\alpha} = 0$. This solution corresponds to the minimum of Φ if all $A_p(T)$ are positive. The transition into the ordered state occurs if one of the quantities $A_p(T)$ changes its sign. This means that the transition temperature T_c is the temperature at which one of the coefficients $A_p(T_c) = 0$. This coefficient has the form:

$$A_p(T) = \lambda(T - T_c). \tag{1.5.3.14}$$

Accordingly, the corresponding magnetic structure is defined by the order parameters $c_{p,\alpha}$ and belongs to the representation p.

The representation of the space group is realized by a set of functions of the following type:

$$\varphi_{\mathbf{k}_\beta}(\mathbf{r}) = u_{\mathbf{k}_\beta}(\mathbf{r}) \exp(i\mathbf{k}_\beta\mathbf{r}), \tag{1.5.3.15}$$

where the values of the vectors $\mathbf{k}$ are confined to the Brillouin zone in the reciprocal lattice and the function $u_{\mathbf{k}_\beta}(\mathbf{r})$ is periodic in the real lattice. The irreducible representation defined by the vector $\mathbf{k}_\beta$ contains the functions with all the vectors $\mathbf{k}_\beta$ that belong to the same star. The star is the set of the vectors $\mathbf{k}_\beta$ obtained by applying all the transformations g_i of the corresponding point group to any vector of the star (see also Section 1.2.3.3). If we denote it as $\mathbf{k}_1$, then the set of the vectors of the star consists of all inequivalent vectors of the form $g_i\mathbf{k}_1$.

There are three types of transition we have to consider: (1) the magnetic lattice is commensurate with the crystallographic one and $\mathbf{k} \neq 0$; (2) the magnetic lattice is incommensurate with the crystallographic one; (3) $\mathbf{k} = 0$ and the magnetic lattice coincides with the crystallographic lattice. Below we shall discuss in detail only the first and the third type of transition.

(a) $\mathbf{k} \neq 0$.

It is found that the first type of transition occurs if the arms of the star $\mathbf{k}_\beta$ are aligned along specific isolated crystallographic directions and its vectors are equal to 1/2, 1/3 or 1/4 of some translation in the reciprocal lattice (Lifshitz, 1942). Then the magnetic structure is described by one of the 22 nontrivial Bravais types of magnetic lattices shown in Figs. 1.5.2.1–1.5.2.7.

As an example, let us consider a magnetic transition in UO_2. In the paramagnetic state, it is a crystal with a face-centred cubic structure (space group $O_h^5 = Fm\bar{3}m$) (for details see Dzyaloshinskii & Man'ko, 1964; Izyumov & Naish, 1979; Izyumov, Naish & Petrov, 1979; Izyumov, Naish & Syromiatnikov, 1979; Barbara *et al.*, 1988). Primitive translations of the crystallographic lattice are (see Fig. 1.5.3.5):

$$\mathbf{a}_1 = (a/2)(0, 1, 1), \quad \mathbf{a}_2 = (a/2)(1, 0, 1), \quad \mathbf{a}_3 = (a/2)(1, 1, 0). \tag{1.5.3.16}$$

Primitive translations of the reciprocal lattice are:

$$\mathbf{b}_1 = (2\pi/a)(-1, 1, 1), \quad \mathbf{b}_2 = (2\pi/a)(1, -1, 1),$$
$$\mathbf{b}_3 = (2\pi/a)(1, 1, -1). \tag{1.5.3.17}$$

Let us assume that there is one magnetic ion in the primitive cell in the position (0, 0, 0) and that the transition takes place over a three-armed star $\{\mathbf{K}_{10}\}$ (for the definition of the symbols of the stars see Kovalev, 1987):

$$\begin{aligned} \mathbf{k}_1 &= (\mathbf{b}_1 + \mathbf{b}_2)/2 = (2\pi/a)(0, 0, 1) \\ \mathbf{k}_2 &= (\mathbf{b}_1 + \mathbf{b}_3)/2 = (2\pi/a)(0, 1, 0) \\ \mathbf{k}_3 &= (\mathbf{b}_2 + \mathbf{b}_3)/2 = (2\pi/a)(1, 0, 0). \end{aligned} \tag{1.5.3.18}$$

If $\boldsymbol{\mu}_1$ is the magnetic moment at the site (0, 0, 0), the value of $\boldsymbol{\mu}_i(\mathbf{k}_j)$ at $\mathbf{t}_i = (a/2)(h_i, k_i, l_i)$ may be obtained for each $\mathbf{k}_j$ with the help of the following relation:

$$\boldsymbol{\mu}_i(\mathbf{k}_j) = \boldsymbol{\mu}_1 \exp[i(\mathbf{k}_j\mathbf{t}_i)]. \tag{1.5.3.19}$$

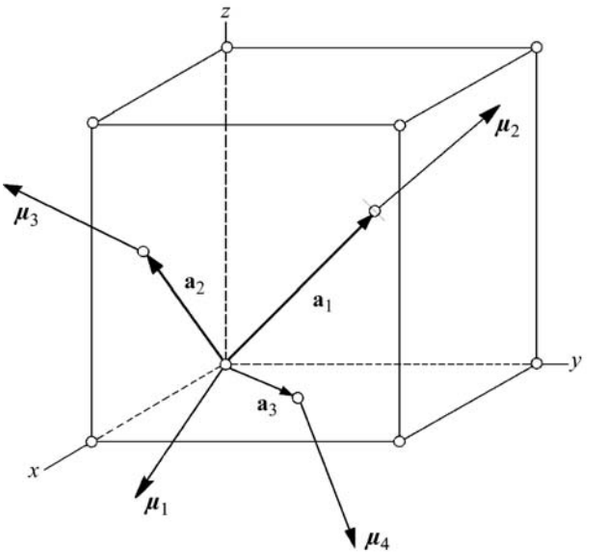

Fig. 1.5.3.5. The conventional unit cell of UO_2. Only the positions of the magnetic U^{4+} ions are shown. The vectors $\mathbf{a}_1, \mathbf{a}_2, \mathbf{a}_3$ form a basis of a primitive cell of the crystallographic lattice; $\boldsymbol{\mu}_1, \boldsymbol{\mu}_2, \boldsymbol{\mu}_3, \boldsymbol{\mu}_4$ are the magnetic moments of the ions belonging to the four magnetic lattices.

From this relation, it follows that $\boldsymbol{\mu}_i(\mathbf{k}_j) = \pm\boldsymbol{\mu}_1$ for different combinations of $\mathbf{t}_i$ and $\mathbf{k}_j$. The signs of the magnetic moments $\boldsymbol{\mu}_i$ at the four sites at the corner and the face centres of the conventional unit cell are displayed in Table 1.5.3.5.

Table 1.5.3.5 shows that for each arm of the vector star $\mathbf{k}_j$, there exists a linear combination of the four vectors $\boldsymbol{\mu}_i$ (i = lattice site) which is a basis of the representation of one of the arms. According to Table 1.5.3.5, these linear combinations have the following forms:

$$\begin{aligned} \mathbf{l}_1 &= \boldsymbol{\mu}_1 - \boldsymbol{\mu}_2 - \boldsymbol{\mu}_3 + \boldsymbol{\mu}_4 \\ \mathbf{l}_2 &= \boldsymbol{\mu}_1 - \boldsymbol{\mu}_2 + \boldsymbol{\mu}_3 - \boldsymbol{\mu}_4 \\ \mathbf{l}_3 &= \boldsymbol{\mu}_1 + \boldsymbol{\mu}_2 - \boldsymbol{\mu}_3 - \boldsymbol{\mu}_4. \end{aligned} \tag{1.5.3.20}$$

None of the vectors $\mathbf{l}_\alpha$ is a basis of an irreducible representation of the whole space group $O_h^5 = Fm\bar{3}m$ in the case under consideration. The basis functions of the irreducible representation are formed by linear superposition of the basis functions of each arm. One of these representations, τ_3, is a superposition of the following components of $\mathbf{l}_\alpha$: l_{1z}, l_{2y} and l_{3x}. This corresponds to the following orientations of the magnetic moments located in different corners of the primitive unit cell:

$$\boldsymbol{\mu}_1 \sim [\bar{1}, \bar{1}, \bar{1}], \ \boldsymbol{\mu}_2 \sim [\bar{1}, 1, 1], \ \boldsymbol{\mu}_3 \sim [1, \bar{1}, 1], \ \boldsymbol{\mu}_4 \sim [1, 1, \bar{1}]. \tag{1.5.3.21}$$

Thus the magnetic structure of UO_2 consists of four primitive cubic magnetic sublattices $\mathbf{M}_i$ inserted into each other. According to (1.5.3.21), the magnetization vectors of these sublattices $\mathbf{M}_i$ are aligned along the space diagonals of the cubic lattice. This magnetic structure for UO_2 was predicted theoretically by Dzyaloshinskii & Man'ko (1964) (using the representation approach in the way discussed above) and established by neutron scattering by Faber *et al.* (1975).

Table 1.5.3.5. *The signs of $\boldsymbol{\mu}_i(\mathbf{k}_j)$ for four sites $\mathbf{t}_i$ of the conventional unit cell (the corners of a primitive cell)*

	$\mathbf{t}_1$ $a(0, 0, 0)$	$\mathbf{t}_2$ $(a/2)(0, 1, 1)$	$\mathbf{t}_3$ $(a/2)(1, 0, 1)$	$\mathbf{t}_4$ $(a/2)(1, 1, 0)$
$\mathbf{k}_1$	+	−	−	+
$\mathbf{k}_2$	+	−	+	−
$\mathbf{k}_3$	+	+	−	−

This example shows that the Landau theory can solve complicated problems of phase transitions where the magnetic lattice does not coincide with the crystallographic one and the magnetic structure is strongly non-collinear. Here only a qualitative analysis has been given; Section 1.5.3.3.1 and Section 1.5.3.3.2 will be devoted to quantitative solutions connected with phase transitions into an ordered state.

As was discussed in Section 1.5.2, Andreev & Marchenko (1976, 1980) introduced the concept of exchange magnetic symmetry. This concept is based on neglecting the relativistic interactions in comparison with the exchange interaction. In such an approach, the orientation of the magnetic moments relative to the crystallographic axis is arbitrary and the crystallographic transformations act on the magnetic moments not as on vectors but as on scalars. In the exchange approximation, three magnetic vectors can be introduced that describe any magnetic structure. These vectors are mutually orthogonal. All magnetic structures can be classified into four types. (1) Collinear ferromagnets or ferrimagnets are described by one ferromagnetic vector **M**. (2) Collinear antiferromagnets are described by one antiferromagnetic vector **L**. (3) Non-collinear ferromagnets are described by one ferromagnetic vector **M** and one or two antiferromagnetic vectors $\mathbf{L}_\alpha$. (4) Non-collinear antiferromagnets are described by two or three antiferromagnetic vectors $\mathbf{L}_\alpha$. The Andreev and Marchenko approach describes the magnetic structure of UO_2 considered above by three antiferromagnetic vectors which are aligned along [1, 0, 0], [0, 1, 0] and [0, 0, 1], respectively.

(*b*) *Incommensurate structures* (see also Section 1.10.1).

In the second type of transition, $\mathbf{k}_\beta$ differs slightly from one of the rational values (1/2, 1/3, 1/4). Then the magnetic structure is incommensurate with the crystallographic lattice. Such non-collinear structures are shown in Fig. 1.5.1.4 (antiferromagnetic and ferromagnetic helices). A detailed analysis of this problem is given by Andreev & Marchenko (1976, 1980).

(*c*) $\mathbf{k}_\beta = 0$.

To the third type belong transitions for which $\mathbf{k}_\beta = 0$. In this case, the magnetic primitive cell coincides with the crystallographic one and antiferromagnetic ordering is allowed only if there is more than one magnetic ion in the primitive cell. As stated above, only this type of ordering allows collinear ferromagnetism. Therefore, we shall discuss this type of transition later in more detail.

Let us consider the phase transition in a uniaxial crystal with four magnetic ions in the primitive cell, as was done by Dzyaloshinskii (1957*a*). Now the average density of the magnetic moment $m^i(\mathbf{r})$ in (1.5.3.12) is determined by the average values of the magnetic moments of each ion, $\boldsymbol{\mu}_1$, $\boldsymbol{\mu}_2$, $\boldsymbol{\mu}_3$, $\boldsymbol{\mu}_4$. In (1.5.3.12), there is no longer any need to distinguish the coefficients $M^i_{n\alpha}$ and the functions $\varphi_{n,\alpha}(\mathbf{r})$. Their product $M^i_{n,\alpha}\varphi_{n,\alpha}(\mathbf{r})$ is now replaced by the linear combinations of the components of $\boldsymbol{\mu}_1$, $\boldsymbol{\mu}_2$, $\boldsymbol{\mu}_3$, $\boldsymbol{\mu}_4$ transforming according to the corresponding irreducible representation of the point group $\mathcal{P}$ of the crystal (the space group of which is $\mathcal{G}$). To illustrate this, we shall take for $\mathcal{G}$ the group $\boldsymbol{D}^6_{3d} = R\bar{3}c$, which was discussed in Section 1.5.3.1. There we introduced the linear combinations (1.5.3.2) $\mathbf{l}_1$, $\mathbf{l}_2$, $\mathbf{l}_3$, $\mathbf{m}$ of the vectors $\boldsymbol{\mu}_1$, $\boldsymbol{\mu}_2$, $\boldsymbol{\mu}_3$, $\boldsymbol{\mu}_4$. The components of these linear combinations are basis functions of the irreducible representations of the corresponding point group $\boldsymbol{D}_{3d} = \bar{3}m$. The characters of the representations of this group are given in Table 1.5.3.6. It follows from this table that all z components of the vectors $\mathbf{l}_\alpha$ and $\mathbf{m}$ are transformed according to different one-dimensional representations of $\boldsymbol{D}_{3d}$ (*i.e.* $\Gamma_1, \ldots, \Gamma_4$). Following the rule introduced in Section 1.5.2.1 [see relation (1.5.2.2)], we established the magnetic point groups displayed in the last column of Table 1.5.3.6. The symbols for the magnetic structures are given in the corresponding column. The x, y components are transformed by two-dimensional representations: m_x, m_y and l_{3x}, l_{3y} are transformed according to the same representation Γ_5; a similar situation holds for the pairs l_{1x}, l_{1y} and l_{2x}, l_{2y}, which are transformed according to Γ_6. It is obvious that if the magnetic structure possesses x, y components of the magnetic vectors, the magnetic point group (which must be a subgroup of $\boldsymbol{D}_{3d}$) will contain only four elements of the group $\boldsymbol{D}_{3d}$: E, C_2, I, $\sigma_\perp$. These elements form the point group $\boldsymbol{C}_{2h} = 2/m$. The point group $\boldsymbol{C}_{2h}$ has four one-dimensional representations, which according to relation (1.5.2.2) generate the four magnetic point groups listed in the last column of Table 1.5.3.6. To each of these magnetic point groups corresponds a definite magnetic structure, which is a mixture of x and y components of $\mathbf{l}_3$ and $\mathbf{m}$ or $\mathbf{l}_1$ and $\mathbf{l}_2$. The symbols of these structures are also listed in the table (by definition, the twofold axis is aligned along the x axis).

According to the relation (1.5.3.13), the thermodynamic potential Φ contains a sum of quadratic terms of basis functions for each irreducible representation. Thus it contains the following invariants, which correspond to the one-dimensional representations:

$$A'_1 l^2_{1z} + A'_2 l^2_{2z} + A'_3 l^2_{3z} + B' m^2_z. \tag{1.5.3.22}$$

The invariants formed with the x, y components of the vectors $\mathbf{l}_1$, $\mathbf{l}_2$, $\mathbf{l}_3$, $\mathbf{m}$, which are basis functions of two-dimensional representations, have the following form:

$$A''_1(l^2_{1x} + l^2_{1y}) + A''_2(l^2_{2x} + l^2_{2y}) + A''_3(l^2_{3x} + l^2_{3y}) + B''(m^2_x + m^2_y). \tag{1.5.3.23}$$

The thermodynamic potential for any uniaxial crystal possesses such invariants of second order. For crystals belonging to the space group $\boldsymbol{D}^6_{3d}$ it is possible to construct additional invariants, which are linear combinations of the mixed products of the x and y components of the pairs of vectors $\mathbf{l}_1, \mathbf{l}_2$ and $\mathbf{l}_3, \mathbf{m}$ and are transformed according to the same two-dimensional representations. These invariants have the following form:

$$l_{1x}l_{2y} - l_{1y}l_{2x}, \quad l_{3x}m_y - l_{3y}m_x. \tag{1.5.3.24}$$

These terms are responsible for 'weakly non-collinear' structures; we discuss their properties in the Section 1.5.5 and shall not take them into account now.

Before writing the whole expression of the thermodynamic potential, let us combine expressions (1.5.3.22) and (1.5.3.23) to

Table 1.5.3.6. *Characters of the irreducible representations of the group* $\boldsymbol{D}_{3d} = \bar{3}m$ *and corresponding magnetic structures*

Representation	Magnetic vector components	Elements of symmetry						Magnetic structure	Magnetic point group
		E	$2C_3$	$3U_2$	I	$2S_6$	$3\sigma_d$		
Γ_1	l_{3z}	1	1	1	1	1	1	$\boldsymbol{C}_z$	$\boldsymbol{D}_{3d} = \bar{3}m$
Γ_2	m_z	1	1	−1	1	1	−1	$\boldsymbol{F}_z$	$\boldsymbol{D}_{3d}(\boldsymbol{S}_6) = \bar{3}m'$
Γ_3	l_{1z}	1	1	−1	−1	−1	1	$\boldsymbol{A}_z$	$\boldsymbol{D}_{3d}(\boldsymbol{C}_{3v}) = \bar{3}'m$
Γ_4	l_{2z}	1	1	1	−1	−1	−1	$\boldsymbol{G}_z$	$\boldsymbol{D}_{3d}(\boldsymbol{D}_3) = \bar{3}'m'$
Γ_5	l_{3x} m_y	2	−1	0	2	−1	0	$\boldsymbol{C}_x$ $\boldsymbol{F}_y$	$\boldsymbol{C}_{2h}(\boldsymbol{C}_i) = 2'/m'$
	m_x l_{3y}							$\boldsymbol{C}_y$ $\boldsymbol{F}_x$	$\boldsymbol{C}_{2h} = 2/m$
Γ_6	l_{1x} l_{2y}	2	−1	0	−2	1	0	$\boldsymbol{A}_x$ $\boldsymbol{G}_y$	$\boldsymbol{C}_{2h}(\boldsymbol{C}_2) = 2/m'$
	l_{2x} l_{1y}							$\boldsymbol{A}_y$ $\boldsymbol{G}_x$	$\boldsymbol{C}_{2h}(\boldsymbol{C}_s) = 2'/m$

separate the exchange terms from the relativistic ones. This can be performed in two ways:

$$A_1' l_{1z}^2 + A_1''(l_{1x}^2 + l_{1y}^2) = (A_1/2)\mathbf{l}_1^2 + (a_1/2) l_{1z}^2 \quad \text{or}$$
$$A_1' l_{1z}^2 + A_1''(l_{1x}^2 + l_{1y}^2) = (A_1/2)\mathbf{l}_1^2 + (a_1/2)(l_{1x}^2 + l_{1y}^2). \tag{1.5.3.25}$$

Similar rearrangements are performed for $\mathbf{l}_2$, $\mathbf{l}_3$ and $\mathbf{m}$. Summing expressions (1.5.3.22) and (1.5.3.23) and taking into account expression (1.5.3.25), we obtain the final expression for the thermodynamic potential Φ limited to the terms of second order:

$$\Phi_1 = \Phi_0 + (A_1/2)\mathbf{l}_1^2 + (A_2/2)\mathbf{l}_2^2 + (A_3/2)\mathbf{l}_3^2 + (B/2)\mathbf{m}^2 + (a_1/2) l_{1z}^2 + (a_2/2) l_{2z}^2 + (a_3/2) l_{3z}^2 + (b/2) m_z^2. \tag{1.5.3.26}$$

In this expression, the coefficients of the terms representing the exchange interaction are denoted by capital letters. It is mainly these terms that are responsible for the transition to the ordered state. The much smaller relativistic terms are responsible for the orientation of the vectors $\mathbf{l}_\alpha$ or $\mathbf{m}$. Their coefficients are denoted by small letters.

To minimize the potential (1.5.3.26), it is necessary to add terms of the fourth order, which are restricted to the exchange terms. The total expression for the thermodynamic potential Φ will then be

$$\Phi = \Phi_1 + \tfrac{1}{4}\sum_\alpha C_\alpha \mathbf{l}_\alpha^4 + \tfrac{1}{4} C' \mathbf{m}^4 + \tfrac{1}{2}\sum_\alpha D_\alpha (\mathbf{l}_\alpha \mathbf{m})^2 + \tfrac{1}{2}\sum_\alpha D_\alpha' \mathbf{l}_\alpha^2 \mathbf{m}^2. \tag{1.5.3.27}$$

As pointed out above, one of the coefficients A_α or B vanishes at the transition temperature T_0. This coefficient may be expanded in a series of $(T - T_0)$ [see (1.5.3.14)]. At $T < T_0$, a ferro- or antiferromagnetic structure will be realized, the type of which is determined by minimization of the thermodynamic potential (1.5.3.27).

As an example, we shall consider in the next two sections the simplest cases, the uniaxial ferromagnet and the uniaxial antiferromagnet. When doing this, we shall not restrict ourselves to a certain crystallographic structure as in the case above. For the sake of simplicity, it will be assumed that the primitive cell contains only two magnetic ions and therefore there is only one antiferromagnetic vector $\mathbf{l}$. Further, we shall introduce new variables:

$$\mathbf{M} = (N/2)\mathbf{m}, \quad \mathbf{L} = (N/2)\mathbf{l}, \tag{1.5.3.28}$$

where N is the number of magnetic ions per cm^3.

1.5.3.3.1. *Uniaxial ferromagnet*

The temperature of transition from the paramagnetic to the ferromagnetic state is called the Curie temperature. The thermodynamic treatment of the behaviour of uniaxial ferromagnets in the neighbourhood of the Curie temperature T_c is given below.

In the case of a ferromagnet ($\mathbf{L} = 0$), the thermodynamic potential (1.5.3.27) near T_c including the magnetic energy $-\mathbf{MH}$ is given by (see 1.5.3.25)

$$\tilde{\Phi} = \Phi_0 + (B/2)\mathbf{M}^2 + (b/2)(M_x^2 + M_y^2) + (C/4)\mathbf{M}^4 - \mathbf{MH}, \tag{1.5.3.29}$$

where $\tilde{\Phi}$ is used to designate the thermodynamic potential in variables $p, T, \mathbf{H}$ [instead of $\Phi(p, T, \mathbf{M})$]; at the given field, $\tilde{\Phi}$ should be a minimum. The equilibrium value of the magnetization $\mathbf{M}$ is found by minimizing the thermodynamic potential.

First consider the ferromagnet in the absence of the external field ($\mathbf{H} = 0$). The system of equations $\partial\tilde{\Phi}/\partial\mathbf{M} = 0$ has three solutions:

$$\text{(I)} \qquad M_x = M_y = M_z = 0 \tag{1.5.3.30}$$

$$\text{(II)} \qquad M_z = 0; \quad M_x^2 + M_y^2 = M_\perp^2 = -\frac{B+b}{C} \tag{1.5.3.31}$$

$$\text{(III)} \qquad M_x = M_y = 0; \quad M_z^2 = -\frac{B}{C}. \tag{1.5.3.32}$$

In the whole range of temperatures $T > T_c$ when $B > 0$, the minimum of the potential is determined by solution (I) (*i.e.* absence of a spontaneous magnetization). The realization of the second or third state depends on the sign of the coefficient b. If $b > 0$, then the third state is realized, the magnetization $\mathbf{M}$ being directed along the axis. In this case, the transition from the paramagnetic into the ferromagnetic state will take place at $T_c = T_0$ (when $B = 0$). If $b < 0$, the magnetization is directed perpendicular to the axis. In this case, the Curie temperature is $T_c = T_0 - b/\lambda$ (when $B + b = 0$). In the absence of a magnetic field, the difference between the two values of T_c has no physical meaning, since it only means another value of the coefficient B [see (1.5.3.25)]. In a magnetic field, both temperatures may be determined experimentally, *i.e.* when B becomes zero and when $B + b$ becomes zero.

If a magnetic field $\mathbf{H}$ is applied parallel to the z axis and $b > 0$, the minimization of the thermodynamic potential Φ leads to

$$H/M = CM^2 + B. \tag{1.5.3.33}$$

This relation has been verified in many experiments and the corresponding graphical representations are known in the literature as Arrott–Belov–Kouvel plots (see Kouvel & Fisher, 1964). Putting $B = \lambda(T - T_c)$ according to (1.5.3.14), equations (1.5.3.32) and (1.5.3.33) may be used to derive expressions for the initial magnetic susceptibilities (for $H \to 0$):

$$\chi_0 = \frac{1}{2\lambda(T_c - T)^\gamma}, \quad T < T_c, \tag{1.5.3.34}$$

$$\chi_0 = \frac{1}{\lambda(T - T_c)^\gamma}, \quad T > T_c, \tag{1.5.3.35}$$

where $\gamma = 1$.

The Landau theory of phase transitions does not take account of fluctuations of the order parameter. It gives qualitative predictions of all the possible magnetic structures that are allowed for a given crystal if it undergoes a second-order transition. The theory also explains which of the coefficients in the expression for the thermodynamic potential is responsible for the corresponding magnetic structure. It describes also quantitative relations for the magnetic properties of the material if

$$1 \gg (T - T_c)/T_c \gg T_c B^2/b\alpha^3, \tag{1.5.3.36}$$

where α is the coefficient in the term which describes the gradient energy. In this chapter, we shall not discuss the behaviour of the material in the fluctuation region. It should be pointed out that, in this region, γ in relations (1.5.3.34) and (1.5.3.35) depends on the dimensionality of the structure n and equals 1.24 for $n = 1$, 1.31 for $n = 2$ and 1.39 for $n = 3$. Similar considerations are relevant to the relations (1.5.3.31) and (1.5.3.32), which describe the temperature dependence of spontaneous magnetization.

The relations (1.5.3.31) and (1.5.3.32) describe the behaviour of the ferromagnet in the 'saturated' state when the applied magnetic field is strong enough to destroy the domain structure. The problem of the domains will be discussed later (see Section 1.5.4).

The transition from the paramagnetic to the ferromagnetic state is a second-order transition, provided that there is no magnetic field. In the presence of a magnetic field that is parallel to the easy axis of magnetization, the magnetic symmetry of the crystal is the same ($M_z \neq 0$) both above and below T_c. From the point of view of symmetry, no transition occurs in this case.

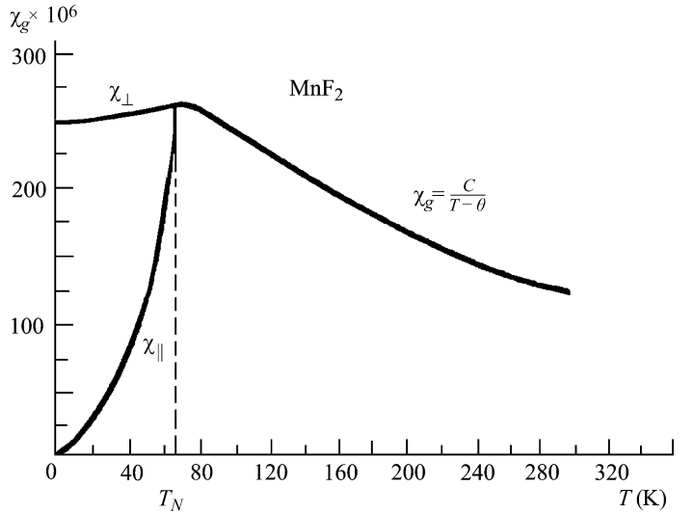

Fig. 1.5.3.6. Temperature dependence of the mass susceptibility χ_g for a uniaxial antiferromagnet along ($\chi_\parallel$) and perpendicular ($\chi_\perp$) to the axis of antiferromagnetism (see Foner, 1963).

1.5.3.3.2. *Uniaxial antiferromagnet*

Now let us proceed to the uniaxial antiferromagnet with two ions in the primitive cell. The thermodynamic potential $\tilde{\Phi}$ for such an antiferromagnet is given in accordance with (1.5.3.26) and (1.5.3.27) by (Landau, 1933)

$$\begin{aligned}\tilde{\Phi} = \Phi_0 &+ (A/2)\mathbf{L}^2 + (B/2)\mathbf{M}^2 + (a/2)(L_x^2 + L_y^2) \\ &+ (b/2)(M_x^2 + M_y^2) + (C/4)\mathbf{L}^4 + (D/2)(\mathbf{LM})^2 \\ &+ (D'/2)\mathbf{L}^2\mathbf{M}^2 - \mathbf{MH}. \end{aligned} \tag{1.5.3.37}$$

If the magnetic field is absent ($\mathbf{H} = 0$), then $\mathbf{M} = 0$ because B, D and $D' > 0$. Then three possible magnetic states are obtained by minimizing the potential with respect to $\mathbf{L}$ only:

(I) $$L_x = L_y = L_z = 0 \tag{1.5.3.38}$$

(II) $$L_z = 0; \quad L_x^2 + L_y^2 = L_\perp^2 = -\frac{A + a}{C} \tag{1.5.3.39}$$

(III) $$L_x = L_y = 0; \quad L_z^2 = -\frac{A}{C}. \tag{1.5.3.40}$$

When $a < 0$, state (II) with $L_z = 0$ is thermodynamically stable. When $a > 0$, state (III) is stable and the antiferromagnetic vector is directed along the axis. This means that the term with the coefficient a is responsible for the anisotropy of the uniaxial antiferromagnet. We introduce the effective anisotropy field:

$$H_a = aL = 2aM_0, \tag{1.5.3.41}$$

where M_0 is the sublattice magnetization.

Formulas (1.5.3.39) and (1.5.3.14) in the form $A = \lambda(T - T_c)$ yield the expression for the temperature dependence of the sublattice magnetization:

$$L^2 = (\lambda/C)(T_N - T), \tag{1.5.3.42}$$

where T_N is the Néel temperature. The assertions relating to formulas (1.5.3.34) and (1.5.3.35) concerning the fluctuation region are also valid for the temperature dependence of the sublattice magnetization.

The minimization of the potential $\tilde{\Phi}$ with respect to $\mathbf{M}$ for given $\mathbf{L} \neq 0$ when $\mathbf{H} \neq 0$ yields the following relation for the magnetization:

$$\mathbf{M} = \chi_\perp \mathbf{H} - (\chi_\perp - \chi_\parallel)(\mathbf{qH})\mathbf{q}, \tag{1.5.3.43}$$

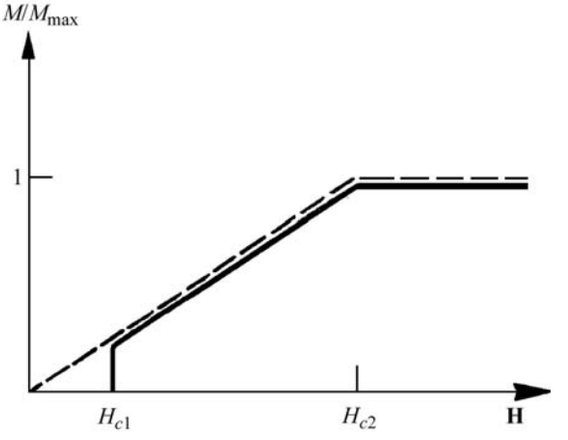

Fig. 1.5.3.7. Dependence of the relative magnetization M/M_{max} on the magnetic field at $T = 0$. The dashed line corresponds to $\mathbf{H} \perp Oz$, the full line to $\mathbf{H} \parallel Oz$. H_{c1} is the field of spin-flop, H_{c2} is the field of spin-flip.

where $\mathbf{q} = \mathbf{L}/|L|$. Thus the magnetization of an antiferromagnet is linear with the magnetic field, as for a paramagnet, if the magnetic field is not too strong. The main difference is in the anisotropy and temperature dependence of the susceptibility. The parallel susceptibility $\chi_\parallel$ decreases when the temperature is lowered, and $\chi_\perp$ does not depend on temperature ($\chi_\perp = 1/B$) (see Fig. 1.5.3.6). The coefficient B belongs to the exchange term and defines the effective exchange field

$$H_e = \tfrac{1}{2}BL = BM_0. \tag{1.5.3.44}$$

As seen from Fig. 1.5.3.6, $\chi_\perp > \chi_\parallel$. Therefore, when the magnetic field applied parallel to the axis of a uniaxial antiferromagnet reaches the critical value

$$H_{c1}^2 = aL^2/(\chi_\perp - \chi_\parallel) \simeq aBL_0^2 = 2H_aH_e \tag{1.5.3.45}$$

(L_0 is the value of L at $T = 0$), a flopping of the sublattices from the direction along the axis to some direction in the plane perpendicular to the axis occurs. In this spin-flop transition (which is a first-order transition into a new magnetic structure), the magnetization jumps as shown in Fig. 1.5.3.7.

A second-order transition into a saturated paramagnetic state takes place in a much stronger magnetic field $H_{c2} = 2H_e$. This transition is called a spin-flip transition. Fig. 1.5.3.7 shows the magnetic field dependence of the magnetization of a uniaxial antiferromagnet. Fig. 1.5.3.8 shows the temperature dependence of both critical fields.

The quantitative behaviour of the critical magnetic fields in the neighbourhood of T_N for both directions of the magnetic field ($\mathbf{H} \parallel Oz$ and $\mathbf{H} \perp Oz$) can be determined from the theory of second-order phase transitions starting from the thermodynamic potential $\tilde{\Phi}$ and taking into account that L is small and $DL^2 \ll B$ close to T_N.

In the presence of the magnetic field $\mathbf{H} \perp Oz$, $\mathbf{L}$ is parallel to Oz, $\mathbf{LM} = 0$, the coefficient A at L^2 is replaced by $A + 2D'H^2/B^2$ and the latter is zero at the new transition point. The critical field is given by the relation

$$H_{c2}^2 = (\lambda B^2/2D')(T_N - T), \quad \mathbf{H} \perp Oz. \tag{1.5.3.46}$$

If the field is applied parallel to the z axis, then $\mathbf{L}$ remains parallel to Oz if $H < H_{c1}$ ($H_{c1} \simeq aB^2/D$ in the neighbourhood of T_N). Therefore,

$$H_{c2}^2 = \frac{\lambda B^2}{2(D + D')}(T_N - T), \quad \mathbf{H} \parallel Oz, \; H < H_{c1}. \tag{1.5.3.47}$$

If $H > H_{c1}$, $\mathbf{L}$ becomes perpendicular to the z axis and the anisotropy term has to be taken into account:

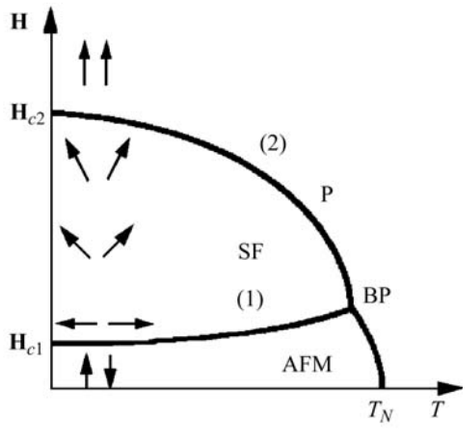

Fig. 1.5.3.8. Magnetic phase diagram for a uniaxial antiferromagnet in a magnetic field applied parallel to the axis. (1) The line of spin-flop transition (H_{c1}); (2) the line of spin-flip transition (H_{c2}); P, paramagnetic phase; AFM, easy-axis antiferromagnetic phase; SF, spin-flop phase; BP, bicritical point.

$$H_{c2}^2 = \frac{\lambda B^2}{2D'}(T_N - T - a/\lambda), \quad \mathbf{H} \parallel Oz,\ H > H_{c1}. \qquad (1.5.3.48)$$

Formulas (1.5.3.46)–(1.5.3.48) show that the transition temperature is reduced by applying the magnetic field. The displacement of the transition point is directly proportional to the square of the applied field. Fig. 1.5.3.9 shows the phase diagram of an antiferromagnet in the neighbourhood of T_N. Unlike ferromagnets, antiferromagnets maintain the second-order phase transition when a magnetic field is applied because the symmetry of the crystal in the antiferromagnetic state differs essentially from that in the paramagnetic state also if the crystal is placed into a magnetic field.

Formula (1.5.3.43) describes the magnetization process only in easy-axis antiferromagnets. For easy-plane antiferromagnets, the anisotropy in the plane is usually extremely small and the antiferromagnetic vector rotates freely in the basic plane. Therefore, for any direction of the magnetic field, the vector **L** becomes

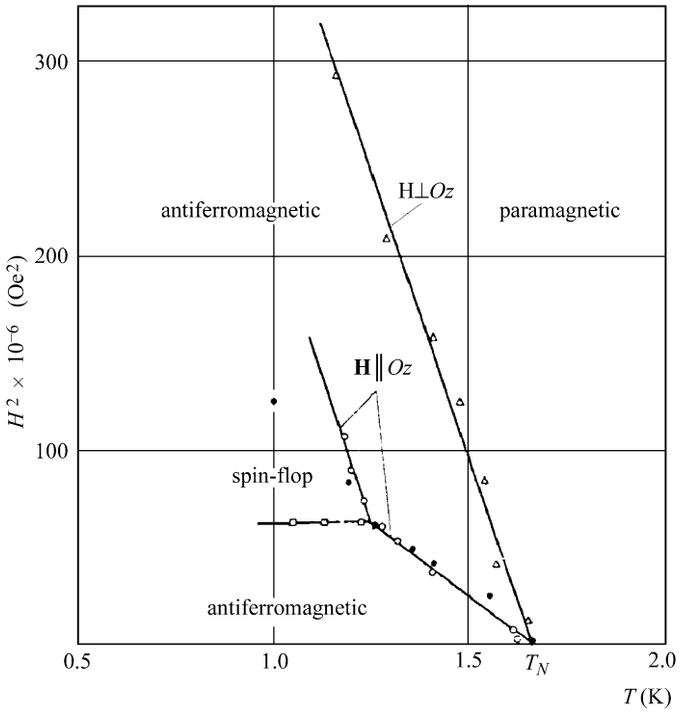

Fig. 1.5.3.9. Phase diagram for a uniaxial antiferromagnet in the proximity of T_N, calculated for $MnCl_2{\cdot}4H_2O$. Experimental data are taken from Gijsman *et al.* (1959).

aligned perpendicular to the applied magnetic field. Correspondingly the magnetization becomes

$$\mathbf{M} = \chi_z H_z \hat{\mathbf{z}} + \chi_\perp H_\perp \hat{\mathbf{x}}, \qquad (1.5.3.49)$$

where $\hat{\mathbf{z}}$ and $\hat{\mathbf{x}}$ are unit vectors parallel and perpendicular to the axis.

1.5.4. Domain structure

1.5.4.1. *180° domains*

Neither symmetry nor energy considerations can determine the alignment of the magnetization vector **n** in a non-chiral easy-axis magnetic (of ferro- or antiferromagnetic type). The vector **n** may be aligned parallel or antiparallel to the positive direction of the z axis. Therefore, specimens of any magnetic are usually split into separate regions called domains. In each domain of an easy-axis magnetic, the vector **n** has one of its two possible directions. Such domains are called 180° domains. Adjacent domains are separated by a domain wall, in which the magnetic moments are no longer strictly parallel (or antiparallel). As a result of this, both the exchange and the anisotropy energy rise inside the volume of the domain wall.

In ferromagnets (and ferrimagnets), the loss in the exchange and anisotropy energy in a multidomain sample is compensated by the gain in the magnetostatic energy. The existence of the domain structure is responsible for the behaviour of a ferromagnet in an applied magnetic field. There are two kinds of magnetization processes that one has to distinguish: the displacement of the domain walls and the rotation of the spontaneous magnetization vector from the easy direction to the direction of the applied magnetic field. The magnetization process will first be considered without taking the demagnetizing field into account. If the magnetic field is applied parallel to the axis of an easy-axis ferromagnet, the displacement of the domain wall will completely determine the magnetization process. If the sample contains no impurities and crystal defects, such a displacement must take place in an infinitely small magnetic field [see curve (1) in Fig. 1.5.4.1 and Fig. 1.5.4.3*a*]. If the magnetic field is applied perpendicular to the easy axis, the size of the domains does not change but their magnetization vectors rotate. Let us denote the spontaneous magnetization by M_s. Then the sample magnetization M rises linearly with respect to the applied magnetic field:

$$M = HM_s^2/2K_1, \qquad (1.5.4.1)$$

where K_1 is defined by relations (1.5.3.8)–(1.5.3.10). Some nonlinearity in H can arise from the fourth-order term with K_2 [see curve (2) in Fig. 1.5.4.1 and Fig. 1.5.4.3*c*]. When $H = 2K_1/M_s = H_s$, the magnetizations of all the domains are rotated by 90° and the magnetization of the sample becomes oriented along the magnetic field; its value is saturated and is equal to the spontaneous magnetization M_s. If $T \neq 0$ K, there is an additional rise in magnetization with the magnetic field. This rise, which is called true magnetization, is relatively very small at all temperatures except for the temperature region close to the transition temperature. If the magnetic field is applied at an arbitrary angle θ to the easy axis, the magnetization process occurs in two steps [see curves (2) in Fig. 1.5.4.2 and Fig. 1.5.4.3*b*]. First, as a result of the wall displacement, the magnetization jumps to the value M_1 in a small magnetic field. Next, the rotation process follows and at H_s the sample becomes saturated [see curves (2) in Fig. 1.5.4.2]. It is essential to take the shape of the sample into account in considering the problem of the magnetization processes in ferromagnets, as the demagnetizing field can be up to $4\pi M$. In real materials, the displacement process is partly (at low fields) reversible and partly (at higher fields) irreversible. Therefore, complicated hysteresis processes arise in magnetizing ferromagnets.

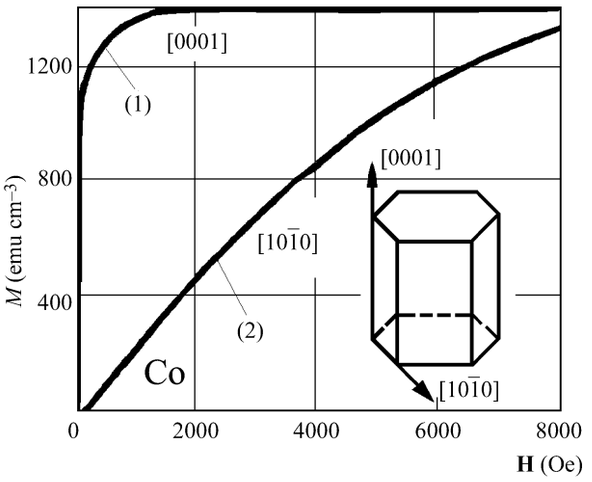

Fig. 1.5.4.1. Magnetization curves of hexagonal cobalt for two main crystallographic directions: (1) [0001] and (2) [10$\bar{1}$0].

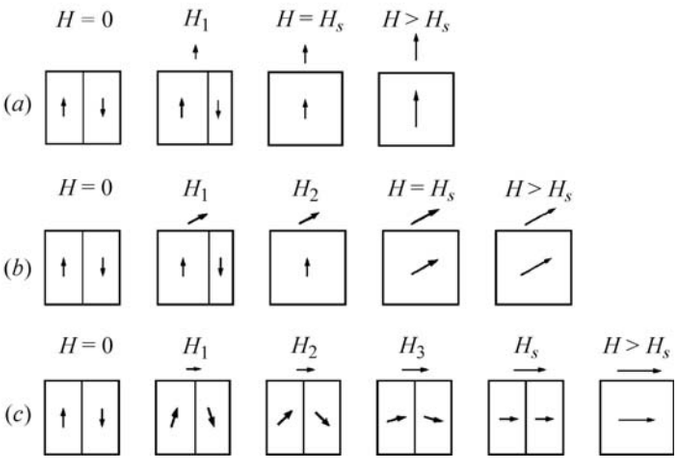

Fig. 1.5.4.3. Schematic display of the magnetization: (*a*) along the easy axis; (*b*) at an arbitrary angle to the easy axis; (*c*) perpendicular to the easy axis.

The problem of 180° domains in antiferromagnets is not as clear. These domains differ in the sign of the antiferromagnetic vector **L**. This vector was defined as the difference of the vectors of sublattice magnetizations in a two-sublattice antiferromagnet, *i.e.* $\mathbf{M}_1 - \mathbf{M}_2$. Thus two such antiferromagnetic domains differ only by the numbering of the sites in the sublattices. Antiferromagnetic 180° domains are also called S-domains. The wall between two S-domains is schematically represented in Fig. 1.5.4.4.

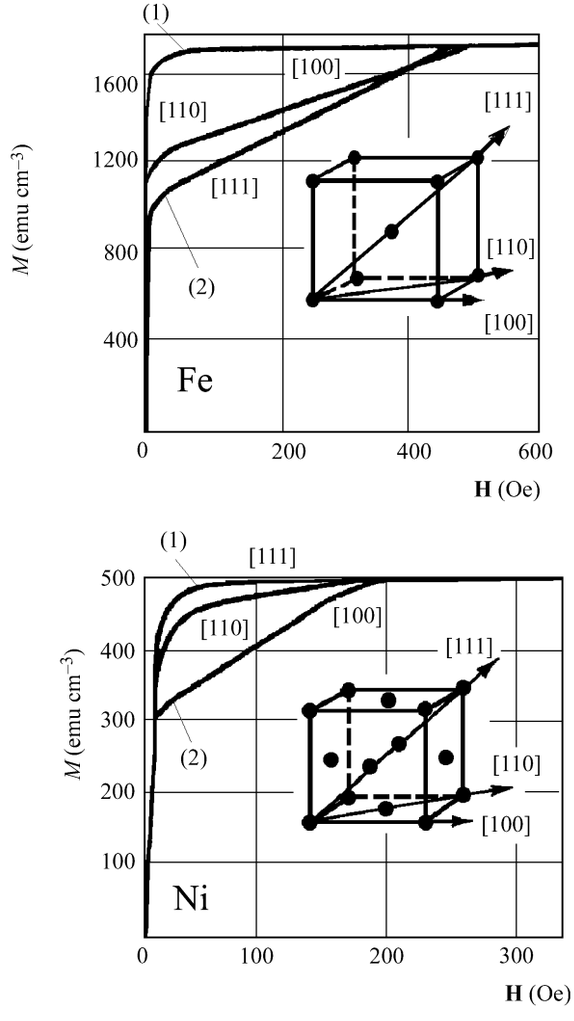

Fig. 1.5.4.2. Magnetization curves of two cubic crystals (iron and nickel) for three crystallographic directions.

The origin of the antiferromagnetic S-domains cannot be explained from the point of view of energy balance as in a ferromagnet. These domains give rise to additional exchange and anisotropy energies which are not compensated by a decrease of any other kind of energy. Thus the S-domain structure is thermodynamically not stable. However, experiments show that S-domains exist in most easy-axis antiferromagnets.

The formation of S-domains can be explained by assuming that when the material is cooled down to the Néel temperature, antiferromagnetic ordering arises in different independent regions. The direction of the vector **L** in these regions is accidental. When growing regions with different directions of **L** meet, the regular alternation of the directions of magnetic moments of the ions is broken on the border between these regions. Domain walls are created on such borders. Such domain structures can be metastable.

The existence of S-domains in easy-axis antiferromagnets was first proved in experiments in which effects that depend on the sign of **L** were investigated. These are piezomagnetism, linear magnetostriction and the linear magnetoelectric effect. The sign of these effects depends on the sign of **L**. We shall discuss this problem in detail in Sections 1.5.7 and 1.5.8. Later, 180° domain walls were observed in neutron scattering experiments (Schlenker & Baruchel, 1978), and the domains themselves in magneto-optical experiments (see Kharchenko *et al.*, 1979; Kharchenko & Gnatchenko, 1981).

1.5.4.2. *Twin domains*

As pointed out in Section 1.5.3, in tetragonal non-easy-axis magnetics, in easy-plane hexagonal and trigonal and in cubic magnetics there is more than one easy magnetization direction (3, 4 or 6). As a result, domains arise in which vectors $\mathbf{M}_s$ or **L** are directed to each other at 120, 109.5, 90, 70.5 and 60°. Such domains are called twin or T-domains. The formation of magnetic

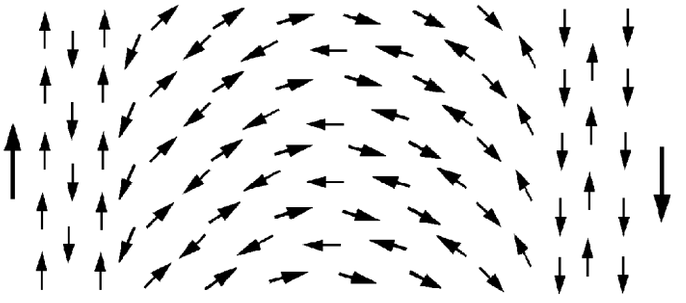

Fig. 1.5.4.4. A 180° domain wall in an antiferromagnet.

T-domains is accompanied by the formation of crystallographic domains as a result of spontaneous magnetostriction. But mostly this is very small. Each of the T-domains may split into 180° domains.

The magnetization process in ferromagnets possessing T-domains is similar to the previously described magnetization of an easy-axis ferromagnet in a magnetic field directed at an oblique angle. First the displacement process allows those 180° domains that are directed unfavourably in each T-domain to disappear, and then the rotation process follows.

In easy-plane antiferromagnets, the T-domain structure is destroyed by a small magnetic field and the antiferromagnetic vector **L** in the whole specimen becomes directed perpendicular to the applied magnetic field, as was explained in Section 1.5.3.

There are four kinds of T-domains in cubic antiferromagnets, in which the vectors **L** are directed parallel or perpendicular to the four ⟨111⟩ axes. Such a T-domain structure can be destroyed only when the applied magnetic field is so strong that the antiferromagnetic order is destroyed at a spin-flip transition.

1.5.4.3. *Ferroic domains*

Aizu (1970) gave a classification of domain formation when a crystal undergoes a transition from an unordered to a magnetically ordered state that has a lower point-group symmetry (see also Section 3.1.1). The unordered state (called the prototype phase) has a grey point group. The number of elements in this group is equal to the product of the number of elements in the point group of the ordered state (called the ferroic state) times the number of domains. Aizu found that there are 773 possible combinations of the point-group symmetries of the prototype and the ferroic state, if crystallographically inequivalent orientations of the subgroup in the group of the prototype are distinguished. These 773 combinations are called ferroic species and are characterized by a symbol giving first the point group of the prototype, then the letter F, then the point group of the ferroic state and finally a letter between parentheses if different orientations are possible. As an example, the $2'$ axis of the ferroic state is parallel to the fourfold axis of the prototype in $4221'F2'(p)$ and perpendicular to it in $4221'F2'(s)$.

Let us discuss the ferroic states of rhombohedral transition-metal oxides given in Table 1.5.3.4. The paramagnetic prototype has point group $\bar{3}m1'$. The four monoclinic ferroic species have six domains ('orientation states') each, which form three pairs of 180° domains ('time-conjugate orientation states'). All four species are 'fully ferroelastic', *i.e.* the three pairs show different orientations of the spontaneous strain; two of the four species ($\bar{3}m1'F2'/m'$ and $\bar{3}m1'F2/m$) are also 'fully ferromagnetic' because all six domains have different orientations of the spontaneous magnetization. Switching a domain into another with a different orientation of the spontaneous strain can be achieved by applying mechanical stress. If the domain was spontaneously magnetized, the orientation of the magnetization is changed simultaneously. Similarly, a domain can be switched into another with a different orientation of the spontaneous magnetization by means of a magnetic field. If the two spontaneous magnetizations have different directions (not just opposite sign), the direction of the spontaneous strain will change at the same time.

The Aizu classification is of interest for technological applications because it gives an overall view not only of domain formation but also of the possibilities for domain switching.

1.5.5. Weakly non-collinear magnetic structures

As was indicated above (see Tables 1.5.3.3 and 1.5.3.6), certain magnetic space groups allow the coexistence of two different types of magnetic ordering. Some magnetic structures can be described as a superposition of two antiferromagnetic structures with perpendicular antiferromagnetic vectors $\mathbf{L}_\alpha$. Such structures may be called weakly non-collinear antiferromagnets. There can also be a superposition of an antiferromagnetic structure **L** with a ferromagnetic one **M** (with $\mathbf{L} \perp \mathbf{M}$). This phenomenon is called weak ferromagnetism. We shall demonstrate in this section why one of the magnetic vectors has a much smaller value than the other in such mixed structures.

1.5.5.1. *Weak ferromagnetism*

The theory of weak ferromagnetism was developed by Dzyaloshinskii (1957*a*). He showed that the expansion of the thermodynamic potential $\tilde{\Phi}$ may contain terms of the following type: $L_i M_k$ $(i, k = x, y)$. Such terms are invariant with respect to the transformations of many crystallographic space groups (see Section 1.5.3.3). If there is an antiferromagnetic ordering in the material ($L_i \neq 0$) and the thermodynamic potential of the material contains such a term, the minimum of the potential will be obtained only if $M_k \neq 0$ as well. The term $L_i M_k$ is a relativistic one. Therefore this effect must be small.

We shall consider as an example the origin of weak ferromagnetism in the two-sublattice antiferromagnets $MnCO_3$, $CoCO_3$ and $NiCO_3$, discussed in Section 1.5.3.1. The following analysis can be applied also to the four-sublattice antiferromagnet α-Fe_2O_3 (assuming $\mathbf{L}_1 = \mathbf{L}_2 = 0$, $\mathbf{L}_3 = \mathbf{L}$). All these rhombohedral crystals belong to the crystallographic space group $\boldsymbol{D}_{3d}^6 = R\bar{3}c$. The thermodynamic potential $\tilde{\Phi}$ for these crystals was derived in Section 1.5.3.3. For the case of a two-sublattice antiferromagnet, one has to add to the expression (1.5.3.26) the invariant (1.5.3.24):

$$\tilde{\Phi} = (A/2)\mathbf{L}^2 + (B/2)\mathbf{M}^2 + (a/2)L_z^2 + (b/2)M_z^2 + d(L_x M_y - L_y M_x) - \mathbf{MH}. \quad (1.5.5.1)$$

The coefficients of the isotropic terms (A and B) are of exchange origin. They are much larger than the coefficients of the relativistic terms (a, b, d). Minimization of $\tilde{\Phi}$ for a fixed value of $\mathbf{L}^2$ and $\mathbf{H} = 0$ gives two solutions:

(1) $\mathbf{L} \parallel Oz$ $(L_x = L_y = 0,\ \mathbf{M} = 0)$. $FeCO_3$ and the low-temperature modification of α-Fe_2O_3 possess such purely antiferromagnetic structures.

(2) $\mathbf{L} \perp Oz$ $[M_x = (d/B)L_y,\ M_y = (d/B)L_x,\ M_z = 0]$. This structure exhibits a spontaneous ferromagnetic moment

$$M_D = (M_x^2 + M_y^2)^{1/2} = (d/B)L. \quad (1.5.5.2)$$

The magnetic moment M_D is smaller than the magnetization of the sublattices ($M_0 = L/2$) in the ratio $2d/B$. This phenomenon is therefore called weak ferromagnetism. The vectors $\mathbf{M}_D$ and **L** are mutually perpendicular. Their direction in the plane is determined by the sixth-order terms of the anisotropy energy (see Section 1.5.3.2). This anisotropy is extremely small in most materials. The vectors of magnetization of the sublattices $\mathbf{M}_0$ are deflected by a small angle $\varphi \simeq 2d/B$ away from the direction of the antiferromagnetic axis **L** in such weak ferromagnets (see Fig. 1.5.5.1).

Weak ferromagnetism was first observed in the following trigonal crystals: the high-temperature modification of haematite, α-Fe_2O_3 (Townsend Smith, 1916; Néel & Pauthenet, 1952), $MnCO_3$ (Borovik-Romanov & Orlova, 1956) and later also in $CoCO_3$, $NiCO_3$ and $FeBO_3$. In accordance with theory, weak ferromagnetism does not occur in trigonal crystals with a positive anisotropy coefficient a. Such crystals become easy-axis antiferromagnets. Of this type are $FeCO_3$ and the low-temperature modification of α-Fe_2O_3. For four-sublattice antiferromagnets, the sequence of the directions of the magnetic moments of the sublattices is also essential. For example, the structures of the types $\boldsymbol{A}_1$ and $\boldsymbol{A}_2$ (see Fig. 1.5.3.4 and Table 1.5.3.3) do not exhibit weak ferromagnetism.

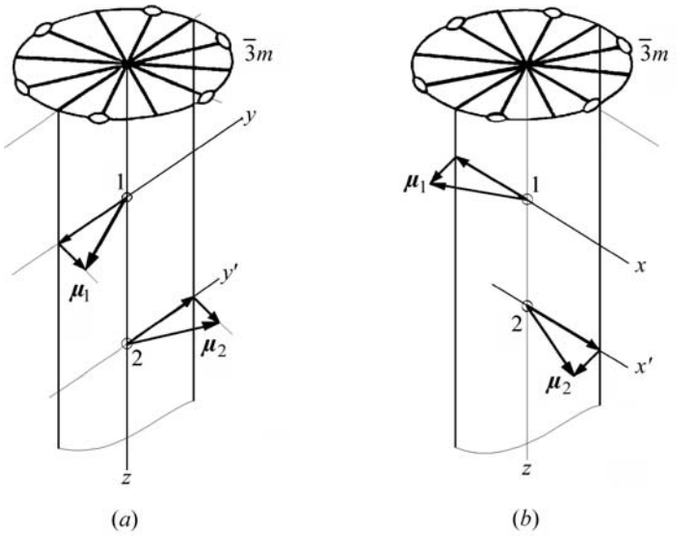

Fig. 1.5.5.1. Diagrams demonstrating two weakly ferromagnetic structures in rhombohedral crystals with two magnetic ions in the primitive cell (compare with Fig. 1.5.3.1). (*a*) Magnetic space group $P2/c$; (*b*) magnetic space group $P2'/c'$.

The behaviour of weak ferromagnets in magnetic fields applied perpendicular ($H_\perp$) and parallel ($H_\parallel$) to the trigonal axis is described by the following relations:

$$M_\perp = M_D + \chi_\perp H_\perp, \quad M_\parallel = \chi_\parallel H_\parallel, \tag{1.5.5.3}$$

where

$$\chi_\perp = 1/B, \quad \chi_\parallel = 1/(B+b). \tag{1.5.5.4}$$

An external magnetic field can freely rotate the ferromagnetic moment in the basal plane of the easy-plane weak ferromagnets under consideration because their anisotropy in the basal plane is extremely small. During such a rotation, both vectors **M** and **L** move simultaneously as a rigid structure. On the other hand, it is impossible to deflect the vector $\mathbf{M}_D$ out of the basal plane, as this is forbidden by symmetry. This is illustrated by the magnetization curves plotted in Fig. 1.5.5.2, which confirm the relations (1.5.5.3).

It is worth mentioning that when the weakly ferromagnetic structure is rotated in the basal plane, a change of the magnetic space groups occurs in the following order: $P2/c \leftrightarrow P\bar{1} \leftrightarrow P2'/c' \leftrightarrow P\bar{1} \leftrightarrow P2/c \leftrightarrow \ldots$. Each of these symmetry transformations corresponds to a second-order phase transition. Such transitions are allowed because $P\bar{1}$ is a subgroup of both groups $P2/c$ and $P2'/c'$.

NiF_2 was one of the first weak ferromagnets to be discovered (Matarrese & Stout, 1954). In the paramagnetic state, it is a tetragonal crystal. Its crystallographic space group is $\boldsymbol{D}_{4h}^{14} = P4_2/mnm$. In the ordered state its magnetic point group is $\boldsymbol{D}_{2h}(\boldsymbol{C}_{2h}) = mm'm'$ and the vectors **L** and **M** are directed along two twofold axes (one of which is primed) in the plane perpendicular to the former fourfold axis (see Fig. 1.5.5.3*a*). The invariant term responsible for the weak ferromagnetism in tetragonal fluorides has the form

$$d(L_x M_y + L_y M_x). \tag{1.5.5.5}$$

The anisotropy of the crystals of NiF_2 and the relation given above for the invariant lead to the same dependence on the magnetic field as for trigonal crystals. However, the anisotropy of the magnetic behaviour in the basal plane is much more complicated than for rhombohedral crystals (see Bazhan & Bazan, 1975). The anisotropy constant K_1 is positive for most other fluorides (MnF_2, FeF_2 and CoF_2) and their magnetic structure is described by the magnetic point group

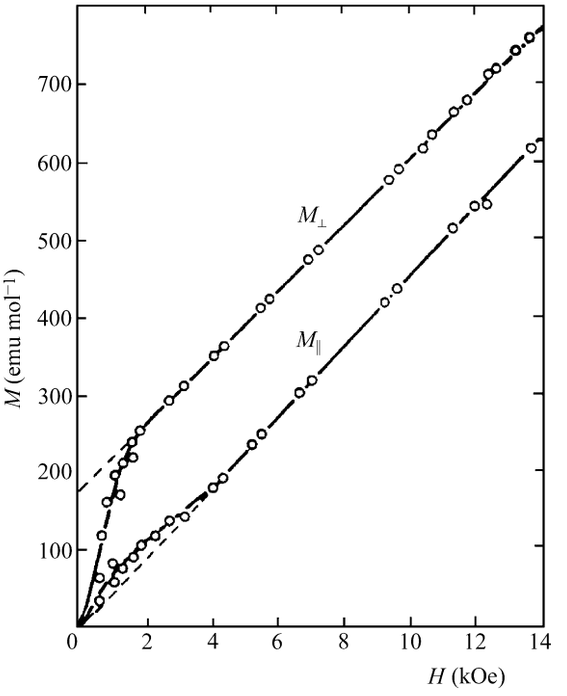

Fig. 1.5.5.2. Dependence of magnetization $M_\perp$ and $M_\parallel$ on the magnetic field H for the weak ferromagnet $MnCO_3$ at 4.2 K (Borovik-Romanov, 1959*a*).

$\boldsymbol{D}_{4h}(\boldsymbol{D}_{2h}) = 4'/mmm'$. They are easy-axis antiferromagnets without weak ferromagnetism.

The interaction described by the invariant $d(L_x M_y - L_y M_x)$ in equation (1.5.5.1) is called Dzyaloshinskii–Moriya interaction. It corresponds to the interaction between the spins of neighbouring ions, which can be represented in the form

$$\mathbf{d}[\mathbf{S}_i \times \mathbf{S}_j], \tag{1.5.5.6}$$

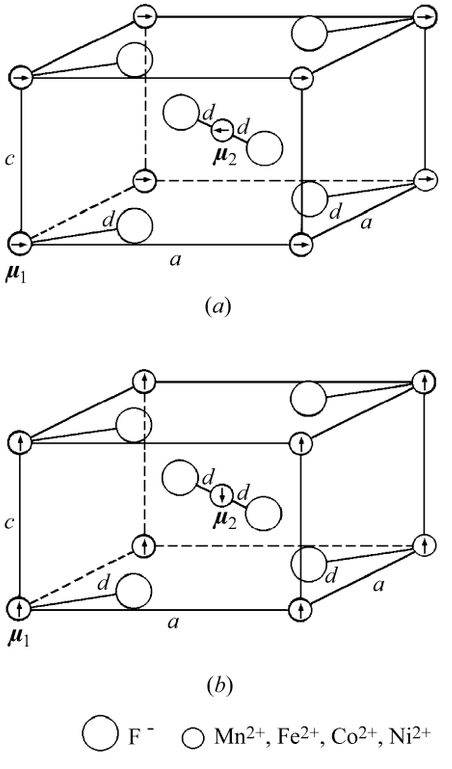

Fig. 1.5.5.3. Magnetic structures of fluorides of transition metals. (*a*) The weak ferromagnet NiF_2; (*b*) the easy-axis antiferromagnets MnF_2, FeF_2 and CoF_2.

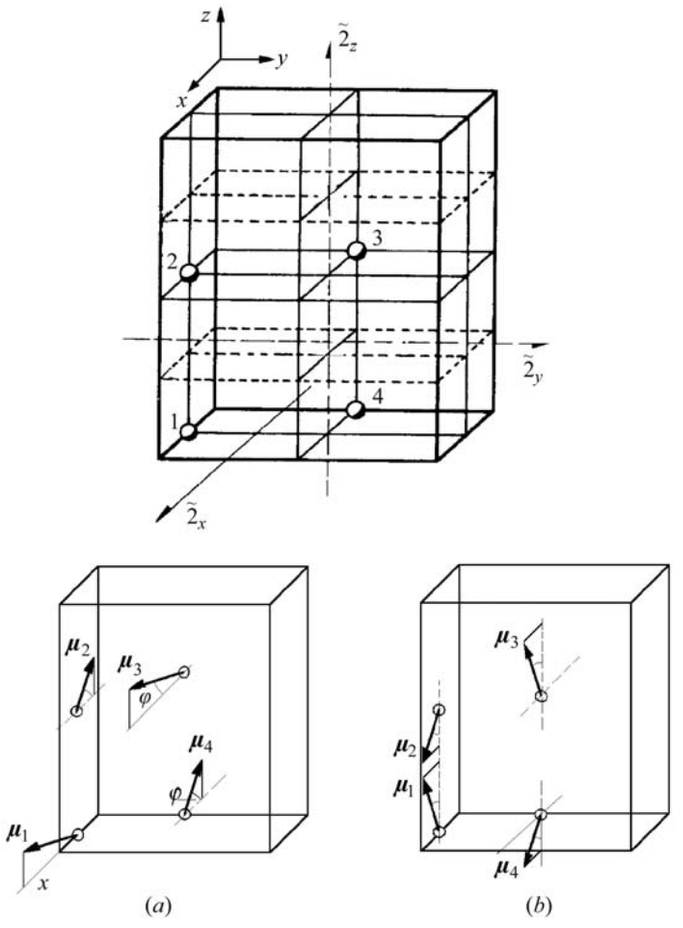

Fig. 1.5.5.4. Magnetic structures of orthoferrites and orthochromites RMO_3. (Only the transition-metal ions are shown; the setting *Pbnm* is used.) (*a*) $\boldsymbol{G}_x\boldsymbol{F}_z$ weakly ferromagnetic state; (*b*) $\boldsymbol{G}_z\boldsymbol{F}_x$ weakly ferromagnetic state.

where the vector **d** has the components $(0, 0, d_z)$. Terms of such type are allowed by symmetry for crystals that in the paramagnetic state belong to certain space groups of the trigonal, tetragonal and hexagonal systems. In some groups of the tetragonal system, weak ferromagnetism is governed by the term $d(L_xM_y + L_yM_x)$ (as for NiF_2) and in the orthorhombic system by $(d_1L_iM_k + d_2L_kM_i)$, $(i, k = x, y, z)$. In the monoclinic system, the latter sum contains four terms. The weak ferromagnetism in most groups of the hexagonal and cubic systems is governed by invariants of fourth and sixth order of L_i, M_k. Turov (1963) determined for all crystallographic space groups the form of the invariants of lowest order that allow for collinear or weakly non-collinear antiferromagnetic structures a phase transition into a state with weak ferromagnetism. The corresponding list of the numbers of the space groups that allow the transition into an antiferromagnetic state with weak ferromagnetism is given in Table 1.5.5.1. The form of the invariant responsible for weak ferromagnetism is also displayed in the table. Turov (1963) showed that weak ferromagnetism is forbidden for the triclinic system, for the six trigonal groups with point groups $C_3 = 3$ or $C_{3i} = \bar{3}$, and the 12 cubic groups with point groups $T = 23$ or $T_h = m\bar{3}$.

The microscopic theory of the origin of weak ferromagnetism was given by Moriya (1960*a*,*b*, 1963). In this chapter, however, we have restricted our consideration to the phenomenological approach to this problem.

A large number of orthorhombic orthoferrites and orthochromites with the formula RMO_3 (where R is a trivalent rare-earth ion and M is Fe^{3+} or Cr^{3+}) have been investigated in many laboratories (*cf.* Wijn, 1994). Some of them exhibit weak ferromagnetism. The space group of these compounds is $\boldsymbol{D}_{2h}^{16} = Pnma$ in the paramagnetic state. The primitive cell is the same in the paramagnetic and magnetically ordered states. It contains four magnetic transition-metal ions (see Fig. 1.5.5.4). They determine to a large extent the properties of orthoferrites (outside the region of very low temperatures). For a four-sublattice antiferromagnet, there are four possible linear combinations of the sublattice vectors, which define three types of antiferromagnetic vectors $\mathbf{L}_\alpha$ and one ferromagnetic vector **F** [see relations (1.5.3.2) and Table 1.5.3.1]. The exchange interaction in these compounds governs magnetic structures, which to a first approximation are described by the following antiferromagnetic vector (which is usually denoted by the symbol $\boldsymbol{G}$):

$$\boldsymbol{G} = \mathbf{L}_2 = (N/4)(\boldsymbol{\mu}_1 - \boldsymbol{\mu}_2 + \boldsymbol{\mu}_3 - \boldsymbol{\mu}_4). \qquad (1.5.5.7)$$

In the case of orthoferrites, the other two antiferromagnetic vectors $\mathbf{L}_1$ and $\mathbf{L}_3$ [see relations (1.5.3.2)] are named $\boldsymbol{A}$ and $\boldsymbol{C}$, respectively.

The magnetic structure of the compounds under consideration is usually called the $\boldsymbol{G}_i$ or $\boldsymbol{G}_i\boldsymbol{F}_k$ state. Depending on the signs and

Table 1.5.5.1. *The numbers of the crystallographic space groups that allow a phase transition into a weakly ferromagnetic state and the invariants of lowest order that are responsible for weak ferromagnetism*

Note that the standard numbering of space groups is used in this table, not the one employed by Turov (1963).

System	Nos. of the space groups	Invariants	Case No.
Monoclinic	3–15	M_xL_y, M_zL_y, M_yL_x, M_yL_z	1
Orthorhombic	16–74	M_xL_y, M_yL_x	2
		M_yL_z, M_zL_y	3
		M_xL_z, M_zL_x	4
Tetragonal	75–88	$M_xL_y + M_yL_x$, $M_xL_x - M_yL_y$	5
	89–142	$M_xL_y - M_yL_x$	6
		$M_xL_y + M_yL_x$	7
		$M_xL_x - M_yL_y$	8
Trigonal	149–167	$M_xL_y - M_yL_x$	9, 10
Hexagonal	168–176	$M_z(L_x \pm iL_y)^3$, $(M_x \pm iM_y)(L_x \pm iL_y)^2L_z$	11
	177–194	$M_xL_y - M_yL_x$	12
		$iM_z[(L_x + iL_y)^3 - (L_x - iL_y)^3]$, $i[(M_x + iM_y)(L_x + iL_y)^2 - (M_x - iM_y)(L_x - iL_y)^2]L_z$	13
		$M_z[(L_x + iL_y)^3 + (L_x - iL_y)^3]$, $[(M_x + iM_y)(L_x + iL_y)^2 + (M_x - iM_y)(L_x - iL_y)^2]L_z$	14
Cubic	207–230	$M_xL_x(L_y^2 - L_z^2) + M_yL_y(L_z^2 - L_x^2) + M_zL_z(L_x^2 - L_y^2)$	15

the values of the anisotropy constants, there are three possible magnetic states:

$$\text{(I)} \quad \boldsymbol{G}_x\boldsymbol{F}_z \quad L_{2x} \neq 0; \quad M_{Dz} \neq 0, \tag{1.5.5.8}$$

$$\text{(II)} \quad \boldsymbol{G}_y \quad L_{2y} \neq 0; \quad \mathbf{M}_D = 0, \tag{1.5.5.9}$$

$$\text{(III)} \quad \boldsymbol{G}_z\boldsymbol{F}_x \quad L_{2z} \neq 0; \quad M_{Dx} \neq 0. \tag{1.5.5.10}$$

The magnetic structures (I) and (III) are weak ferromagnets. They are displayed schematically in Fig. 1.5.5.4. Both are described by the same magnetic point group $\boldsymbol{D}_{2h}(\boldsymbol{C}_{2h})$ yet in different orientations: $m'm'm$ (*i.e.* $2'_x/m'_x\ 2'_y/m'_y\ 2_z/m_z$) for structure (I) and $mm'm'$ (*i.e.* $2_x/m_x\ 2'_y/m'_y\ 2'_z/m'_z$) for structure (III). The magnetic point group of structure (II) is $\boldsymbol{D}_{2h} = mmm$.

Weak ferromagnetism is observed in boracites with chemical formula $M_3B_7O_{13}X$ (where M = Co, Ni and X = Br, Cl, I). These compounds are unique, being simultaneously antiferromagnets, weak ferromagnets and ferroelectrics. Section 1.5.8.3 is devoted to these ferromagnetoelectrics.

Concerning the magnetic groups that allow weak ferromagnetism, it should be noted that, as for any ferromagnetism, weak ferromagnetism is allowed only in those space groups that have a trivial magnetic Bravais lattice. There must be at least two magnetic ions in the primitive cell to get antiferromagnetic order. Among the 31 magnetic point groups that admit ferromagnetism (see Table 1.5.2.4), weak ferromagnetism is forbidden in the magnetic groups belonging to the tetragonal, trigonal and hexagonal systems. Twelve magnetic point groups that allow weak ferromagnetism remain. These groups are listed in Table 1.5.5.2.

A material that becomes a weak ferromagnet below the Néel temperature T_N differs from a collinear antiferromagnet in its behaviour above T_N. A magnetic field applied to such a material above T_N gives rise to an ordered antiferromagnetic state with vector **L** directed perpendicular and magnetization **M** parallel to the field. Thus, as in usual ferromagnets, the magnetic symmetry of a weak ferromagnet in a magnetic field is the same above and below T_N. As a result, the magnetic susceptibility has a maximum at $T = T_N$ [like the relations (1.5.3.34) and (1.5.3.35)]. This is true only if the magnetic field is aligned along the easy axis for weak ferromagnetism. Fig. 1.5.5.5 shows the anomalous anisotropy of the temperature dependence of the magnetic susceptibility in the neighbourhood of T_N for weak ferromagnets.

Similar anomalies in the neighbourhood of T_N are observed in materials with a symmetry allowing a transition into a weakly ferromagnetic state for which the sign of the anisotropy constant causes their transition into purely antiferromagnetic states.

1.5.5.2. *Other weakly non-collinear magnetic structures*

A thermodynamic potential $\tilde{\Phi}$ of the form (1.5.5.1) may give rise not only to the weak ferromagnetism considered above but also to the reverse phenomenon. If the coefficient B (instead of A) changes its sign and $b > 0$, the material will undergo a transition into a slightly canted ferromagnetic structure, in which $M_s \gg L_D$ and the expression for L_D is

Table 1.5.5.2. *Magnetic point groups that allow weak ferromagnetism*

Schoenflies	Hermann–Mauguin
$\boldsymbol{C}_1$	1
$\boldsymbol{C}_i$	$\bar{1}$
$\boldsymbol{C}_2$	2
$\boldsymbol{C}_2(\boldsymbol{C}_1)$	$2'$
$\boldsymbol{C}_s$	m
$\boldsymbol{C}_s(\boldsymbol{C}_1)$	m'
$\boldsymbol{C}_{2h}$	$2/m$
$\boldsymbol{C}_{2h}(\boldsymbol{C}_i)$	$2'/m'$
$\boldsymbol{D}_2(\boldsymbol{C}_2)$	$22'2'$
$\boldsymbol{C}_{2v}(\boldsymbol{C}_2)$	$m'm'2$
$\boldsymbol{C}_{2v}(\boldsymbol{C}_s)$	$m'm2'$
$\boldsymbol{D}_{2h}(\boldsymbol{C}_{2h})$	$mm'm'$

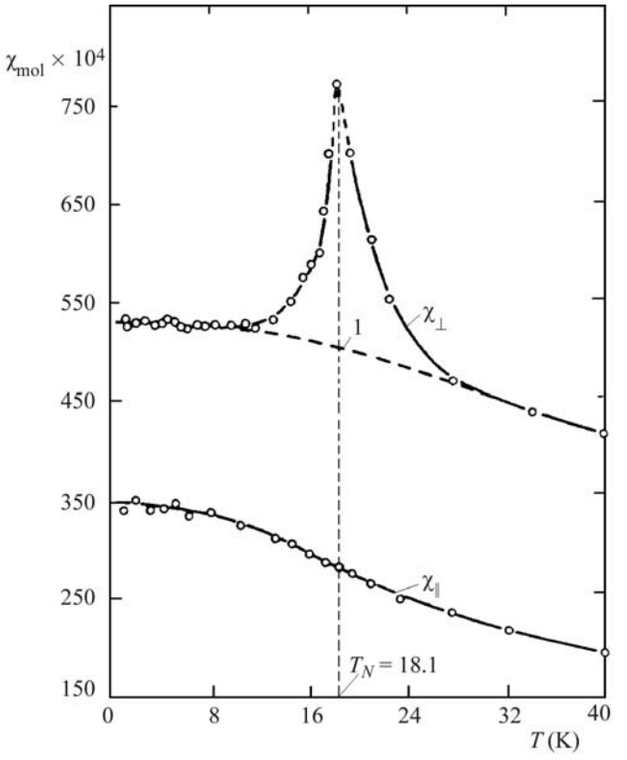

Fig. 1.5.5.5. Temperature dependence of the susceptibility for $CoCO_3$ (Borovik-Romanov & Ozhogin, 1960).

$$L_D = (d/B)M_{s\perp}. \tag{1.5.5.11}$$

Experimental detection of such structures is a difficult problem and to date no-one has observed such a phenomenon.

The thermodynamic potential $\tilde{\Phi}$ of a four-sublattice antiferromagnet may contain the mixed invariant [see (1.5.3.24)]

$$d_1(L_{1x}L_{2y} - L_{1y}L_{2x}). \tag{1.5.5.12}$$

Such a term gives rise to a structure in which all four vectors of sublattice magnetization $\mathbf{M}_\alpha$ form a star, as shown in Fig. 1.5.5.6 (see also Fig. 1.5.1.3*b*). The angle 2α between the vectors $\boldsymbol{\mu}_1$ and $\boldsymbol{\mu}_3$ (or $\boldsymbol{\mu}_2$ and $\boldsymbol{\mu}_4$) is equal to d_1/A_2 if the main antiferromagnetic structure is defined by the vector $\mathbf{l}_2$ [see relation (1.5.3.2)]. Such a structure may occur in Cr_2O_3. In most orthoferrites discussed above, such non-collinear structures are observed for all three cases: purely antiferromagnetic ($\boldsymbol{G}_y$) and weakly ferromagnetic ($\boldsymbol{G}_x\boldsymbol{F}_z$ and $\boldsymbol{G}_z\boldsymbol{F}_x$). The structure $\boldsymbol{G}_y$ is not coplanar. Apart from the main antiferromagnetic vector **G** aligned along the y axis, it possesses two other antiferromagnetic vectors: **A** (aligned along the x axis) and **C** (aligned along the z axis). The weakly ferromagnetic structure $\boldsymbol{G}_x\boldsymbol{F}_z$ has an admixture of the $\boldsymbol{A}_y$ antiferromagnetic structure.

The helical (or spiral) structure described in Section 1.5.1.2.3 and depicted in Fig. 1.5.1.4 is also a weakly non-collinear antiferromagnetic structure. As mentioned above, this structure consists of atomic layers in which all the magnetic moments are

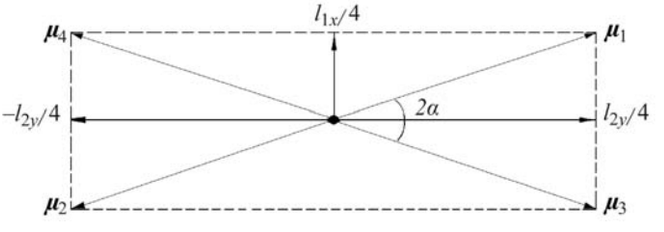

Fig. 1.5.5.6. A weakly non-collinear magnetic structure corresponding to (1.5.5.12).

parallel to each other and parallel to the layer. The magnetizations of neighbouring layers are antiparallel to a first approximation; but, more specifically, there is a small deviation from a strictly antiparallel alignment. The layers are perpendicular to a vector **k**, which is parallel to the axis of the helix. The two mutually perpendicular antiferromagnetic vectors $\mathbf{L}_\alpha$ are both perpendicular to **k**. These vectors define the helical structure by the following relation for the density of the magnetization $\mathbf{M}(\mathbf{r})$ in the layer with the coordinate **r** (Dzyaloshinskii, 1964; Andreev & Marchenko, 1980):

$$\mathbf{M}(\mathbf{r}) = \mathbf{L}_1 \sin \mathbf{kr} - \mathbf{L}_2 \cos \mathbf{kr}. \qquad (1.5.5.13)$$

Most helical structures are incommensurate, which means that the representation defined by the vector **k** does not satisfy the Lifshitz condition (see Section 1.5.3.3).

1.5.6. Reorientation transitions

In many materials, the anisotropy constants change sign at some temperature below the critical temperature. As a result, the direction of the vector **L** (or $\mathbf{M}_s$) changes relative to the crystallographic axes. Correspondingly, the magnetic symmetry of the material also changes. Such phase transitions are called reorientation transitions.

Cobalt is a typical ferromagnet and experiences two such reorientation transitions. It is a hexagonal crystal, which at low temperatures behaves as an easy-axis ferromagnet; its magnetic point group is $\boldsymbol{D}_{6h}(\boldsymbol{C}_{6h}) = 6/mm'm'$. If the anisotropy energy were described by the relations (1.5.3.6) and (1.5.3.7) with only one anisotropy constant K_1, the change of the sign of this constant would give rise to a first-order transition from an easy-axis to an easy-plane antiferromagnet. This transition would occur at the temperature T_c at which $K_1(T) = 0$. In fact, the polar angle θ which determines the direction of the spontaneous magnetization increases progressively over a finite temperature interval. The behaviour of θ during the process of this reorientation may be obtained by minimizing the expression of the anisotropy energy (1.5.3.10), which contains two anisotropy coefficients K_1 and K_2. If $K_2 > 0$, the minimum of U_a corresponds to three magnetic phases, which belong to the following magnetic point groups:

(1) $\boldsymbol{D}_{6h}(\boldsymbol{C}_{6h}) = 6/mm'm'$; for this phase $\theta = 0, \pi$. It is realized at temperatures $T < T_1 = 520$ K, where $K_1 > 0$.

(2) $\boldsymbol{C}_{2h}(\boldsymbol{C}_i) = 2'/m'$; for this phase $\sin\theta = \pm(-K_1/2K_2)^{1/2}$. It is realized at temperatures $T_1 = 520 < T < T_2 = 580$ K, where $-2K_2 < K_1 < 0$.

(3) $\boldsymbol{D}_{2h}(\boldsymbol{C}_{2h}) = mm'm'$; for this phase $\theta = \pi/2$. It is realized at temperatures $T_2 = 580 < T < T_c = 690$ K, where $K_1 < -2K_2$.

The low-temperature phase is of the easy-axis type and the high-temperature phase is of the easy-plane type. The intermediate phase is called the angular phase. The two second-order phase transitions occur at temperatures which are the roots of the two equations

$$K_1(T_1) = 0; \quad K_1(T_2) + 2K_2(T_2) = 0. \qquad (1.5.6.1)$$

The chain of these transitions (including the transition to the paramagnetic state at $T = T_c$) may be represented by the following chain of the corresponding magnetic point groups:

$$\begin{aligned} \boldsymbol{D}_{6h}(\boldsymbol{C}_{6h}) = 6/mm'm' &\longleftrightarrow \boldsymbol{C}_{2h}(\boldsymbol{C}_i) = 2'/m' \\ &\longleftrightarrow \boldsymbol{D}_{2h}(\boldsymbol{C}_{2h}) = mm'm' \\ &\longleftrightarrow (\boldsymbol{D}_{6h} + \boldsymbol{R}\boldsymbol{D}_{6h}) = 6/mmm1'. \end{aligned}$$

In Co and most of the other ferromagnets, the rotation of the spontaneous magnetization described above may be obtained by applying an external magnetic field in an appropriate direction. In many antiferromagnets, there occur similar reorientation transitions, which cannot be achieved by means of a magnetic field.

The first reorientation transition in antiferromagnets was observed in haematite (α-Fe_2O_3), which at room temperature is a weak ferromagnet with magnetic structure $\boldsymbol{A}_{3x}$ or $\boldsymbol{A}_{3y}$ (see Tables 1.5.3.3 and 1.5.3.4 in Section 1.5.3.1). Morin (1950) found that the weak ferromagnetism in haematite disappears below $T_M \simeq 260$ K. At low temperature, haematite becomes an easy-axis antiferromagnet with the structure $\boldsymbol{A}_{3z}$. Unlike in cobalt, the transition at T_M is a first-order transition in haematite. This is so because the anisotropy constant K_2 is negative in haematite. As a result, there are only two solutions for the angle θ that lead to a minimum of the anisotropy energy $U_a(3)$ [(1.5.3.9)], $\theta = 0$ if $K_1 > -K_2$ and $\theta = \pi/2$ if $K_1 < -K_2$. The transition temperature T_M is defined by

$$K_1(T_M) + K_2(T_M) = 0. \qquad (1.5.6.2)$$

There is the following change in the magnetic space groups at this transition:

$$R\bar{3}c' \overset{T_M}{\longleftrightarrow} \begin{cases} P2/c & (1.5.6.3) \\ P2'/c' & (1.5.6.4) \end{cases}$$

Which of the two groups is realized at high temperatures depends on the sign of the anisotropy constant $K'_\perp$ in equation (1.5.3.9). Neither of the high-temperature magnetic space groups is a subgroup of the low-temperature group. Therefore the transition under consideration cannot be a second-order transition.

Reorientation transitions have been observed in many orthoferrites and orthochromites. Orthoferrites of Ho, Er, Tm, Nd, Sm and Dy possess the structure $\boldsymbol{G}_x\boldsymbol{F}_z$ [see (1.5.5.8)] at room temperature. The first five of them undergo reorientation transitions to the structure $\boldsymbol{G}_z\boldsymbol{F}_x$ at lower temperatures. This reorientation occurs gradually, as in Co. Both vectors **L** and $\mathbf{M}_D$ rotate simultaneously, as shown in Fig. 1.5.6.1. These vectors remain perpendicular to each other, but the value of $\mathbf{M}_D$ varies from $(d_1/B)L$ for M_{Dz} to $(d_2/B)L$ for M_{Dx}. The coefficients d_1 and d_2 belong to the terms L_xM_z and L_zM_x, respectively. The following magnetic point groups are observed when these transitions occur:

$$\frac{2'_x}{m'_x}\frac{2'_y}{m'_y}\frac{2_z}{m_z} \overset{T_1}{\longleftrightarrow} \frac{2'_y}{m'_y} \overset{T_2}{\longleftrightarrow} \frac{2_x}{m_x}\frac{2'_y}{m'_y}\frac{2'_z}{m'_z}. \qquad (1.5.6.5)$$

Anomalies typical for second-order transitions were observed at the temperatures T_1 and T_2. The interval $T_2 - T_1$ varies from 10 to 100 K.

At low temperatures, $DyFeO_3$ is an easy-axis antiferromagnet without weak ferromagnetism – $\boldsymbol{G}_y$. It belongs to the trivial magnetic point group $\boldsymbol{D}_{2h} = mmm$. At $T_M = 40$ K, $DyFeO_3$ transforms into a weak ferromagnet $\boldsymbol{G}_x\mathbf{F}_z$. This is a first-order reorientation transition of the type

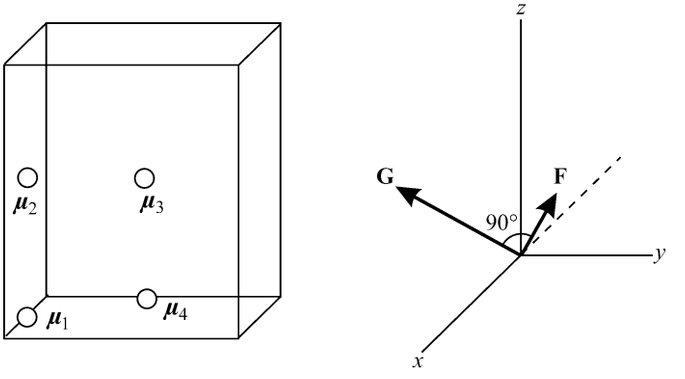

Fig. 1.5.6.1. Schematic representation of the rotation of the vectors **G** and **F** (in the *xz* plane) at a reorientation transition in orthoferrites.

$$\boldsymbol{D}_{2h} = mmm \overset{T_M}{\longleftrightarrow} \boldsymbol{D}_{2h}(\boldsymbol{C}_{2h}) = m'm'm. \qquad (1.5.6.6)$$

Reorientation transitions in antiferromagnets occur not only as a result of a sign change of the anisotropy constant. They can be governed by the applied magnetic field. In Section 1.5.3.3.2, we described the spin-flop first-order reorientation transition in an easy-axis antiferromagnet. This transition splits into two second-order transitions if the magnetic field is not strictly parallel to the axis of the crystal. There is a specific type of reorientation transition, which occurs in antiferromagnets that do not exhibit weak ferromagnetism, but would become weak ferromagnets if the antiferromagnetic vector was directed along another crystallographic direction. As an example, let us consider such a transition in CoF_2. It is a tetragonal crystal with crystallographic space group $\boldsymbol{D}_{4h}^{14} = P4_2/mnm$. Below T_N, CoF_2 becomes an easy-axis antiferromagnet. The magnetic structure of this crystal is shown in Fig. 1.5.5.3. Its magnetic point group is $\boldsymbol{D}_{4h}(\boldsymbol{D}_{2h}) = 4'/mmm'$. Let us apply the magnetic field H parallel to the twofold axis x (see Fig. 1.5.6.2). In a typical antiferromagnet, the field stimulates a magnetization $M = \chi_\perp H$. The structure $\boldsymbol{D}_{4h}^{14} = P4_2/mnm$ allows weak ferromagnetism if **L** is perpendicular to the z axis. As a result, if the vector **L** is deflected from the z axis by an angle θ in the plane yz perpendicular to the x axis, the magnetization will rise according to the relation

$$M = \chi_\perp(H + H_D \sin\theta), \qquad (1.5.6.7)$$

where $H_D = M_D/\chi_\perp$ [see (1.5.5.3) and (1.5.5.4)]. As a result, there is a gain in the magnetic energy, which compensates the loss in the anisotropy energy. The beginning of the deflection is a second-order transition. The balance of both energies determines the value of θ:

$$\sin\theta = (H_e/H_a H_D)H. \qquad (1.5.6.8)$$

The second second-order transition occurs when θ becomes equal to $\pi/2$ at the critical field H_c:

$$H_c = H_D H_a/H_e. \qquad (1.5.6.9)$$

After the reorientation transition, CoF_2 has the same magnetic point group as the weak ferromagnet NiF_2, *i.e.* $\boldsymbol{D}_{2h}(\boldsymbol{C}_{2h}) = mm'm'$.

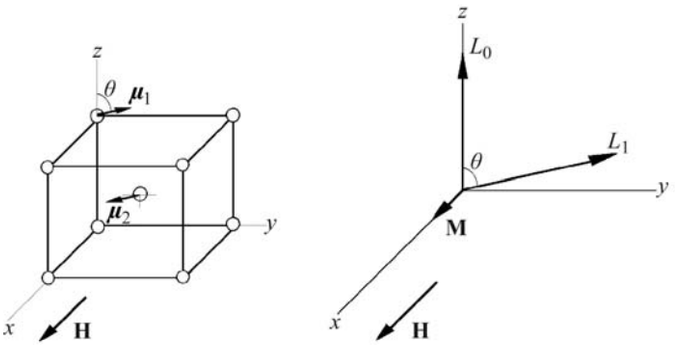

Fig. 1.5.6.2. Schematic representation of the rotation of the vector **L** under the action of a magnetic field applied to CoF_2 perpendicular to the fourfold axis z (reorientation transition) (see Figs. 1.5.5.3*a* and *b*).

1.5.7. Piezomagnetism

As we have seen, the appearance of weak ferromagnetism in antiferromagnets is closely connected with their magnetic symmetry. If the magnetic point group of the antiferromagnetic crystal contains an axis of higher than twofold symmetry, the magnetic structure is purely antiferromagnetic. By applying an external force that disturbs the symmetry of the crystal and destroys the axis of high symmetry, one may create a structure possessing weak ferromagnetism. In the previous section, we considered such reduction of the symmetry with the aid of a magnetic field applied perpendicular to the main axis of the crystal. Another possibility for symmetry reduction is to apply an external pressure and to deform the crystal. Thus, in some antiferromagnetic crystals, a ferromagnetic moment may be produced on application of external stress. This phenomenon is called piezomagnetism.

To investigate the piezomagnetic effect from the phenomenological point of view, we have to add the terms of the magnetoelastic energy in the expansion of the thermodynamic potential. The magnetoelastic terms of the least degree in the expansion of the thermodynamic potential $\tilde{\Phi}$ for a given stable magnetic structure will be of the type $T_{ij}M_kL_l$ (T_{ij} are the components of the elastic stress tensor **T**). These terms must be invariant relative to the crystallographic group of the material under examination.

If we consider the potential Φ, which is a function of T, **T**, **H**, the terms of the magnetoelastic energy that are responsible for piezomagnetism are of the form $H_i T_{jk}$. Thus, for the piezomagnetic crystals the expansion of the thermodynamic potential should be expressed by

$$\Phi(T, \mathbf{T}, \mathbf{H}) = \Phi_0(T, \mathbf{H}) - \sum_{i,j,k} \Lambda_{ijk} H_i T_{jk}. \qquad (1.5.7.1)$$

If at least one term of this expansion remains invariant under the magnetic symmetry of the given crystal, then the corresponding component Λ_{ijk} will not be zero and hence

$$M_i = -\partial\Phi/\partial H_i = -\partial\Phi_0/\partial H_i + \Lambda_{ijk} T_{jk}. \qquad (1.5.7.2)$$

Thus, when a stress T_{jk} is applied, a magnetic moment is produced which is linear with the stress.

It follows from expression (1.5.7.1) that the converse of the piezomagnetic effect also exists, *i.e.* linear magnetostriction:

$$S_{jk} = -\partial\Phi/\partial T_{jk} = \Lambda_{ijk} H_i, \qquad (1.5.7.3)$$

where S_{jk} are the components of the deformation tensor.

1.5.7.1. *Piezomagnetic effect*

The possibility of the existence of a piezomagnetic effect was first foreseen by Voigt (1928). However, he assumed that it is sufficient to consider only the crystallographic symmetry in order to predict this effect. In reality, the crystals that do not possess a magnetic structure are characterized by the transformation R being contained in the magnetic group as an independent element. The transformation R changes the sign of the magnetic vectors **H**, **L**, **M**. Hence, for such crystals all values of Λ_{ijk} vanish and piezomagnetism is forbidden. The magnetic groups of magnetically ordered crystals (ferromagnets and antiferromagnets) contain R only in combination with other elements of symmetry, or do not contain this transformation at all. Hence the piezomagnetic effect may occur in such crystals. This statement was first made by Tavger & Zaitsev (1956). The most interesting manifestation of the piezomagnetic effect is observed in antiferromagnets, as there is no spontaneous magnetization in these materials.

From equation (1.5.7.1) it follows that Λ_{ijk} is an axial tensor of third rank. Hence, apart from the restriction that piezomagnetism is forbidden for all para- and diamagnetic materials, it must be absent from the 21 magnetic point groups that contain the element $C_i R = \bar{1}'$ (see Table 1.5.7.1). The stress tensor T_{jk} is symmetrical ($T_{jk} = T_{kj}$); see Section 1.3.2.4. Thus the tensor Λ_{ijk} is symmetrical in its last two indices. This is the reason why piezomagnetism is prohibited for three more magnetic point groups: $\boldsymbol{O} = 432$, $\boldsymbol{T}_d = \bar{4}3m$ and $\boldsymbol{O}_h = m\bar{3}m$. The remaining 66 magnetic point groups were found by Tavger (1958), who also

Table 1.5.7.1. *The forms of the matrix characterizing the piezomagnetic effect*

Magnetic crystal class		Matrix representation $\Lambda_{i\alpha}$ of the piezomagnetic tensor
Schoenflies	Hermann–Mauguin	
$\boldsymbol{C}_1$ $\boldsymbol{C}_i$	1 $\bar{1}$	$\begin{bmatrix} \Lambda_{11} & \Lambda_{12} & \Lambda_{13} & \Lambda_{14} & \Lambda_{15} & \Lambda_{16} \\ \Lambda_{21} & \Lambda_{22} & \Lambda_{23} & \Lambda_{24} & \Lambda_{25} & \Lambda_{26} \\ \Lambda_{31} & \Lambda_{32} & \Lambda_{33} & \Lambda_{34} & \Lambda_{35} & \Lambda_{36} \end{bmatrix}$
$\boldsymbol{C}_2$ $\boldsymbol{C}_s$ $\boldsymbol{C}_{2h}$	$2\,(=121)$ $m\,(=1m1)$ $2/m\,(=1\,2/m\,1)$ (unique axis y)	$\begin{bmatrix} 0 & 0 & 0 & \Lambda_{14} & 0 & \Lambda_{16} \\ \Lambda_{21} & \Lambda_{22} & \Lambda_{23} & 0 & \Lambda_{25} & 0 \\ 0 & 0 & 0 & \Lambda_{34} & 0 & \Lambda_{36} \end{bmatrix}$
$\boldsymbol{C}_2(\boldsymbol{C}_1)$ $\boldsymbol{C}_s(\boldsymbol{C}_1)$ $\boldsymbol{C}_{2h}(\boldsymbol{C}_i)$	$2'\,(=12'1)$ $m'\,(=1m'1)$ $2'/m'\,(=1\,2'/m'\,1)$ (unique axis y)	$\begin{bmatrix} \Lambda_{11} & \Lambda_{12} & \Lambda_{13} & 0 & \Lambda_{15} & 0 \\ 0 & 0 & 0 & \Lambda_{24} & 0 & \Lambda_{26} \\ \Lambda_{31} & \Lambda_{32} & \Lambda_{33} & 0 & \Lambda_{35} & 0 \end{bmatrix}$
$\boldsymbol{D}_2$ $\boldsymbol{C}_{2v}$ $\boldsymbol{D}_{2h}$	222 $mm2\,[2mm, m2m]$ mmm	$\begin{bmatrix} 0 & 0 & 0 & \Lambda_{14} & 0 & 0 \\ 0 & 0 & 0 & 0 & \Lambda_{25} & 0 \\ 0 & 0 & 0 & 0 & 0 & \Lambda_{36} \end{bmatrix}$
$\boldsymbol{D}_2(\boldsymbol{C}_2)$ $\boldsymbol{C}_{2v}(\boldsymbol{C}_2)$ $\boldsymbol{C}_{2v}(\boldsymbol{C}_s)$ $\boldsymbol{D}_{2h}(\boldsymbol{C}_{2h})$	$2'2'2$ $m'm'2$ $m'2'm\,[2'm'm]$ $m'm'm$	$\begin{bmatrix} 0 & 0 & 0 & 0 & \Lambda_{15} & 0 \\ 0 & 0 & 0 & \Lambda_{24} & 0 & 0 \\ \Lambda_{31} & \Lambda_{32} & \Lambda_{33} & 0 & 0 & 0 \end{bmatrix}$
$\boldsymbol{C}_4,\ \boldsymbol{C}_6$ $\boldsymbol{S}_4,\ \boldsymbol{C}_{3h}$ $\boldsymbol{C}_{4h},\ \boldsymbol{C}_{6h}$	$\bar{4},\ \bar{6}$ $\bar{4},\ \bar{6}$ $4/m,\ 6/m$	$\begin{bmatrix} 0 & 0 & 0 & \Lambda_{14} & \Lambda_{15} & 0 \\ 0 & 0 & 0 & \Lambda_{15} & -\Lambda_{14} & 0 \\ \Lambda_{31} & \Lambda_{31} & \Lambda_{33} & 0 & 0 & 0 \end{bmatrix}$
$\boldsymbol{C}_4(\boldsymbol{C}_2)$ $\boldsymbol{S}_4(\boldsymbol{C}_2)$ $\boldsymbol{C}_{4h}(\boldsymbol{C}_{2h})$	$4'$ $\bar{4}'$ $4'/m$	$\begin{bmatrix} 0 & 0 & 0 & \Lambda_{14} & \Lambda_{15} & 0 \\ 0 & 0 & 0 & -\Lambda_{15} & \Lambda_{14} & 0 \\ \Lambda_{31} & -\Lambda_{31} & 0 & 0 & 0 & \Lambda_{36} \end{bmatrix}$
$\boldsymbol{D}_4,\ \boldsymbol{D}_6$ $\boldsymbol{C}_{4v},\ \boldsymbol{C}_{6v}$ $\boldsymbol{D}_{2d},\ \boldsymbol{D}_{3h}$ $\boldsymbol{D}_{4h},\ \boldsymbol{D}_{6h}$	$422,\ 622$ $4mm,\ 6mm$ $\bar{4}2m\,[\bar{4}m2],\ \bar{6}m2\,[\bar{6}2m]$ $4/mmm,\ 6/mmm$	$\begin{bmatrix} 0 & 0 & 0 & \Lambda_{14} & 0 & 0 \\ 0 & 0 & 0 & 0 & -\Lambda_{14} & 0 \\ 0 & 0 & 0 & 0 & 0 & 0 \end{bmatrix}$
$\boldsymbol{D}_4(\boldsymbol{C}_4),\ \boldsymbol{D}_6(\boldsymbol{C}_6)$ $\boldsymbol{C}_{4v}(\boldsymbol{C}_4),\ \boldsymbol{C}_{6v}(\boldsymbol{C}_6)$ $\boldsymbol{D}_{2d}(\boldsymbol{S}_4),\ \boldsymbol{D}_{3h}(\boldsymbol{C}_{3h})$ $\boldsymbol{D}_{4h}(\boldsymbol{C}_{4h}),\ \boldsymbol{D}_{6h}(\boldsymbol{C}_{6h})$	$42'2',\ 62'2'$ $4m'm',\ 6m'm'$ $\bar{4}2'm'\,[\bar{4}m'2'],\ \bar{6}m'2'\,[\bar{6}2'm']$ $4/mm'm',\ 6/mm'm'$	$\begin{bmatrix} 0 & 0 & 0 & 0 & \Lambda_{15} & 0 \\ 0 & 0 & 0 & \Lambda_{15} & 0 & 0 \\ \Lambda_{31} & \Lambda_{31} & \Lambda_{33} & 0 & 0 & 0 \end{bmatrix}$
$\boldsymbol{D}_4(\boldsymbol{D}_2)$ $\boldsymbol{C}_{4v}(\boldsymbol{C}_{2v})$ $\boldsymbol{D}_{2d}(\boldsymbol{D}_2),\ \boldsymbol{D}_{2d}(\boldsymbol{C}_{2v})$ $\boldsymbol{D}_{4h}(\boldsymbol{D}_{2h})$	$4'22'$ $4'mm'$ $\bar{4}'2m',\ \bar{4}'m2'$ $4'/mmm'$	$\begin{bmatrix} 0 & 0 & 0 & \Lambda_{14} & 0 & 0 \\ 0 & 0 & 0 & 0 & \Lambda_{14} & 0 \\ 0 & 0 & 0 & 0 & 0 & \Lambda_{36} \end{bmatrix}$
$\boldsymbol{C}_3$ $\boldsymbol{S}_6$	3 $\bar{3}$	$\begin{bmatrix} \Lambda_{11} & -\Lambda_{11} & 0 & \Lambda_{14} & \Lambda_{15} & -2\Lambda_{22} \\ -\Lambda_{22} & \Lambda_{22} & 0 & \Lambda_{15} & -\Lambda_{14} & -2\Lambda_{11} \\ \Lambda_{31} & \Lambda_{31} & \Lambda_{33} & 0 & 0 & 0 \end{bmatrix}$
$\boldsymbol{D}_3$ $\boldsymbol{C}_{3v}$ $\boldsymbol{D}_{3d}$	$32\,(=321)$ $3m\,(=3m1)$ $\bar{3}m\,(=\bar{3}m1)$	$\begin{bmatrix} \Lambda_{11} & -\Lambda_{11} & 0 & \Lambda_{14} & 0 & 0 \\ 0 & 0 & 0 & 0 & -\Lambda_{14} & -2\Lambda_{11} \\ 0 & 0 & 0 & 0 & 0 & 0 \end{bmatrix}$
$\boldsymbol{D}_3(\boldsymbol{C}_3)$ $\boldsymbol{C}_{3v}(\boldsymbol{C}_3)$ $\boldsymbol{D}_{3d}(\boldsymbol{S}_6)$	$32'\,(=32'1)$ $3m'\,(=3m'1)$ $\bar{3}m'\,(=\bar{3}m'1)$	$\begin{bmatrix} 0 & 0 & 0 & 0 & \Lambda_{15} & -2\Lambda_{22} \\ -\Lambda_{22} & \Lambda_{22} & 0 & \Lambda_{15} & 0 & 0 \\ \Lambda_{31} & \Lambda_{31} & \Lambda_{33} & 0 & 0 & 0 \end{bmatrix}$
$\boldsymbol{C}_6(\boldsymbol{C}_3)$ $\boldsymbol{C}_{3h}(\boldsymbol{C}_3)$ $\boldsymbol{C}_{6h}(\boldsymbol{S}_6)$	$6'$ $\bar{6}'$ $6'/m'$	$\begin{bmatrix} \Lambda_{11} & -\Lambda_{11} & 0 & 0 & 0 & -2\Lambda_{22} \\ -\Lambda_{22} & \Lambda_{22} & 0 & 0 & 0 & -2\Lambda_{11} \\ 0 & 0 & 0 & 0 & 0 & 0 \end{bmatrix}$
$\boldsymbol{D}_6(\boldsymbol{D}_3)$ $\boldsymbol{C}_{6v}(\boldsymbol{C}_{3v})$ $\boldsymbol{D}_{3h}(\boldsymbol{D}_3),\ \boldsymbol{D}_{3h}(\boldsymbol{C}_{3v})$ $\boldsymbol{D}_{6h}(\boldsymbol{D}_{3d})$	$6'22'$ $6'mm'$ $\bar{6}'2m',\ \bar{6}'m2'$ $6'/m'mm'$	$\begin{bmatrix} \Lambda_{11} & -\Lambda_{11} & 0 & 0 & 0 & 0 \\ 0 & 0 & 0 & 0 & 0 & -2\Lambda_{11} \\ 0 & 0 & 0 & 0 & 0 & 0 \end{bmatrix}$
$\boldsymbol{T},\ \boldsymbol{T}_h$ $\boldsymbol{O}(\boldsymbol{T})$ $\boldsymbol{T}_d(\boldsymbol{T})$ $\boldsymbol{O}_h(\boldsymbol{T}_h)$	$23,\ m\bar{3}$ $4'32'$ $\bar{4}'3m'$ $m\bar{3}m'$	$\begin{bmatrix} 0 & 0 & 0 & \Lambda_{14} & 0 & 0 \\ 0 & 0 & 0 & 0 & \Lambda_{14} & 0 \\ 0 & 0 & 0 & 0 & 0 & \Lambda_{14} \end{bmatrix}$

constructed the 16 corresponding forms of the piezomagnetic tensors appropriate to each point group. They are represented in Table 1.5.7.1. (See also Birss & Anderson, 1963; Birss, 1964.)

Since the stress tensor T_{jk} is symmetrical, it has only six independent components. Therefore the notation of its components can be replaced by a matrix notation (Voigt's notation, see Section 1.3.2.5) in the following manner:

Tensor notation	Matrix notation
T_{11}	T_1
T_{22}	T_2
T_{33}	T_3
T_{23}, T_{32}	T_4
T_{31}, T_{13}	T_5
T_{12}, T_{21}	T_6

In matrix notation, equation (1.5.7.2) may be written in the form

$$M_i = \Lambda_{i\alpha} T_\alpha, \tag{1.5.7.4}$$

where $i = 1, 2, 3$ and $\alpha = 1, 2, 3, 4, 5, 6$. These notations are used in Table 1.5.7.1. Notice that $\Lambda_{ij} = \Lambda_{ijj}$ for $j = 1, 2, 3$, $\Lambda_{i4} = 2\Lambda_{i23}$, $\Lambda_{i5} = 2\Lambda_{i31}$, and $\Lambda_{i6} = 2\Lambda_{i12}$.

The form of the matrix $\Lambda_{i\alpha}$ depends on the orientation of the axes of the Cartesian coordinate system (CCS) with respect to the symmetry axes of the point group of the crystal under consideration. These symmetry axes may be rotation axes, rotoinversion axes or mirror-plane normals, all possibly combined with time reversal. The usual orientations of the CCS with respect to the symmetry axes can be expressed by the order of the entries in the Hermann–Mauguin symbol. An entry consists (apart from possible primes and bars) of a number $N = 1, 2, 3, 4$ or 6 or the letter m or N/m ($= \frac{N}{m}$). The conventional rules will be followed: in the monoclinic and orthorhombic crystal systems the x, y and z axes of the CCS are parallel to the symmetry axes given in the first, second and third entries, respectively. In the monoclinic system, there is only one symmetry axis, which is usually chosen parallel to the y axis, and a short Hermann–Mauguin symbol with only one entry is usually used, *e.g.* $2/m$ instead of $1\,2/m\,1$. In the trigonal and hexagonal systems, the z, x and y axes are parallel to the symmetry axes given in the first, second and third entries, respectively. In the tetragonal system, the z axis is parallel to the symmetry axis given in the first entry, and the x and y axes are parallel to the symmetry axes given in the second entry, which appear in two mutually perpendicular directions. In the cubic system, the symmetry axes given in the first entry appear in three mutually perpendicular directions; the x, y and z axes of the CCS are chosen parallel to these directions. Alternative orientations of the same point group that give rise to the same form of $\Lambda_{i\alpha}$ have been added between square brackets [] in Table 1.5.7.1. Notice that the Schoenflies notation does not allow us to distinguish different orientations of the CCS with respect to the symmetry axes.

The forms of $\Lambda_{i\alpha}$ for frequently encountered orientations of the CCS other than those given in Table 1.5.7.1 are

(1) $112, 11m, 11\,2/m$ (unique axis z):

$$\begin{bmatrix} 0 & 0 & 0 & \Lambda_{14} & \Lambda_{15} & 0 \\ 0 & 0 & 0 & \Lambda_{24} & \Lambda_{25} & 0 \\ \Lambda_{31} & \Lambda_{32} & \Lambda_{33} & 0 & 0 & \Lambda_{36} \end{bmatrix};$$

(2) $112', 11m', 11\,2'/m'$ (unique axis z):

$$\begin{bmatrix} \Lambda_{11} & \Lambda_{12} & \Lambda_{13} & 0 & 0 & \Lambda_{16} \\ \Lambda_{21} & \Lambda_{22} & \Lambda_{23} & 0 & 0 & \Lambda_{26} \\ 0 & 0 & 0 & \Lambda_{34} & \Lambda_{35} & 0 \end{bmatrix};$$

(3) $22'2', 2m'm', mm'2'$ $[m2'm']$, $mm'm'$:

$$\begin{bmatrix} \Lambda_{11} & \Lambda_{12} & \Lambda_{13} & 0 & 0 & 0 \\ 0 & 0 & 0 & 0 & 0 & \Lambda_{26} \\ 0 & 0 & 0 & 0 & \Lambda_{35} & 0 \end{bmatrix};$$

(4) $2'22', m'2m', 2'mm'$ $[m'm2']$, $m'mm'$:

$$\begin{bmatrix} 0 & 0 & 0 & 0 & 0 & \Lambda_{16} \\ \Lambda_{21} & \Lambda_{22} & \Lambda_{23} & 0 & 0 & 0 \\ 0 & 0 & 0 & \Lambda_{34} & 0 & 0 \end{bmatrix};$$

(5) $4'2'2, 4'm'm, \bar{4}'m'2, \bar{4}'2'm, 4'/mm'm$:

$$\begin{bmatrix} 0 & 0 & 0 & 0 & \Lambda_{15} & 0 \\ 0 & 0 & 0 & -\Lambda_{15} & 0 & 0 \\ \Lambda_{31} & -\Lambda_{31} & 0 & 0 & 0 & 0 \end{bmatrix};$$

(6) $6'2'2, 6'm'm, \bar{6}'m'2, \bar{6}'2'm, 6'/m'm'm$:

$$\begin{bmatrix} 0 & 0 & 0 & 0 & 0 & -2\Lambda_{22} \\ -\Lambda_{22} & \Lambda_{22} & 0 & 0 & 0 & 0 \\ 0 & 0 & 0 & 0 & 0 & 0 \end{bmatrix};$$

(7) $312, 31m, \bar{3}1m$:

$$\begin{bmatrix} 0 & 0 & 0 & \Lambda_{14} & 0 & -2\Lambda_{22} \\ -\Lambda_{22} & \Lambda_{22} & 0 & 0 & -\Lambda_{14} & 0 \\ 0 & 0 & 0 & 0 & 0 & 0 \end{bmatrix};$$

(8) $312', 31m', \bar{3}1m'$:

$$\begin{bmatrix} \Lambda_{11} & -\Lambda_{11} & 0 & 0 & \Lambda_{15} & 0 \\ 0 & 0 & 0 & \Lambda_{15} & 0 & -2\Lambda_{11} \\ \Lambda_{31} & \Lambda_{31} & \Lambda_{33} & 0 & 0 & 0 \end{bmatrix}.$$

Many connections between the different forms of $\Lambda_{i\alpha}$ given above and in Table 1.5.7.1 have been derived by Kopský (1979*a*,*b*) and Grimmer (1991). These connections between the forms that the matrix can assume for the various magnetic or crystallographic point groups hold for all matrices and tensors that describe properties of materials, not just for the special case of piezomagnetism.

Dzyaloshinskii (1957*b*) pointed out a number of antiferromagnets that may display the piezomagnetic effect. These include the fluorides of the transition metals, in which the piezomagnetic effect was first observed experimentally (see Fig. 1.5.7.1) (Borovik-Romanov, 1959*b*). Below we shall discuss the origin of the piezomagnetic effect in fluorides in more detail.

The fluorides of transition metals MnF_2, CoF_2 and FeF_2 are tetragonal easy-axis antiferromagnets (see Fig. 1.5.5.3). It is easy to check that the expansion of the thermodynamic potential $\tilde{\Phi}$ up to terms that are linear in stress T_{ij} and invariant relative to the transformations of the crystallographic space group $\boldsymbol{D}_{4h}^{14} = P4_2/mnm$ is represented by

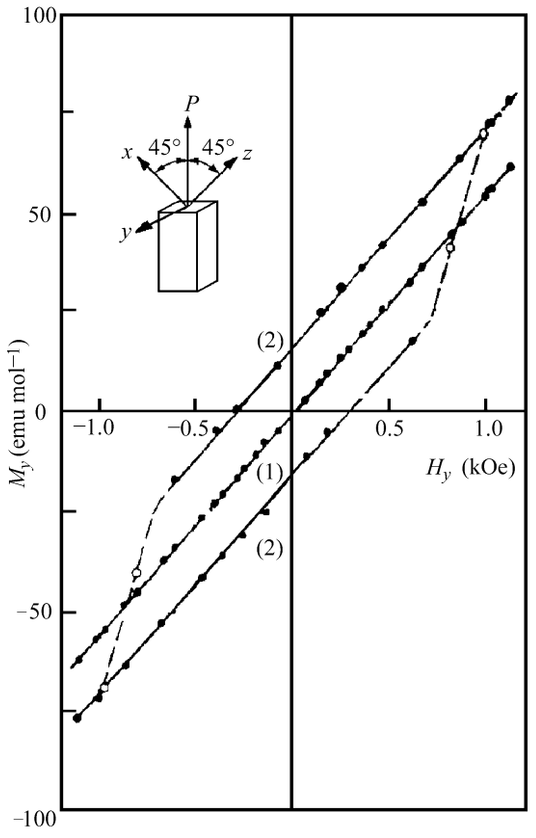

Fig. 1.5.7.1. The dependence of the magnetic moment of CoF_2 on the magnetic field. (1) Without stress; (2) under the stress $T_{xz} = 33.3$ MPa (Borovik-Romanov, 1960).

$$\begin{aligned}\tilde{\Phi} = \tilde{\Phi}_0 &+ (A/2)\mathbf{L}^2 + (a/2)(L_x^2 + L_y^2) \\ &+ (B/2)\mathbf{M}^2 + (b/2)(M_x^2 + M_y^2) \\ &+ d(L_x M_y + L_y M_x) \\ &+ 2\lambda_1(M_x T_{yz} + M_y T_{xz})L_z \\ &+ 2\eta_1(L_y T_{yz} + L_x T_{xz})L_z \\ &+ 2\lambda_2 M_z L_z T_{xy} + 2\eta_2 L_x L_y T_{xy} - \mathbf{MH}. \end{aligned} \tag{1.5.7.5}$$

In this expression, the sums $(T_{ij} + T_{ji})$ that appear in the magnetoelastic terms have been replaced by $2T_{ij}$, as $T_{ij} \equiv T_{ji}$.

The analysis of expression (1.5.7.5) in the absence of stresses proves that fluorides may possess weak ferromagnetism provided that $a < 0$ ($L_z = 0$) (see Section 1.5.5.1). Here we shall discuss the easy-axis structure of the fluorides MnF_2, CoF_2, FeF_2 (see Fig. 1.5.5.3*b*). In the absence of magnetic fields and stresses only $L_z \neq 0$ for this structure. All other components of the vector **L** and the magnetization vector **M** are equal to zero. The magnetic point group is $\boldsymbol{D}_{4h}(\boldsymbol{D}_{2h}) = 4'/mmm'$.

To transform the potential $\tilde{\Phi}(L_i, M_j, T_{k\ell})$ [(1.5.7.5)] into the form $\Phi(T, \mathbf{T}, \mathbf{H})$ [(1.5.7.1)], one has to insert into the magnetoelastic terms the dependence of the components of **L** and **M** on the magnetic field. The corresponding relations, obtained by minimization of (1.5.7.5) without the magnetoelastic terms, are

$$\begin{aligned} M_x &= \frac{a}{a(B+b) - d^2} H_x; \quad & L_x &= -\frac{d}{a(B+b) - d^2} H_y; \\ M_y &= \frac{a}{a(B+b) - d^2} H_y; \quad & L_y &= -\frac{d}{a(B+b) - d^2} H_x; \\ M_z &= \frac{1}{B} H_z; & L_z &\simeq \text{constant}. \end{aligned} \tag{1.5.7.6}$$

To a first approximation, the component L_z does not depend on the magnetic field.

Inserting the relations (1.5.7.6) for M_i and L_i into the magnetoelastic terms of (1.5.7.5), one gets the following expression for the corresponding terms in $\Phi(T, H_i, T_{jk})$:

$$\begin{aligned}\Phi(T, H_i, T_{jk}) = \Phi_0(T, H_i) &+ 2L_z \frac{a\lambda_1 - d\eta_1}{a(B+b) - d^2} T_{yz} H_x \\ &+ 2L_z \frac{a\lambda_1 - d\eta_1}{a(B+b) - d^2} T_{xz} H_y + 2L_z \frac{\lambda_2}{B} T_{xy} H_z. \end{aligned} \tag{1.5.7.7}$$

In this case, the expression for the magnetoelastic energy contains only three components of the stress tensor: T_{yz}, T_{xz} and T_{xy}. Using (1.5.7.2), we get formulas for the three main components of the piezomagnetic effect:

$$M_x = 2L_z \frac{d\eta_1 - a\lambda_1}{a(B+b) - d^2} T_{yz} = 2\Lambda_{xyz} T_{yz} = \Lambda_{14} T_4, \tag{1.5.7.8}$$

$$M_y = 2L_z \frac{d\eta_1 - a\lambda_1}{a(B+b) - d^2} T_{xz} = 2\Lambda_{yxz} T_{xz} = \Lambda_{25} T_5, \tag{1.5.7.9}$$

$$M_z = -2L_z \frac{\lambda_2}{B} T_{xy} = 2\Lambda_{zxy} T_{xy} = \Lambda_{36} T_6. \tag{1.5.7.10}$$

In all three cases, the piezomagnetic moment is produced in the direction perpendicular to the shear plane. Comparing (1.5.7.8) and (1.5.7.9), we see that $\Lambda_{25} = \Lambda_{14}$. This is in agreement with the equivalence of the axes x and y in the tetragonal crystals. If the stress is applied in the plane xz (or yz), the vector **L** turns in the shear plane and a component L_x (or L_y) is produced:

$$L_x = 2L_z \frac{\eta_1(B+b) - d\lambda_1}{a(B+b) - d^2} T_{xz}. \tag{1.5.7.11}$$

For T_{xy} stress, no rotation of the vector **L** occurs.

Formulas (1.5.7.8)–(1.5.7.10) show that in accordance with Table 1.5.7.1 the form of the matrix $\Lambda_{i\alpha}$ for the magnetic point group $\boldsymbol{D}_{4h}(\boldsymbol{D}_{2h}) = 4'/mmm'$ is

$$\boldsymbol{\Lambda}_{i\alpha} = \begin{bmatrix} 0 & 0 & 0 & \Lambda_{14} & 0 & 0 \\ 0 & 0 & 0 & 0 & \Lambda_{14} & 0 \\ 0 & 0 & 0 & 0 & 0 & \Lambda_{36} \end{bmatrix}. \tag{1.5.7.12}$$

The relations (1.5.7.8)–(1.5.7.10) show that the components of the piezomagnetic tensor Λ_{ijk} are proportional to the components of the antiferromagnetic vector **L**. Thus the sign of the piezomagnetic moment depends on the sign of the vector **L** and the value of the piezomagnetic effect depends on the domain structure of the sample (we are referring to S-domains). The piezomagnetic moment may become equal to zero in a polydomain sample. On the other hand, piezomagnetism may be used to obtain single-domain antiferromagnetic samples by cooling them from the paramagnetic state in a magnetic field under suitably oriented external pressure.

There are relatively few publications devoted to experimental investigations of the piezomagnetic effect. As mentioned above, the first measurements of the values of the components of the tensor Λ_{ijk} were performed on crystals of MnF_2 and CoF_2 (Borovik-Romanov, 1960). In agreement with theoretical prediction, three components were observed: $\Lambda_{xyz} = \Lambda_{yxz}$ and Λ_{zxy}. The largest value obtained for these components was $\Lambda_{14} = 21 \times 10^{-10}$ Oe^{-1}. The piezomagnetic effect was also observed for two modifications of α-Fe_2O_3 (Andratskii & Borovik-Romanov, 1966). The magnetic point group of the low-temperature modification of this compound is $\boldsymbol{D}_{3d} = \bar{3}m$. In accordance with form (7) given above, the following nonzero components Λ_{ijk} were found for the low-temperature state:

$$\Lambda_{xyz} = -\Lambda_{yxz}, \tag{1.5.7.13}$$

$$\Lambda_{yyy} = -\Lambda_{yxx} = -\Lambda_{xxy}. \tag{1.5.7.14}$$

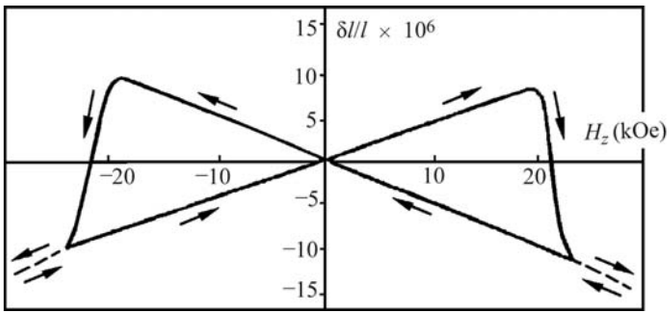

Fig. 1.5.7.2. Linear magnetostriction of CoF_2 (Prokhorov & Rudashevskii, 1975).

The values of these components are one order of magnitude smaller than for CoF_2.

The temperature dependence of the components is similar for the piezomagnetic tensor and the sublattice magnetization. This means that the magnetoelastic constants λ_1 and λ_2 (as well as the constants B and d) in the relations (1.5.7.7) and (1.5.7.8) depend only slightly on temperature.

1.5.7.2. *Linear magnetostriction*

From expression (1.5.7.3), it follows that a deformation of the sample may occur in a magnetic field. This deformation is linear with respect to the field. By its linear dependence, this effect differs essentially from ordinary magnetostriction, which is quadratic in the magnetic field. Most substances display such quadratic magnetostriction. The linear magnetostriction may be observed only in those ordered magnetics that belong to one of the 66 magnetic point groups that allow piezomagnetism and are listed in Table 1.5.7.1. The distinctive feature of linear magnetostriction is the dependence of its sign on the sign of the magnetic field and on the sign of the antiferromagnetic vector **L**. The sign of **L** characterizes the domain state of the specimen. Thus, observation of linear magnetostriction gives information about the domain state. In some materials, it has been observed that a sudden transition from one domain state to the opposite may occur in strong magnetic fields.

Linear magnetostriction (LM) was observed in CoF_2 by Borovik-Romanov & Yavelov (1963) in a magnetic field applied parallel to the fourfold axis. The relations for the LM in CoF_2 can be obtained by differentiating the expression of the thermodynamic potential Φ [(1.5.7.7)]. If the magnetic field is applied along the y axis, a deformation S_{xz} appears:

$$S_{xz} = -\partial\Phi/\partial T_{xz} = 2L_z \frac{d\eta_1 - a\lambda_1}{a(B+b) - d^2} H_y = 2\Lambda_{yxz} H_y = \Lambda_{25} H_2. \tag{1.5.7.15}$$

A similar formula holds for S_{yz} if the magnetic field is applied parallel to the x axis (with Λ_{14}, which is equal to Λ_{25}).

If the magnetic field is applied parallel to the fourfold axis, the S_{xy} component of the deformation appears:

$$S_{xy} = -\partial\Phi/\partial T_{xy} = -2L_z(\lambda_2/B)H_z = -2L_z\lambda_2\chi_\parallel H_z = 2\Lambda_{zxy} H_z = \Lambda_{36} H_3. \tag{1.5.7.16}$$

If the relations (1.5.7.15) and (1.5.7.16) are compared with (1.5.7.8)–(1.5.7.10), it is apparent that in accordance with theory the components of the tensors of the piezomagnetic effect (PM) and LM are identical.

Prokhorov & Rudashevskii (1969, 1975) extended the investigation of LM in CoF_2. They discovered that if the applied field becomes larger than 20 kOe, a jump in the magnetostriction occurs and it changes its sign (see Fig. 1.5.7.2). This jump is the result of a transition of the magnetic structure from one domain state ($\mathbf{L}_+$) into the opposite state ($\mathbf{L}_-$). To explain such a transition, one has to take into account the term of third power in the expansion of the magnetic energy (Scott & Anderson, 1966),

$$U_m = A_i H_i + \tfrac{1}{2}\chi_{ij} H_i H_j + C_{ijk} H_i H_j H_k. \tag{1.5.7.17}$$

C_{ijk} is an axial time-antisymmetric tensor, the sign of which depends on the sign of the domain. This term defines the dependence of the magnetic energy on the sign of the antiferromagnetic domain.

To date, CoF_2 and MnF_2 are unique in that LM and PM occur without rotating the antiferromagnetic vector **L** if the magnetic field is applied along the fourfold axis (or pressure along a ⟨110⟩ axis). In all other cases, these effects are accompanied by a rotation of **L** and, as a result, the creation of new components L_i. To the latter belongs the LM in the low-temperature modification of α-Fe_2O_3, which was observed by Anderson *et al.* (1964) (see also Scott & Anderson, 1966; Levitin & Shchurov, 1973). This compound displays PM, therefore it is obvious that LM will also occur (see Table 1.5.7.1).

LM has been observed in some orthoferrites. One of the orthoferrites, $DyFeO_3$ at low temperatures, is a pure antiferromagnet, the vector **L** of which is aligned along the y axis. Its magnetic point group ($\boldsymbol{D}_{2h} = mmm$) allows PM and LM. The latter was observed when a magnetic field was applied parallel to the z axis by Zvezdin *et al.* (1985). There it was shown that $\Lambda_{zxy} \neq 0$ if $0 < H < H_c$. At $H_c \simeq 4$ kOe, a first-order phase transition into a weakly ferromagnetic state with magnetic point group $\boldsymbol{D}_{2h}(\boldsymbol{C}_{2h}) = m'm'm$ ($\mathbf{L} \parallel Ox, \mathbf{M}_D \parallel Oz$) occurs.

Many orthoferrites and orthochromites that possess weak ferromagnetism belong to the same point group, which possesses an ordinary centre of symmetry. Thus PM and LM are allowed for these phases of orthoferrites. If the magnetic field is applied parallel to Ox, they undergo a reorientation transition at which both vectors, **L** and $\mathbf{M}_D$, being orthogonal, rotate in the xz plane. These intermediate angular phases belong to the magnetic point group $\boldsymbol{C}_{2h}(\boldsymbol{C}_i) = 2'/m'$.

LM was observed by Kadomtseva and coworkers (Kadomtseva, Agafonov, Lukina *et al.*, 1981; Kadomtseva, Agafonov, Milov *et al.*, 1981) in two such compounds, $YFeO_3$ and $YCrO_3$. The Λ_{xxz} components of the LM tensor were measured, which are allowed for the $\boldsymbol{D}_{2h}(\boldsymbol{C}_{2h}) = m'm'm$ state.

The experimental data obtained to date for PM and LM are summarized in Table 1.5.7.2. The values of the components $\Lambda_{i\alpha}$ can be converted to SI units using $1\ \mathrm{Oe}^{-1} = 4\pi \times 10^{-3}\ \mathrm{m\ A}^{-1} = 4\pi \times 10^{-3}\ \mathrm{T\ Pa}^{-1}$.

Table 1.5.7.2. *Experimental data for the piezomagnetic effect (PM) and for linear magnetostriction (LM)*

a: antiferromagnetic phase; *w*: weak ferromagnetic phase.

Compound	$\Lambda_{i\alpha} \times 10^{10}$ (Oe^{-1})	T (K)	PM or LM	Reference†
MnF_2	$\Lambda_{14} \simeq 0.2$	20	PM	(1)
CoF_2	$\Lambda_{14} = 21$	20	PM	(1)
	$\Lambda_{36} = 8.2$	20	PM	(1)
	$\Lambda_{36} = 9.8$	4	LM	(3)
$DyFeO_3$	$\Lambda_{36} = 6.0$	6	LM	(8)
$YFeO_3$	$\Lambda_{15} = 1.7$	6	LM	(6)
$YCrO_3$	$\Lambda_{15} \simeq 1$	6	LM	(7)
α-Fe_2O_3 (*a*)	$\Lambda_{22} = 1.9$	78	LM	(4)
	$\Lambda_{22} = 3.2$	77	PM	(2)
	$\Lambda_{22} = 1.3$	100	LM	(5)
	$\Lambda_{14} = 0.3$	78	LM	(4)
	$\Lambda_{14} = 1.7$	77	PM	(2)
	$\Lambda_{14} = 0.9$	100	LM	(5)
α-Fe_2O_3 (*w*)	$\Lambda_{23} = 2.5$	292	PM	(2)

† References: (1) Borovik-Romanov (1959*b*, 1960); (2) Andratskii & Borovik-Romanov (1966); (3) Prokhorov & Rudashevskii (1969, 1975); (4) Anderson *et al.* (1964); (5) Levitin & Shchurov (1973); (6) Kadomtseva, Agafonov, Milov *et al.* (1981); (7) Kadomtseva, Agafonov, Lukina *et al.* (1981); (8) Zvezdin *et al.* (1985).

1.5.7.3. *Linear magnetic birefringence*

The magnetic contribution to the component of the dielectric permittivity $\delta\varepsilon_{ij}$ can be represented as a series in the powers of the components of the magnetization and the antiferromagnetic vector. The magnetic birefringence (also called the Cotton–Mouton or Voigt effect) is described by the real symmetrical part of the tensor $\delta\varepsilon_{ij}$. In paramagnetic crystals, the magnetization $\mathbf{M}$ is proportional to the applied magnetic field $\mathbf{H}$, and the series has the form

$$\delta\varepsilon_{ij} = Q^{MM}_{ijk\ell} M_k M_\ell = Q^{MM}_{ijk\ell} \chi^M_{kr} \chi^M_{\ell s} H_r H_s = \Gamma_{ijrs} H_r H_s. \quad (1.5.7.18)$$

The tensor Γ_{ijrs} is symmetric with respect to both the first and the second pair of indices. The symmetry of this tensor implies that the diagonal components of the permittivity tensor include magnetic corrections. The modification of the diagonal components gives rise to birefringence in cubic crystals and to a change $\Delta n^{\rm pm}$ of the birefringence in uniaxial and lower-symmetry crystals. It follows from (1.5.7.18) that this birefringence is bilinear in the applied field. Bilinear magnetic birefringence can be observed in uniaxial crystals if the magnetic field is applied along the x axis perpendicular to the principal z axis. In the simplest case, a difference in the refractive indices n_x and n_y arises:

$$\Delta n^{\rm pm} = n_x - n_y = \frac{1}{2n_0}(\delta\varepsilon_{xx} - \delta\varepsilon_{yy}) = \frac{1}{2n_0}(\Gamma_{xxxx} - \Gamma_{yyxx}) H_x^2, \quad (1.5.7.19)$$

where n_0 is the refractive index for the ordinary beam.

Consider now a magnetically ordered crystal which can be characterized by an antiferromagnetic vector $\mathbf{L}_0$ and a magnetization vector $\mathbf{M}_0$ in the absence of a magnetic field. Applying a magnetic field with components H_r, we change the direction and size of $\mathbf{L}_0$ and $\mathbf{M}_0$, getting additional components $L^H_k = \chi^L_{kr} H_r$ and $M^H_k = \chi^M_{kr} H_r$. This is illustrated by the relations (1.5.7.6). Instead of (1.5.7.18) we get

$$\begin{aligned}\delta\varepsilon_{ij} &= Q^{LL}_{ijk\ell} L_k L_\ell + Q^{ML}_{ijk\ell} M_k L_\ell + Q^{MM}_{ijk\ell} M_k M_\ell \\ &= Q^{LL}_{ijk\ell} L_{0k} L_{0\ell} + Q^{ML}_{ijk\ell} M_{0k} L_{0\ell} + Q^{MM}_{ijk\ell} M_{0k} M_{0\ell} \\ &\quad + [2Q^{LL}_{ijk\ell} \chi^L_{kr} L_{0\ell} + Q^{ML}_{ijk\ell} (\chi^M_{kr} L_{0\ell} + M_{0k} \chi^L_{\ell r}) + 2Q^{MM}_{ijk\ell} \chi^M_{kr} M_{0\ell}] H_r. \end{aligned} \quad (1.5.7.20)$$

The terms in the middle line of (1.5.7.20) show that in an ordered state a change in the refractive indices occurs that is proportional to L_0^2 in antiferromagnets and to M_0^2 in ferromagnets. The terms in square brackets show that a linear magnetic birefringence may exist. In the special case of a tetragonal antiferromagnet belonging to the space group $\boldsymbol{D}^{14}_{4h} = P4_2/mnm$ with $\mathbf{L}_0$ parallel to the principal axis z, the linear birefringence occurs in the xy plane if the magnetic field is applied along the z axis (see Fig. 1.5.5.3). In this case, $\mathbf{M}_0 = 0$, $\chi^L_{kz} = 0$ for all k, $\chi^M_{xz} = \chi^M_{yz} = 0$ and $\chi^M_{zz} = 1/B$ [see (1.5.7.6)]. Therefore the terms in square brackets in (1.5.7.20) differ from zero only for one component of $\delta\varepsilon_{ij}$,

$$\delta\varepsilon_{ij} = Q^{ML}_{xyzz} L_{0z} H_z / B = q_{zxy} H_z \,\mathrm{sign}(L_{0z}). \quad (1.5.7.21)$$

As a result,

$$\Delta n^{\rm af} = n_{x'} - n_{y'} = \frac{1}{2n_0}\delta\varepsilon_{xy} = \frac{1}{2n_0} q_{zxy} H_z \,\mathrm{sign}(L_{0z}), \quad (1.5.7.22)$$

where x', y' are the optic axes, which in these tetragonal crystals are rotated by $\pi/4$ relative to the crystallographic axes.

Comparing relation (1.5.7.22) with (1.5.7.3), one can see that like LM, there may be linear magnetic birefringence. The forms of the tensors that describe the two effects are the same.

Linear magnetic birefringence has been observed in the uniaxial antiferromagnetic low-temperature α-Fe_2O_3 when the magnetic field was applied perpendicular to the threefold axis (Le Gall *et al.*, 1977; Merkulov *et al.*, 1981). The most impressive effect was observed in CoF_2 when the magnetic field was applied along the fourfold axis. The crystal ceased to be optically uniaxial and a difference $(n_{x'} - n_{y'}) \propto H_z$ was observed in accordance with (1.5.7.22). Such linear magnetic birefringence does not exist in the paramagnetic state. Linear birefringence has also been observed in $CoCO_3$ and $DyFeO_3$. For details of these experiments, see Eremenko *et al.* (1989). These authors also used linear birefringence to make the antiferromagnetic domains visible. A further review of linear magnetic birefringence has been given by Ferré & Gehring (1984).

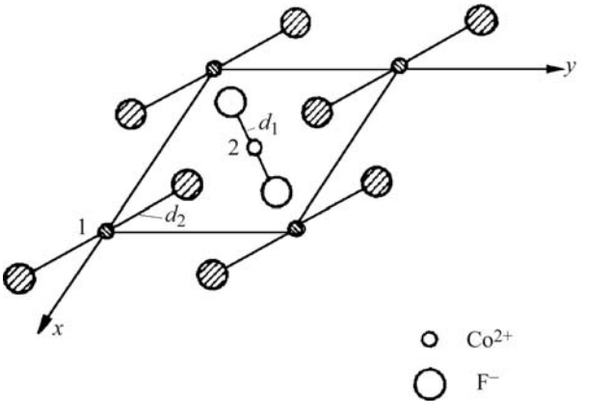

Fig. 1.5.7.3. Variation of symmetry of the crystal field in the presence of the piezomagnetic effect in CoF_2. The unshaded atoms lie at height $c/2$ above the xy plane (see Fig. 1.5.5.3).

Piezomagnetism, linear magnetostriction and linear birefringence in fluorides can be clearly demonstrated qualitatively for one particular geometry. As shown in Fig. 1.5.7.3, the crystallographically equivalent points 1 and 2 are no longer equivalent after a shear deformation applied in the plane xy. During such a deformation, the distances from the magnetic ions to the nearest fluoride ions increase in points 1 and decrease in points 2. As a result, the values of the g-factors for the ions change. Evidently, the changes of the values of the g-factors for different sublattices are opposite in sign. Thus the sublattice magnetizations are no longer equal, and a magnetic moment arises along the direction of sublattice magnetization. On the other hand, if we increase the magnetization of one sublattice and decrease the magnetization of the other by applying a magnetic field parallel to the z axis, the interactions with the neighbouring fluoride ions also undergo changes with opposite signs. This gives rise to the magnetostriction. These considerations can be applied only to antiferromagnets with the fluoride structure. In these structures, single-ion anisotropy is responsible for the weak ferromagnetism, not the antisymmetric exchange interaction of the form $\mathbf{d}[\mathbf{S}_i \times \mathbf{S}_k]$.

1.5.8. Magnetoelectric effect

Curie (1894) stated that materials that develop an electric polarization in a magnetic field or a magnetization in an electric field may exist. This prediction was given a more precise form by Landau & Lifshitz (1957), who considered the invariants in the expansion of the thermodynamic potential up to linear terms in H_i. For materials belonging to certain magnetic point groups, the thermodynamic potential Φ can be written in the form

$$\Phi = \Phi_0 - \alpha_{ij} E_i H_j. \quad (1.5.8.1)$$

If (in the absence of a magnetic field) an electric field $\mathbf{E}$ is applied to a crystal with potential (1.5.8.1), a magnetization will be produced:

$$M_j = -\frac{\partial\Phi}{\partial H_j} = \alpha_{ij} E_i. \quad (1.5.8.2)$$

Conversely, an electric polarization **P** arises at zero electric field if a magnetic field is applied:

$$P_i = -\frac{\partial \Phi}{\partial E_i} = \alpha_{ij} H_j. \qquad (1.5.8.3)$$

This phenomenon is called the magnetoelectric effect. A distinction is made between the linear magnetoelectric effect described above and two types of bilinear magnetoelectric effects. These bilinear effects arise if the thermodynamic potential contains terms of the form $E_i H_j H_k$ or $H_i E_j E_k$. They will be described in Section 1.5.8.2.

1.5.8.1. *Linear magnetoelectric effect*

It is obvious that the linear magnetoelectric effect is forbidden for all dia- and paramagnets as their magnetic groups possess R as a separate element. The effect is also forbidden if the magnetic space group contains translations multiplied by R because in these cases the point group also possesses R as a separate element. Since **H** is an axial vector that changes sign under R and **E** is a polar vector that is invariant under time inversion, α_{ij} is an axial tensor of second rank, the components of which all change sign under time inversion (R). From relation (1.5.8.1), it follows that a magnetic group which allows the magnetoelectric effect cannot possess a centre of symmetry ($C_i = \bar{1}$). However, it can possess it multiplied by R ($C_i R = \bar{1}'$) (see Table 1.5.8.1). There are 21 magnetic point groups that possess a centre of symmetry. The detailed analysis of the properties of the tensor α_{ij} shows that among the remaining 69 point groups there are 11 groups for which the linear magnetoelectric effect is also forbidden. These groups are $\boldsymbol{C}_{3h} = \bar{6}$, $\boldsymbol{C}_6(\boldsymbol{C}_3) = 6'$, $\boldsymbol{C}_{6h}(\boldsymbol{C}_{3h}) = 6'/m$, $\boldsymbol{D}_{3h} = \bar{6}m2$, $\boldsymbol{D}_{3h}(\boldsymbol{C}_{3h}) = \bar{6}m'2'$, $\boldsymbol{D}_{6h}(\boldsymbol{D}_{3h}) = 6'/mmm'$, $\boldsymbol{D}_6(\boldsymbol{D}_3) = 6'22'$, $\boldsymbol{C}_{6v}(\boldsymbol{C}_{3v}) = 6'm'm$, $\boldsymbol{T}_d = \bar{4}3m$, $\boldsymbol{O}(\boldsymbol{T}) = 4'32'$ and $\boldsymbol{O}_h(\boldsymbol{T}_d) = m'\bar{3}'m$.

All remaining 58 magnetic point groups in which the linear magnetoelectric effect is possible are listed in Table 1.5.8.1. The 11 forms of tensors that describe this effect are also listed in this table.[3] The orientation of the axes of the Cartesian coordinate system (CCS) with respect to the symmetry axes of the crystal is the same as in Table 1.5.7.1. Alternative orientations of the same point group that give rise to the same form of α_{ij} have been added between square brackets in Table 1.5.8.1. The tensor has the same form for 32 (= 321) and 312, $3m'1$ and $31m'$, $\bar{3}'m'1$ and $\bar{3}'1m'$; it also has the same form for $3m1$ and $31m$, $32'1$ and $312'$, $\bar{3}'m1$ and $\bar{3}'1m$.

The forms of α_{ij} for frequently encountered orientations of the CCS other than those given in Table 1.5.8.1 are (*cf.* Rivera, 1994)

(1) $112, 11m', 11\,2/m'$ (unique axis z):

$$\begin{bmatrix} \alpha_{11} & \alpha_{12} & 0 \\ \alpha_{21} & \alpha_{22} & 0 \\ 0 & 0 & \alpha_{33} \end{bmatrix};$$

(2) $11m, 112', 11\,2'/m$ (unique axis z):

$$\begin{bmatrix} 0 & 0 & \alpha_{13} \\ 0 & 0 & \alpha_{23} \\ \alpha_{31} & \alpha_{32} & 0 \end{bmatrix};$$

(3) $2mm, 22'2', m'm2'\,[m'2'm], m'mm$:

$$\begin{bmatrix} 0 & 0 & 0 \\ 0 & 0 & \alpha_{23} \\ 0 & \alpha_{32} & 0 \end{bmatrix};$$

(4) $m2m, 2'22', mm'2'\,[2'm'm], mm'm$:

$$\begin{bmatrix} 0 & 0 & \alpha_{13} \\ 0 & 0 & 0 \\ \alpha_{31} & 0 & 0 \end{bmatrix};$$

(5) $\bar{4}m2, \bar{4}2'm', 4'2'2, 4'mm', 4'/m'mm'$:

$$\begin{bmatrix} 0 & \alpha_{12} & 0 \\ \alpha_{12} & 0 & 0 \\ 0 & 0 & 0 \end{bmatrix}.$$

Table 1.5.8.1. *The forms of the tensor characterizing the linear magnetoelectric effect*

Magnetic crystal class		Matrix representation of the property tensor α_{ij}
Schoenflies	Hermann–Mauguin	
$\boldsymbol{C}_1$ $\boldsymbol{C}_i(\boldsymbol{C}_1)$	1 $\bar{1}'$	$\begin{bmatrix} \alpha_{11} & \alpha_{12} & \alpha_{13} \\ \alpha_{21} & \alpha_{22} & \alpha_{23} \\ \alpha_{31} & \alpha_{32} & \alpha_{33} \end{bmatrix}$
$\boldsymbol{C}_2$ $\boldsymbol{C}_s(\boldsymbol{C}_1)$ $\boldsymbol{C}_{2h}(\boldsymbol{C}_2)$	$2\,(=121)$ $m'\,(=1m'1)$ $2/m'\,(=1\,2/m'\,1)$ (unique axis y)	$\begin{bmatrix} \alpha_{11} & 0 & \alpha_{13} \\ 0 & \alpha_{22} & 0 \\ \alpha_{31} & 0 & \alpha_{33} \end{bmatrix}$
$\boldsymbol{C}_s$ $\boldsymbol{C}_2(\boldsymbol{C}_1)$ $\boldsymbol{C}_{2h}(\boldsymbol{C}_s)$	$m\,(=1m1)$ $2'\,(=12'1)$ $2'/m\,(=1\,2'/m\,1)$ (unique axis y)	$\begin{bmatrix} 0 & \alpha_{12} & 0 \\ \alpha_{21} & 0 & \alpha_{23} \\ 0 & \alpha_{32} & 0 \end{bmatrix}$
$\boldsymbol{D}_2$ $\boldsymbol{C}_{2v}(\boldsymbol{C}_2)$ $\boldsymbol{D}_{2h}(\boldsymbol{D}_2)$	222 $m'm'2\,[2m'm',\ m'2m']$ $m'm'm'$	$\begin{bmatrix} \alpha_{11} & 0 & 0 \\ 0 & \alpha_{22} & 0 \\ 0 & 0 & \alpha_{33} \end{bmatrix}$
$\boldsymbol{C}_{2v}$ $\boldsymbol{D}_2(\boldsymbol{C}_2)$ $\boldsymbol{C}_{2v}(\boldsymbol{C}_s)$ $\boldsymbol{D}_{2h}(\boldsymbol{C}_{2v})$	$mm2$ $2'2'2$ $2'mm'\,[m2'm']$ mmm'	$\begin{bmatrix} 0 & \alpha_{12} & 0 \\ \alpha_{21} & 0 & 0 \\ 0 & 0 & 0 \end{bmatrix}$
$\boldsymbol{C}_4,\ \boldsymbol{S}_4(\boldsymbol{C}_2),\ \boldsymbol{C}_{4h}(\boldsymbol{C}_4)$ $\boldsymbol{C}_3,\ \boldsymbol{S}_6(\boldsymbol{C}_3)$ $\boldsymbol{C}_6,\ \boldsymbol{C}_{3h}(\boldsymbol{C}_3),\ \boldsymbol{C}_{6h}(\boldsymbol{C}_6)$	$4,\ \bar{4}',\ 4/m'$ $3,\ \bar{3}'$ $6,\ \bar{6}',\ 6/m'$	$\begin{bmatrix} \alpha_{11} & \alpha_{12} & 0 \\ -\alpha_{12} & \alpha_{11} & 0 \\ 0 & 0 & \alpha_{33} \end{bmatrix}$
$\boldsymbol{S}_4$ $\boldsymbol{C}_4(\boldsymbol{C}_2)$ $\boldsymbol{C}_{4h}(\boldsymbol{S}_4)$	$\bar{4}$ $4'$ $4'/m'$	$\begin{bmatrix} \alpha_{11} & \alpha_{12} & 0 \\ \alpha_{12} & -\alpha_{11} & 0 \\ 0 & 0 & 0 \end{bmatrix}$
$\boldsymbol{D}_4,\ \boldsymbol{C}_{4v}(\boldsymbol{C}_4)$ $\boldsymbol{D}_{2d}(\boldsymbol{D}_2),\ \boldsymbol{D}_{4h}(\boldsymbol{D}_4)$ $\boldsymbol{D}_3,\ \boldsymbol{C}_{3v}(\boldsymbol{C}_3),\ \boldsymbol{D}_{3d}(\boldsymbol{D}_3)$ $\boldsymbol{D}_6,\ \boldsymbol{C}_{6v}(\boldsymbol{C}_6)$ $\boldsymbol{D}_{3h}(\boldsymbol{D}_3),\ \boldsymbol{D}_{6h}(\boldsymbol{D}_6)$	$422,\ 4m'm'$ $\bar{4}'2m'\,[\bar{4}'m'2],\ 4/m'm'm'$ $32,\ 3m',\ \bar{3}'m'$ $622,\ 6m'm'$ $\bar{6}'m'2\,[\bar{6}'2m'],\ 6/m'm'm'$	$\begin{bmatrix} \alpha_{11} & 0 & 0 \\ 0 & \alpha_{11} & 0 \\ 0 & 0 & \alpha_{33} \end{bmatrix}$
$\boldsymbol{C}_{4v},\ \boldsymbol{D}_4(\boldsymbol{C}_4)$ $\boldsymbol{D}_{2d}(\boldsymbol{C}_{2v}),\ \boldsymbol{D}_{4h}(\boldsymbol{C}_{4v})$ $\boldsymbol{C}_{3v},\ \boldsymbol{D}_3(\boldsymbol{C}_3),\ \boldsymbol{D}_{3d}(\boldsymbol{C}_{3v})$ $\boldsymbol{C}_{6v},\ \boldsymbol{D}_6(\boldsymbol{C}_6)$ $\boldsymbol{D}_{3h}(\boldsymbol{C}_{3v}),\ \boldsymbol{D}_{6h}(\boldsymbol{D}_{6v})$	$4mm,\ 42'2'$ $\bar{4}'2'm\,[\bar{4}'m2'],\ 4/m'mm$ $3m,\ 32',\ \bar{3}'m$ $6mm,\ 62'2'$ $\bar{6}'m2'\,[\bar{6}'2'm],\ 6/m'mm$	$\begin{bmatrix} 0 & \alpha_{12} & 0 \\ -\alpha_{12} & 0 & 0 \\ 0 & 0 & 0 \end{bmatrix}$
$\boldsymbol{D}_{2d},\ \boldsymbol{D}_{2d}(\boldsymbol{S}_4)$ $\boldsymbol{D}_4(\boldsymbol{D}_2),\ \boldsymbol{C}_{4v}(\boldsymbol{C}_{2v})$ $\boldsymbol{D}_{4h}(\boldsymbol{D}_{2d})$	$\bar{4}2m,\ \bar{4}m'2'$ $4'22',\ 4'm'm$ $4'/m'm'm$	$\begin{bmatrix} \alpha_{11} & 0 & 0 \\ 0 & -\alpha_{11} & 0 \\ 0 & 0 & 0 \end{bmatrix}$
$\boldsymbol{T},\ \boldsymbol{T}_h(\boldsymbol{T})$ $\boldsymbol{O},\ \boldsymbol{T}_d(\boldsymbol{T}),\ \boldsymbol{O}_h(\boldsymbol{O})$	$23,\ m'\bar{3}'$ $432,\ \bar{4}'3m',\ m'\bar{3}'m'$	$\begin{bmatrix} \alpha_{11} & 0 & 0 \\ 0 & \alpha_{11} & 0 \\ 0 & 0 & \alpha_{11} \end{bmatrix}$

[3] Table 1.5.8.1 shows that the tensor describing the magnetoelectric effect does not need to be symmetric for 31 of the 58 point groups. These 31 groups coincide with those that admit a spontaneous toroidal moment (Gorbatsevich & Kopaev, 1994); they were first determined by Ascher (1966) as the magnetic point groups admitting spontaneous currents.

As mentioned above, the components of the linear magnetoelectric tensor change sign under time inversion. The sign of these components is defined by the sign of the antiferromagnetic vector **L**, *i.e.* by the sign of the 180° domains (S-domains). This is like the behaviour of the piezomagnetic effect and therefore everything said above about the role of the domains can be applied to the magnetoelectric effect.

Dzyaloshinskii (1959) proposed the antiferromagnetic Cr_2O_3 as the first candidate for the observation of the magnetoelectric (ME) effect. He showed that the ME tensor for this compound has three nonzero components: $\alpha_{11} = \alpha_{22}$ and α_{33}. The ME effect in Cr_2O_3 was discovered experimentally by Astrov (1960) on an unoriented crystal. He verified that the effect is linear in the applied electric field. Folen *et al.* (1961) and later Astrov (1961) performed measurements on oriented crystals and revealed the anisotropy of the ME effect. In the first experiments, the ordinary magnetoelectric effect ME_E (the electrically induced magnetization) was investigated. This means the magnetic moment induced by the applied electric field was measured. Later Rado & Folen (1961) observed the converse effect ME_H (the electric polarization induced by the magnetic field). The temperature dependence of the components of the magnetoelectric tensor in Cr_2O_3 was studied in detail in both laboratories.

In the following years, many compounds that display the linear magnetoelectric effect were discovered. Both the electrically induced and the magnetically induced ME effect were observed. The values of the components of the magnetoelectric tensor range from 10^{-6} to 10^{-2} in compounds containing the ions of the iron group and from 10^{-4} to 10^{-2} in rare-earth compounds. Cox (1974) collected values of α_{max} of the known magnetoelectrics. Some are listed in Table 1.5.8.2 together with more recent results.

Table 1.5.8.2. *A list of some magnetoelectrics*

Compound	T_N or T_C (K)	Magnetic point group	Maximum α_{obs}	References†
Fe_2TeO_6	219	$4/m'm'm'$	3×10^{-5}	7–9, 70
$DyAlO_3$	3.5	$m'm'm'$	2×10^{-3}	11–13
$GdAlO_3$	4.0	$m'm'm'$	1×10^{-4}	14
$TbAlO_3$	4.0	$m'm'm'$	1×10^{-3}	12, 15–17
$TbCoO_3$	3.3	mmm'	3×10^{-5}	12, 16, 18
Cr_2O_3	318	$\bar{3}'m'$	1×10^{-4}	45–49, 70, 71, W162
$Nb_2Mn_4O_9$	110	$\bar{3}'m'$	2×10^{-6}	52, 53
$Nb_2Co_4O_9$	27	$\bar{3}'m'$	2×10^{-5}	52, 53
$Ta_2Mn_4O_9$	104	$\bar{3}'m'$	1×10^{-5}	53
$Ta_2Co_4O_9$	21	$\bar{3}'m'$	1×10^{-4}	53
$LiMnPO_4$	35	$m'm'm'$	2×10^{-5}	55, 56, 58, 60
$LiFePO_4$	50	mmm'	1×10^{-4}	57, 58
$LiCoPO_4$	22	mmm'	7×10^{-4}	54, 55, R161
$LiNiPO_4$	23	mmm'	4×10^{-5}	54, 55, 61
$GdVO_4$	2.4	$4'/m'm'm$	3×10^{-4}	70
$TbPO_4$	2.2	$4'/m'm'm$	1×10^{-2}	66, 67
$DyPO_4$	3.4	$4'/m'm'm$	1×10^{-3}	68, 69
$HoPO_4$	1.4	$4'/m'm'm$	2×10^{-4}	72
$Mn_3B_7O_{13}I$	26	$m'm2'$	2×10^{-6}	C204
$Co_3B_7O_{13}Cl$	12	m	3×10^{-4}	S204
$Co_3B_7O_{13}Br$	17	$m'm2'$	2×10^{-3}	88C1
$Co_3B_7O_{13}I$	38	$m'm2'$	1×10^{-3}	90C3
$Ni_3B_7O_{13}I$	61.5	m'	2×10^{-4}	74, 75, 77–79, 90C2
$Ni_3B_7O_{13}Cl$	9	$m'm2'$	3×10^{-4}	74R2, 91R1
$Cu_3B_7O_{13}Cl$	8.4	$m'm'2$	3×10^{-6}	88R1
$FeGaO_3$	305	$m'm2'$	4×10^{-4}	84–86
TbOOH	10.0	$2/m'$	4×10^{-4}	114
DyOOH	7.2	$2/m'$	1×10^{-4}	92, 114
ErOOH	4.1	$2'/m$	5×10^{-4}	93, 114
Gd_2CuO_4	6.5	mmm'	1×10^{-4}	W161
$MnNb_2O_6$	4.4	mmm'	3×10^{-6}	101, 102
$MnGeO_3$	16	mmm'	2×10^{-6}	98–100
$CoGeO_3$	31	mmm'	1×10^{-4}	70
$CrTiNdO_5$	13	mmm'	1×10^{-5}	70, 89

† Numbers refer to references quoted by Cox (1974); codes 88C1, 90C3, 88R1, 90C2, 74R2, 91R1 refer to references quoted by Burzo (1993); and codes W162, R161, C204, S204 and W161 refer to articles in *Ferroelectrics*, **162**, 141, **161**, 147, **204**, 125, **204**, 57 and **161**, 133, respectively.

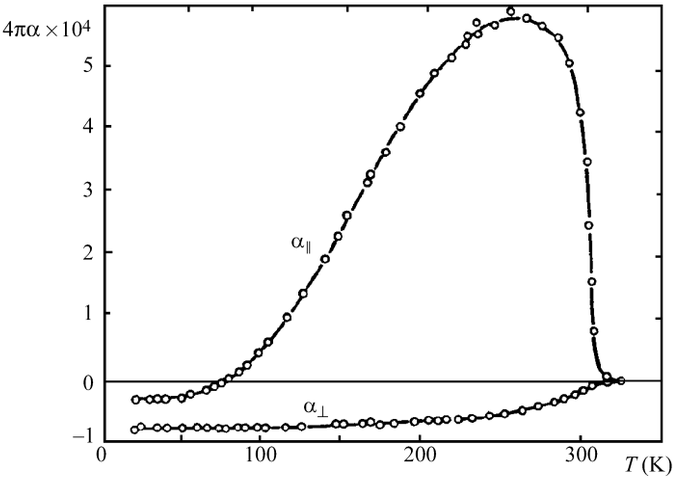

Fig. 1.5.8.1. Temperature dependence of the components $\alpha_\parallel$ and $\alpha_\perp$ in Cr_2O_3 (Astrov, 1961).

Additional information about the experimental data is presented in three conference proceedings (Freeman & Schmid, 1975; Schmid *et al.*, 1994; Bichurin, 1997).

The values of α_{ij} are given in rationalized Gaussian units, where α_{ij} is dimensionless. Some authors follow Dzyaloshinskii (1959) in writing (1.5.8.1) as $\Phi = \Phi_0 - (\alpha'_{ij}/4\pi)E_iH_j$, where α'_{ij} are the non-rationalized Gaussian values of the components of the magnetoelectric tensor. If SI units are used, then (1.5.8.1) becomes $\Phi = \Phi_0 - \alpha^{SI}_{ij}E_iH_j$. The connections between the values of a tensor component expressed in these three systems are

$$4\pi\alpha_{ij} = \alpha'_{ij} = 3 \times 10^8 \alpha^{SI}_{ij}. \qquad (1.5.8.4)$$

The units of α^{SI}_{ij} are s m^{-1}. A detailed discussion of the relations between the descriptions of the magnetoelectric effect in different systems of units is given by Rivera (1994).

Most magnetoelectrics are oxides containing magnetic ions. The ions of the iron group are contained in corundum-type oxides [magnetic point group $\boldsymbol{D}_{3d}(\boldsymbol{D}_3) = \bar{3}'m'$], triphyllite-type oxides with different magnetic groups belonging to the orthorhombic crystallographic structure $\boldsymbol{D}_{2h} = mmm$ and other compounds. The rare-earth oxides are represented by the orthorhombic RMO_3 structure with R = rare earth, $M = Fe^{3+}$, Co^{3+}, Al^{3+} [magnetic point group $\boldsymbol{D}_{2h}(\boldsymbol{D}_2) = m'm'm'$], tetragonal zircon-type compounds RMO_4 (R = rare earth, M = P, V) [magnetic point group $\boldsymbol{D}_{4h}(\boldsymbol{D}_{2d}) = 4'/m'm'm$], monoclinic oxide hydroxides ROOH [magnetic point groups $\boldsymbol{C}_{2h}(\boldsymbol{C}_2) = 2/m'$, $\boldsymbol{C}_{2h}(\boldsymbol{C}_s) = 2'/m$] and other compounds. Of particular interest is $TbPO_4$, which has the highest value of the magnetoelectric tensor components, 1.2×10^{-2} (Rado & Ferrari, 1973; Rado *et al.*, 1984). There are also some weak ferromagnets and ferrimagnets that exhibit the linear magnetoelectric effect. An example is the weakly ferromagnetic boracite $Ni_3B_7O_{13}I$. These orthorhombic compounds will be discussed in Section 1.5.8.3. Another orthorhombic magnetoelectric crystal is ferrimagnetic $FeGaO_3$ (Rado, 1964; see Table 1.5.8.2).

It has been shown in experiments on Cr_2O_3 that in the spin-flop phase $\alpha_\parallel$ becomes zero but a non-diagonal component α_{xz} arises (Popov *et al.*, 1992). Such behaviour is possible if under the spin-flop transition the magnetic point group of Cr_2O_3 transforms from $\boldsymbol{D}_{3d}(\boldsymbol{D}_3) = \bar{3}'m'$ to $\boldsymbol{C}_{2h}(\boldsymbol{C}_s) = 112'/m$. For the latter magnetic point group, the ME tensor possesses only transverse components.

The temperature dependences determined for the ME moduli, $\alpha_\parallel$ and $\alpha_\perp$, in Cr_2O_3 are quite different (see Fig. 1.5.8.1). The temperature dependence of $\alpha_\perp$ is similar to that of the order parameter (sublattice magnetization M_0), which can be explained easily, bearing in mind that the magnetoelectric moduli are

proportional to the magnitude of the antiferromagnetic vector ($\alpha \propto L_z = 2M_0$). However, to explain the rather complicated temperature dependence of $\alpha_\parallel$ it becomes necessary to assume that the moduli α are proportional to the magnetic susceptibility of the crystal so that (Rado, 1961; Rado & Folen, 1962)

$$\alpha_\parallel = a_\parallel \chi_\parallel L_z, \quad \alpha_\perp = a_\perp \chi_\perp L_z, \tag{1.5.8.5}$$

where $a_\parallel$ and $a_\perp$ are new constants of the magnetoelectric effect which do not depend on temperature. Formulas (1.5.8.5) provide a good explanation of the observed temperature dependence of α.

The linear relation between α and $L_z = 2M_0$ is also proved by the fact that when studying the ME effect, the domain structure of the sample is revealed. An annealing procedure to prepare a single-domain sample has been developed. To perform this annealing, the sample must be heated well above the Néel temperature and then cooled below T_N in the presence of electric and magnetic fields. The directions of these fields have to agree with the allowed components of the ME tensor. In some compounds, a single-domain state may be obtained by applying simultaneous pulses of both fields to a multidomain sample at temperatures below T_N (see O'Dell, 1970).

It was shown in the previous section that the piezomagnetic effect can be explained phenomenologically as weak ferromagnetism caused by the change of the symmetry produced by deformation of the lattice. The electric field may act indirectly inducing atomic displacement (similar to the displacement under stress) and as in piezomagnetism may cause the rise of a magnetic moment. Such ideas were proposed by Rado (1964) and expanded by White (1974).

The electric field may act directly to change the admixture of orbital states in the electron wavefunctions. As a result of such direct action, there may be a change of different terms in the microscopic spin Hamiltonian. Correspondingly, the following mechanisms are to be distinguished. Changes in the g-tensor can explain the ME effect in $DyPO_4$ (Rado, 1969). The electric-field-induced changes in single-ion anisotropy may represent the main mechanism of the ME effect in Cr_2O_3 (Rado, 1962). Two other mechanisms have to be taken into account: changes in symmetric and antisymmetric exchange. For details and references see the review article of de Alcantara Bonfim & Gehring (1980).

1.5.8.2. *Nonlinear magnetoelectric effects*

Along with linear terms in E and H, the thermodynamic potential Φ may also contain invariants of higher order in E_k, H_i:

$$\Phi = \Phi_0 - \alpha_{ik}E_iH_k - \tfrac{1}{2}\beta_{ijk}E_iH_jH_k - \tfrac{1}{2}\gamma_{ijk}H_iE_jE_k. \tag{1.5.8.6}$$

From this relation, one obtains the following formulas for the electric polarization P_i and the magnetization M_i:

$$P_i = \alpha_{ik}H_k + \tfrac{1}{2}\beta_{ijk}H_jH_k + \gamma_{jik}H_jE_k, \tag{1.5.8.7}$$

$$M_i = \alpha_{ki}E_k + \beta_{jik}E_jH_k + \tfrac{1}{2}\gamma_{ijk}E_jE_k. \tag{1.5.8.8}$$

The third term in (1.5.8.7) describes the dependence of the dielectric susceptibility ($\chi^e_{ik} = P_i/E_k$) and, consequently, of the dielectric permittivity ε_{ik}, on the magnetic field. Similarly, the second term in (1.5.8.8) points out that the magnetic susceptibility χ^m may depend on the electric field ($\delta\chi^m_{ik} = \beta_{jik}E_j$). The tensors β_{ijk} and γ_{ijk} are symmetric in their last two indices. Symmetry imposes on β_{ijk} the same restrictions as on the piezoelectric tensor and on γ_{ijk} the same restrictions as on the piezomagnetic tensor (see Table 1.5.7.1).

Ascher (1968) determined all the magnetic point groups that allow the terms EHH and HEE in the expansion of the thermodynamic potential Φ. These groups are given in Table 1.5.8.3, which has been adapted from a table given by Schmid (1973). It classifies the 122 magnetic point groups according to which types of magnetoelectric effects (EH, EHH or HEE) they admit and whether they admit spontaneous dielectric polarization (E) or spontaneous magnetization (H). It also classifies the 122 point groups according to whether they contain $\bar{1}$, $1'$ or $\bar{1}'$, as in a table given by Mercier (1974). Ferromagnets, ferrimagnets and weak ferromagnets have a point group characterized by H (the 31 groups of types 4–7 in Table 1.5.8.3); dia- and paramagnets as well as antiferromagnets with a nontrivial magnetic Bravais lattice have a point group containing $1'$ (the 32 groups of types 1, 13, 17 and 19 in Table 1.5.8.3). The 59 remaining point groups describe antiferromagnets with a trivial Bravais lattice. The 31 point groups characterized by E, the 32 containing $\bar{1}$ and the 59 remaining ones correspond to a similar classification of crystals according to their electric properties (see Schmid, 1973).

Table 1.5.8.3 shows that for the 16 magnetic point groups of types 16–19, any kind of magnetoelectric effect is prohibited.

Table 1.5.8.3. *Classification of the 122 magnetic point groups according to magnetoelectric types*

Type	Inversions in the group	Permitted terms in thermodynamic potential	Magnetic point groups	Number of magnetic point groups				
1	$1'$	E EHH	$1'$, $21'$, $m1'$, $mm21'$, $41'$, $4mm1'$, $31'$, $3m1'$, $61'$, $6mm1'$	10	31		49	122
2		E EHH HEE	$6'$, $6'mm'$	2				
3		E EH EHH HEE	$mm2$, $4mm$, $4'$, $4'mm'$, $3m$, $6mm$	6				
4		E H EH EHH HEE	1, 2, m, $2'$, m', $m'm2'$, $m'm'2$, 4, $4m'm'$, 3, $3m'$, 6, $6m'm'$	13		31		
5		H EH EHH HEE	$2'2'2$, $42'2'$, $\bar{4}$, $\bar{4}2'm'$, $32'$, $62'2'$	6				
6		H EHH HEE	$\bar{6}$, $\bar{6}m'2'$	2				
7	$\bar{1}$	H HEE	$\bar{1}$, $2/m$, $2'/m'$, $m'm'm$, $4/m$, $4/mm'm'$, $\bar{3}$, $\bar{3}m'$, $6/m$, $6/mm'm'$	10				
8		EH EHH HEE	222, $\bar{4}'$, 422, $\bar{4}2m$, $4'22'$, $\bar{4}'2m'$, $\bar{4}'2'm$, 32, $\bar{6}'$, 622, $\bar{6}'m'2$, $\bar{6}'m2'$, 23, $\bar{4}'3m'$	14			73	
9		EHH HEE	$\bar{6}m2$, $6'22'$	2				
10		EH	432	1		19		
11	$\bar{1}'$	EH	$\bar{1}'$, $2/m'$, $2'/m$, mmm', $m'm'm'$, $4/m'$, $4'/m'$, $4/m'm'm'$, $4/m'mm$, $4'/m'm'm$, $\bar{3}'$, $\bar{3}'m'$, $\bar{3}'m$, $6/m'$, $6/m'm'm'$, $6/m'mm$, $m'\bar{3}'$, $m'\bar{3}'m'$	18				
12		EHH	$\bar{4}3m$	1		11		
13	$1'$	EHH	$2221'$, $\bar{4}1'$, $4221'$, $\bar{4}2m1'$, $321'$, $\bar{6}1'$, $6221'$, $\bar{6}m21'$, $231'$, $\bar{4}3m1'$	10				
14		HEE	$4'32'$	1		11		
15	$\bar{1}$	HEE	mmm, $4'/m$, $4/mmm$, $4'/mmm'$, $\bar{3}m$, $6'/m'$, $6/mmm$, $6'/m'm'm$, $m\bar{3}$, $m\bar{3}m'$	10				
16	$\bar{1}'$		$6'/m$, $6'/mmm'$, $m'\bar{3}'m$	3		16		
17	$1'$		$4321'$	1				
18	$\bar{1}$		$m\bar{3}m$	1				
19	$\bar{1}$, $1'$, $\bar{1}'$		$\bar{1}1'$, $2/m1'$, $mmm1'$, $4/m1'$, $4/mmm1'$, $\bar{3}1'$, $\bar{3}m1'$, $6/m1'$, $6/mmm1'$, $m\bar{3}1'$, $m\bar{3}m1'$	11				

These are the 11 grey point groups that contain all three inversions, the white group $\boldsymbol{O}_h = m\bar{3}m$, the grey group $(\boldsymbol{O} + R\boldsymbol{O}) = 4321'$ and the three black–white groups $\boldsymbol{C}_{6h}(\boldsymbol{C}_{3h}) = 6'/m$, $\boldsymbol{D}_{6h}(\boldsymbol{D}_{3h}) = 6'/mmm'$ and $\boldsymbol{O}_h(\boldsymbol{T}_d) = m'\bar{3}'m$.

Among the 58 magnetic point groups that allow the linear magnetoelectric effect, there are 19 that do not allow the nonlinear effects EHH and HEE (types 10 and 11 in Table 1.5.8.3). The remaining 39 groups are compatible with all three effects, EH, EHH and HEE; 19 of these groups describe ferromagnets (including weak ferromagnets) and ferrimagnets (types 4 and 5 in Table 1.5.8.3).

The 21 point groups of types 7, 14 and 15 allow only the magnetoelectric effect *HEE*. These groups contain $\boldsymbol{C}_i = \bar{1}$, except $4'32'$. The compounds belonging to these groups possess only one tensor of magnetoelectric susceptibility, the tensor γ_{ijk} of the nonlinear ME effect. The effect is described by

$$P_i = \gamma_{jik} H_j E_k, \tag{1.5.8.9}$$

$$M_i = \tfrac{1}{2}\gamma_{ijk} E_j E_k. \tag{1.5.8.10}$$

The magnetic point group of ferrimagnetic rare-earth garnets $R\mathrm{Fe}_5\mathrm{O}_{12}$ (R = Gd, Y, Dy) is $\boldsymbol{D}_{3d}(\boldsymbol{S}_6) = \bar{3}m'$, which is of type 7. Therefore, the rare-earth garnets may show a nonlinear ME effect corresponding to relations (1.5.8.9) and (1.5.8.10). This was observed by O'Dell (1967) by means of a pulsed magnetic field. As mentioned above, this effect may be considered as the dependence of the dielectric permittivity on the magnetic field, which was the method used by Cardwell (1969) to investigate this ME effect experimentally. Later Lee *et al.* (1970) observed the ME effect defined by relation (1.5.8.10). Applying both static electric fields and alternating ones (at a frequency ω), they observed an alternating magnetization at both frequencies ω and 2ω. A nonlinear ME effect of the form *HEE* was also observed in the weakly ferromagnetic orthoferrites TbFeO_3 and YbFeO_3. Their magnetic point group is $\boldsymbol{D}_{2h}(\boldsymbol{C}_{2h}) = m'm'm$.

Moreover, paramagnets that do not possess an inversion centre $\boldsymbol{C}_i = \bar{1}$ may show an ME effect if the point group is not $4321'$. They have one of the 20 grey point groups given as types 1 or 13 in Table 1.5.8.3. Bloembergen (1962) pointed out that all these paramagnets are piezoelectric crystals. He called the ME effect in these substances the *paramagnetoelectric* (PME) effect. It is defined by the nonzero components of the tensor β_{ijk}:

$$P_i = \tfrac{1}{2}\beta_{ijk} H_j H_k, \tag{1.5.8.11}$$

$$M_i = \beta_{jik} E_j H_k. \tag{1.5.8.12}$$

The PME effect was discovered by Hou & Bloembergen (1965) in $\mathrm{NiSO}_4{\cdot}6\mathrm{H}_2\mathrm{O}$, which belongs to the crystallographic point group $\boldsymbol{D}_4 = 422$. The only nonvanishing components of the third-rank tensor are $\beta_{xyz} = \beta_{xzy} = -\beta_{yzx} = -\beta_{yxz} = \beta$ ($\beta_{14} = -\beta_{25} = 2\beta$ in matrix notation), so that $\mathbf{P} = \beta(H_y H_z, -H_x H_z, 0)$ and $\mathbf{M} = \beta(-E_y H_z,\ E_x H_z,\ E_x H_y - E_y H_x)$. Both effects were observed: the polarization $\mathbf{P}$ by applying static (H_z) and alternating (H_x or H_y) magnetic fields and the magnetization $\mathbf{M}$ by applying a static magnetic field H_z and an alternating electric field in the plane xy. As a function of temperature, the PME effect shows a peak at 3.0 K and changes sign at 1.38 K. The coefficient of the PME effect at 4.2 K is

$$\beta(4.2\ \mathrm{K}) = 2.2 \times 10^{-9}\ \text{cgs units}. \tag{1.5.8.13}$$

The theory developed by Hou and Bloembergen explains the PME effect by linear variation with the applied electric field of the crystal-field-splitting parameter D of the spin Hamiltonian.

Most white and black–white magnetic point groups that do not contain the inversion ($\boldsymbol{C}_i = \bar{1}$), either by itself or multiplied by $R = 1'$, admit all three types of ME effect: the linear (*EH*) and two higher-order (*EHH* and *HEE*) effects. There are many magnetically ordered compounds in which the nonlinear ME effect has been observed. Some of them are listed by Schmid (1973); more recent references are given in Schmid (1994*a*).

In principle, many ME effects of higher order may exist. As an example, let us consider the *piezomagnetoelectric* effect. This is a combination of piezomagnetism (or piezoelectricity) and the ME effect. The thermodynamic potential Φ must contain invariants of the form

$$\Phi = \Phi_0 - \pi_{ijk\ell} E_i H_j T_{k\ell}. \tag{1.5.8.14}$$

The problem of the piezomagnetoelectric effect was considered by Rado (1962), Lyubimov (1965) and recently in detail by Grimmer (1992). All 69 white and black–white magnetic point groups that possess neither $\boldsymbol{C}_i = \bar{1}$ nor $R = 1'$ admit the piezomagnetoelectric effect. (These are the groups of types 2–6, 8–12, 14 and 16 in Table 1.5.8.3.) The tensor $\pi_{ijk\ell}$ that describes the piezomagnetoelectric effect is a tensor of rank 4, symmetric in the last two indices and invariant under space-time inversion. This effect has not been observed so far (Rivera & Schmid, 1994). Grimmer (1992) analyses in which antiferromagnets it could be observed.

1.5.8.3. *Ferromagnetic and antiferromagnetic ferroelectrics*

Neronova & Belov (1959) pointed out that there are ten magnetic point groups that admit the simultaneous existence of spontaneous dielectric polarization **P** and magnetic polarization **M**. Materials with such a complicated ordered structure are called ferromagnetoelectrics. Neronova and Belov considered only structures with parallel alignment of **P** and **M** (or **L**). There are three more groups that allow the coexistence of ferroelectric and ferromagnetic order, in which **P** and **M** are perpendicular to each other. Shuvalov & Belov (1962) published a list of the 13 magnetic point groups that admit ferromagnetoelectric order. These are the groups of type 4 in Table 1.5.8.3; they are given with more details in Table 1.5.8.4.

Notice that **P** and **M** must be parallel in eight point groups, they may be parallel in 1 and m', and they must be perpendicular in $2'$, m and $m'm2'$ (see also Ascher, 1970). The magnetic point groups listed in Table 1.5.8.4 admit not only ferromagnetism (and ferrimagnetism) but the first seven also admit antiferromagnetism with weak ferromagnetism. Ferroelectric pure antiferromagnets of type III^a may also exist. They must belong to one of the following eight magnetic point groups (types 2 and 3 in Table 1.5.8.3): $\boldsymbol{C}_4(\boldsymbol{C}_2) = 4'$; $\boldsymbol{C}_{4v}(\boldsymbol{C}_{2v}) = 4'mm'$; $\boldsymbol{C}_6(\boldsymbol{C}_3) = 6'$; $\boldsymbol{C}_{6v}(\boldsymbol{C}_{3v}) = 6'mm'$; $\boldsymbol{C}_{2v} = mm2$; $\boldsymbol{C}_{4v} = 4mm$; $\boldsymbol{C}_{3v} = 3m$; $\boldsymbol{C}_{6v} = 6mm$.

The first experimental evidence to indicate that complex perovskites may become ferromagnetoelectric was observed by the Smolenskii group (see Smolenskii *et al.*, 1958). They investigated the temperature dependence of the magnetic susceptibility of the ferroelectric perovskites $\mathrm{Pb(Mn_{1/2}Nb_{1/2})O_3}$ and $\mathrm{Pb(Fe_{1/2}Nb_{1/2})O_3}$. The temperature dependence at $T > 77$ K followed the Curie–Weiss law with a very large antiferromagnetic

Table 1.5.8.4. *List of the magnetic point groups of the ferromagnetoelectrics*

Symbol of symmetry group		Allowed direction of	
Schoenflies	Hermann–Mauguin	**P**	**M**
$\boldsymbol{C}_1$	1	Any	Any
$\boldsymbol{C}_2$	2	$\parallel 2$	$\parallel 2$
$\boldsymbol{C}_2(\boldsymbol{C}_1)$	$2'$	$\parallel 2'$	$\perp 2'$
$\boldsymbol{C}_s = \boldsymbol{C}_{1h}$	m	$\parallel m$	$\perp m$
$\boldsymbol{C}_s(\boldsymbol{C}_1)$	m'	$\parallel m'$	$\parallel m'$
$\boldsymbol{C}_{2v}(\boldsymbol{C}_2)$	$m'm'2$	$\parallel 2$	$\parallel 2$
$\boldsymbol{C}_{2v}(\boldsymbol{C}_s)$	$m'm2'$	$\parallel 2'$	$\perp m$
$\boldsymbol{C}_4$	4	$\parallel 4$	$\parallel 4$
$\boldsymbol{C}_{4v}(\boldsymbol{C}_4)$	$4m'm'$	$\parallel 4$	$\parallel 4$
$\boldsymbol{C}_3$	3	$\parallel 3$	$\parallel 3$
$\boldsymbol{C}_{3v}(\boldsymbol{C}_3)$	$3m'$	$\parallel 3$	$\parallel 3$
$\boldsymbol{C}_6$	6	$\parallel 6$	$\parallel 6$
$\boldsymbol{C}_{6v}(\boldsymbol{C}_6)$	$6m'm'$	$\parallel 6$	$\parallel 6$

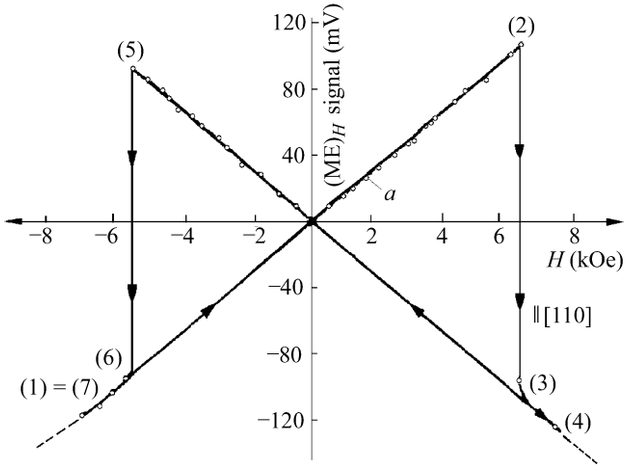

Fig. 1.5.8.2. The hysteresis loop in the linear magnetoelectric effect in ferromagnetoelectric $Ni_3B_7O_{13}I$ at 46 K (Ascher *et al.*, 1966).

Weiss constant. Later, Astrov *et al.* (1968) proved that these compounds undergo a transition into a weakly ferromagnetic state at temperatures $T_N = 11$ and 9 K, respectively.

$BiFeO_3$ is an antiferromagnet below $T_N = 643$ K. This was proved by neutron scattering (Kiselev *et al.*, 1962; Michel *et al.*, 1969) and magnetic measurements (Smolenskii *et al.*, 1962; see also Venevtsev *et al.*, 1987). $BiFeO_3$ also possesses a spontaneous electric polarization. The magnetic point group above T_N is $3m1'$ and below it should have been $3m$ (Kiselev *et al.*, 1962), but in reality it possesses an antiferromagnetic spatially modulated spin structure (Sosnovska *et al.*, 1982). Another ferroelectric antiferromagnet, $YMnO_3$, was found by Bertaut *et al.* (1964). It becomes ferroelectric at $T_c = 913$ K (with paramagnetic point group $6mm1'$) and antiferromagnetic at $T_N = 77$ K. Below this temperature, its magnetic point group is $6'mm'$. The antiferromagnetic ordering was also proved by investigating the Mössbauer effect (Chappert, 1965). The symmetries of both antiferromagnetic ferroelectrics described above do not allow weak ferromagnetism according to Table 1.5.5.2, and, experimentally, a spontaneous ferromagnetic moment has not been observed so far.

Since Schmid (1965) developed a technique for growing single crystals of boracites, these compounds have become the most interesting ferromagnetoelectrics. The boracites have the chemical formula $M_3B_7O_{13}X$ (where $M = Cu^{2+}, Ni^{2+}, Co^{2+}, Fe^{2+}, Mn^{2+}, Cr^{2+}$ and $X = F^-, Cl^-, Br^-, I^-, OH^-, NO_3^-$). Many of them are ferroelectrics and weak ferromagnets at low temperatures. This was first shown for $Ni_3B_7O_{13}I$ (see Ascher *et al.*, 1966). The symmetries of all the boracites are cubic at high temperatures and their magnetic point group is $\bar{4}3m1'$. As the temperature is lowered, most become ferroelectrics with the magnetic point group $mm21'$. At still lower temperatures, the spins of the magnetic ions in the boracites go into an antiferromagnetic state with weak ferromagnetism. For some the ferromagnetoelectric phase belongs to the group $m'm2'$ and for others to $m'm'2$, m', m or 1. In accordance with Table 1.5.8.4, the spontaneous polarization **P** is oriented perpendicular to the weak ferromagnetic moment $\mathbf{M}_D$ for the groups $m'm2'$ and m. There results a complicated behaviour of boracites in external magnetic and electric fields. It depends strongly on the history of the samples. Changing the direction of the electric polarization by an electric field also changes the direction of the ferromagnetic vector (as well as the direction of the antiferromagnetic vector) and *vice versa*.

As an example, Fig. 1.5.8.2 shows the results of measurements on Ni–I boracite with spontaneous polarization along [001] and spontaneous magnetization initially along $[1\bar{1}0]$. A magnetic field was applied along [110] and the polarization induced along [001] was measured. If the applied field was increased beyond 6 kOe, the induced polarization changed sign because the spontaneous magnetization had been reversed. On reversing the applied magnetic field, the rest of the hysteresis loop describing the $ME_{\parallel}$ response was obtained.

If the spontaneous polarization is reversed, *e.g.* by applying an electric field, the spontaneous magnetization will rotate simultaneously by 90° around the polarization axis. Applying magnetic fields as described above will no longer produce a measurable polarization. If, however, the crystal is rotated by 90° around the polarization axis before repeating the experiment, a hysteresis loop similar to Fig. 1.5.8.2 but turned upside down will be obtained (*cf.* Schmid, 1967).

The similarity of the jumps in the curves of linear magnetostriction (see Fig. 1.5.7.2) and magnetoelectric effect in Ni–I boracite is noteworthy. More details about the present state of investigation of the ferromagnetoelectrics are presented in the review article of Schmid (1994*b*).

The ferromagnetoelectrics appear as type 4 and the ferroelectric antiferromagnets of type III^a as types 2 and 3 in Table 1.5.8.3. The table shows that the linear magnetoelectric effect is admitted by all ferromagnetoelectrics and all ferroelectric antiferromagnets of type III^a, except those that belong to the two point groups $\boldsymbol{C}_6(\boldsymbol{C}_3) = 6'$ and $\boldsymbol{C}_{6v}(\boldsymbol{C}_{3v}) = 6'mm'$.

Concluding Section 1.5.8, it is worth noting that the magnetoelectric effect is still actively investigated. Recent results in this field can be found in papers presented at the 1993 and 1996 conferences devoted to this subject (see Schmid *et al.*, 1994; Bichurin, 1997, 2002).

1.5.9. Magnetostriction

The transition to an ordered magnetic state is accompanied by a spontaneous distortion of the lattice, which is denoted spontaneous magnetostriction. The lattice distortion may be specified by the deformation (strain) components S_{ij}. The undeformed state is defined as the crystal structure that would be realized if the crystal remained in the paramagnetic state at the given temperature. This means that it is necessary to separate the magnetostrictive deformation from the ordinary thermal expansion of the crystal. This can be done by measurements of the magnetostriction in external magnetic fields applied in different directions (see Section 1.5.9.2). The magnetostriction arises because the first derivatives of the exchange and relativistic energies responsible for the magnetic order do not vanish at $S_{ij} = 0$. Thus these energies depend linearly on the deformations around $S_{ij} = 0$. That part of the magnetic energy which depends on the deformations (and consequently on the stresses) is called the magnetoelastic energy, $U_{\rm me}$. To find the equilibrium values of the spontaneous magnetostriction, one also has to take the elastic energy into account.

The magnetoelastic energy includes both an exchange and a relativistic part. In some ferromagnets that are cubic in the paramagnetic phase, the exchange interaction does not lower the cubic symmetry. Thus the exchange part of $U_{\rm me}$ satisfies the relations

$$\partial U_{\rm me}/\partial S_{ii} = B_0' \quad \text{and} \quad \partial U_{\rm me}/\partial S_{ij} = 0 \quad (i \neq j). \qquad (1.5.9.1)$$

Such a form of the magnetoelastic energy gives rise to an isotropic spontaneous magnetostriction or volume change (volume striction) which does not depend on the direction of magnetization. In what follows, we shall analyse mainly the anisotropic magnetostriction.

The spontaneous magnetostriction deformations are so small (about 10^{-5}) for some ferro- and antiferromagnets that they cannot be observed by the usual X-ray techniques. However, in materials with ions possessing strong spin–orbit interactions (like Co^{2+}), it may be as large as 10^{-4}. The magnetostriction in rare-

earth metals and their compounds with iron and cobalt are especially large (up to 10^{-3}).

Magnetostriction is observed experimentally as a change δl of the linear dimension along a direction specified by a unit vector $\boldsymbol{\beta} = (\beta_1, \beta_2, \beta_3)$:

$$\lambda_\beta = \delta l/l = \sum_{ij} S_{ij}\beta_i\beta_j, \tag{1.5.9.2}$$

where S_{ij} are the deformation components, which are functions of the components of the unit vector **n** aligned in the direction of the magnetization. Only the symmetric part of the deformation tensor S_{ij} has been taken into account, because the antisymmetric part represents a rotation of the crystal as a whole.

The magnetostriction that arises in an applied magnetic field will be discussed in Section 1.5.9.2; Section 1.5.9.1 is devoted to the spontaneous magnetostriction.

1.5.9.1. *Spontaneous magnetostriction*

In this section, we shall assume that the crystal under consideration undergoes a phase transition from the paramagnetic state into a magnetically ordered state. The latter is a single-domain state with the magnetization (or the antiferromagnetic vector) aligned along the vector **n**. As was mentioned above, to solve the problem of the spontaneous magnetostriction we have to minimize the sum of magnetoelastic and elastic energy.

Like the anisotropy energy, the anisotropic part of the magnetoelastic energy can be represented as a series in the components of the unit vector **n**:

$$U_{\rm me} = Q_{k\ell mn}S_{k\ell}n_m n_n + Q_{k\ell mnop}S_{k\ell}n_m n_n n_o n_p + \ldots = V^0_{k\ell}S_{k\ell}. \tag{1.5.9.3}$$

As for every ordered magnetic, this relation contains only even powers of the magnetization unit vector. The components of the tensors **Q** are called magnetostrictive or magnetoelastic coefficients. They are proportional to even powers of the magnetization M ($Q_{k\ell mn} \propto M^2$ and $Q_{k\ell mnop} \propto M^4$). The symmetry of the tensors $\mathbf{Q}_{k\ell mn}$ and $\mathbf{Q}_{k\ell mnop}$ is defined by the crystallographic point group of the initial paramagnetic phase of the crystal.

It is convenient to consider the magnetoelastic energy as part of a general expansion of the free energy of a magnetic into a series with respect to the deformation (as the magnetostrictive deformations are small):

$$V = V^0 + V^0_{k\ell}S_{k\ell} + \tfrac{1}{2}V^0_{k\ell mn}S_{k\ell}S_{mn} + \ldots, \tag{1.5.9.4}$$

where all the expansion coefficients V^0 are functions of the components of the magnetization unit vector **n**. The superscripts zero indicate that the expansion coefficients have been calculated relative to the undistorted lattice. Such a state in which, at a given temperature, there is no magnetic interaction to distort the crystal is not realizable practically. It will be shown below that the values of the coefficients $V^0_{k\ell}$ may be obtained experimentally by observing the magnetostriction in a magnetic field (see Section 1.5.9.2).

The first term in (1.5.9.4) is the anisotropy energy at zero deformation U^0_a:

$$V^0 = U^0_a = K^0_{ij}n_i n_j + K^0_{ijk\ell}n_i n_j n_k n_\ell + K^0_{ijk\ell mn}n_i n_j n_k n_\ell n_m n_n. \tag{1.5.9.5}$$

This expression has to be compared with the expression for the anisotropy at zero stress introduced in Section 1.5.3.2 [see (1.5.3.5)]. It is obvious that symmetry imposes the same restrictions on the tensors $\boldsymbol{K}$ in both expressions for the anisotropy. Later, we shall discuss these two relations for the anisotropy in more detail.

The second term in (1.5.9.4) is the magnetoelastic energy density, which is displayed in equation (1.5.9.3) and represents the energy of anisotropic deformation.

The third term in (1.5.9.4) is quadratic in $S_{k\ell}$ and can be considered as an additional contribution to the elastic energy arising from the distortion of the lattice by spontaneous magnetostriction. This term is small compared with the main part of the elastic energy, and the effect it produces is called a morphic effect and is usually neglected.

The equilibrium deformation components S^*_{ij} may be found by minimization of the sum of the magnetoelastic and elastic energies. The latter, $U_{\rm el}$, is given by

$$U_{\rm el} = \tfrac{1}{2}c_{ijk\ell}S_{ij}S_{k\ell}, \tag{1.5.9.6}$$

where $c_{ijk\ell}$ are the elastic stiffnesses. The minimization leads to

$$\partial(U_{\rm el} + U_{\rm me})/\partial S_{ij} = c_{ijk\ell}S^*_{k\ell} + V^0_{ij} = 0. \tag{1.5.9.7}$$

We shall replace the elastic stiffnesses $c_{ijk\ell}$ in this equation by the elastic compliances $s_{ijk\ell}$, taking into account that Hooke's law may be written in two forms (see Section 1.3.3):

$$T_{ij} = c_{ijk\ell}S_{k\ell} \quad \text{or} \quad S_{ij} = s_{ijk\ell}T_{k\ell}. \tag{1.5.9.8}$$

Thus the relation for the equilibrium components of the strain S^*_{ij} becomes

$$S^*_{ij} = -s_{ijk\ell}V^0_{k\ell}. \tag{1.5.9.9}$$

Combining the relations (1.5.9.9) and (1.5.9.3), we get the following equation for the magnetostrictive strain components S_{ij} as a function of the magnitude M_s and direction $\mathbf{n} = \mathbf{M}_s/M_s$ of the magnetization $\mathbf{M}_s$:

$$\begin{aligned} S^*_{ij} &= -s_{ijk\ell}(Q_{k\ell mn}n_m n_n + Q_{k\ell mnop}n_m n_n n_o n_p + \ldots) \\ &= M_s^2 N_{ijk\ell}n_k n_\ell + M_s^4 N_{ijk\ell mn}n_k n_\ell n_m n_n + \ldots. \end{aligned} \tag{1.5.9.10}$$

Let us denote the spontaneous magnetostriction by λ^0_β ($\boldsymbol{\beta}$ defines the direction of the magnetostriction relative to the crystallographic axes). According to (1.5.9.2), we obtain

$$\lambda^0_\beta = M_s^2 N_{ijk\ell}\beta_i\beta_j n_k n_\ell + M_s^4 N_{ijk\ell mn}\beta_i\beta_j n_k n_\ell n_m n_n. \tag{1.5.9.11}$$

Relation (1.5.9.11) shows that $\boldsymbol{N}_{ijk\ell mn}$ can be chosen as symmetric in its first two indices and symmetric in its last four indices. It can therefore be represented by a 6×15 matrix $N_{\alpha A}$, where $\alpha = 1, \ldots, 6$ and $A = 01, \ldots, 15$. Table 1.5.9.1 lists the pairs ij that correspond to α and the quadruples $k\ell mn$ that correspond to A.

Similarly, $\boldsymbol{N}_{ijk\ell}$ can be chosen as symmetric in its first two and in its last two indices. It can therefore be represented by a 6×6 matrix $N_{\alpha\beta}$, where $\alpha, \beta = 1, \ldots, 6$. The correspondence between the numbers 1 to 6 and pairs ij or $k\ell$ is given in Table 1.5.9.1.

The tensors $\boldsymbol{N}_{ijk\ell}$ and $\boldsymbol{N}_{ijk\ell mn}$ must satisfy the symmetry of the paramagnetic state of the crystal under consideration. In the case of cubic crystals with fourfold axes (paramagnetic point groups $4321'$, $\bar{4}3m1'$ or $m\bar{3}m1'$), the two matrices $N_{\alpha\beta}$ and $N_{\alpha A}$ possess instead of the 36 and 90 independent components only 3 and 6, *i.e.* N_{11}, N_{12}, N_{44} and $N_{101}, N_{102}, N_{104}, N_{105}, N_{407}, N_{410}$, respectively. The exact form of the two matrices will be given in the following.

(*a*) *Cubic crystals*.

If the point group of the paramagnetic crystal is $4321'$, $\bar{4}3m1'$ or $m\bar{3}m1'$, it follows from the Neumann principle that the only nonvanishing components of $N_{\alpha\beta}$ are $N_{11} = N_{22} = N_{33}, N_{12} = N_{23} = N_{31} = N_{21} = N_{32} = N_{13}$ and $N_{44} = N_{55} = N_{66}$. Similarly, the only nonvanishing components of $N_{\alpha A}$ are $N_{101} = N_{202} = N_{303}$, $N_{102} = N_{203} = N_{301} = N_{103} = N_{201} = N_{302}$, $N_{104} = N_{205} = N_{306}$, $N_{105} = N_{206} = N_{304} = N_{106} = N_{204} = N_{305}$, $N_{407} = N_{508} = N_{609}$,

$N_{410} = N_{511} = N_{612} = N_{413} = N_{514} = N_{615}$. The spontaneous magnetostriction (1.5.9.11) can then be written as

$$\lambda^0_\beta = h_0 + h_1 S(n_1^2\beta_1^2) + 2h_2 S(n_1 n_2 \beta_1\beta_2) + h_3 S(n_1^2 n_2^2) + h_4 S(n_1^4\beta_1^2 + \tfrac{2}{3}n_1^2 n_2^2) + 2h_5 S(n_1 n_2 n_3^2 \beta_1\beta_2). \tag{1.5.9.12}$$

Here an operator $S()$ has been introduced, which denotes the sum of the three quantities obtained by cyclic permutation of the suffixes in the expression within the brackets. For example, $S(n_1^2 n_2 n_3 \beta_2\beta_3) = n_1^2 n_2 n_3 \beta_2\beta_3 + n_2^2 n_3 n_1 \beta_3\beta_1 + n_3^2 n_1 n_2 \beta_1\beta_2$.

The coefficients h_i are related in the following way to the components of the matrices $N_{\alpha\beta}$ and $N_{\alpha A}$ and the spontaneous magnetization M_s:

$$\begin{aligned} h_0 &= N_{12}M_s^2 + N_{102}M_s^4, \\ h_1 &= (N_{11} - N_{12})M_s^2 - 6(N_{104} - N_{105})M_s^4, \\ h_2 &= 2N_{44}M_s^2 + 4N_{410}M_s^4, \\ h_3 &= [-\tfrac{2}{3}(N_{101} + 2N_{102}) + 2(N_{104} + 2N_{105})]M_s^4, \\ h_4 &= [N_{101} - N_{102} + 6(N_{104} - N_{105})]M_s^4, \\ h_5 &= 4(3N_{407} - N_{410})M_s^4. \end{aligned} \tag{1.5.9.13}$$

(*b*) *Hexagonal crystals*.

The equation for the spontaneous magnetostriction of a crystal that, in its paramagnetic state, has a point group $6221'$, $6mm1'$, $\bar{6}m21'$ or $6/mmm1'$, is of the following form [if we restrict ourselves to the quadratic terms in (1.5.9.11)]:

$$\lambda^0_\beta = h_0 + h_1 n_3^2\beta_3^2 + h_2(n_1^2\beta_1^2 + n_2^2\beta_2^2) + h_3(n_1^2\beta_2^2 + n_2^2\beta_1^2) + 2h_4 n_1 n_2 \beta_1\beta_2 + 2h_5 n_3\beta_3(n_1\beta_1 + n_2\beta_2) + h_6\beta_3^2. \tag{1.5.9.14}$$

The coefficients h_i are related to the components $N_{\alpha\beta}$ and the spontaneous magnetization as follows:

$$\begin{aligned} h_0 &= N_{13}M_s^2 \\ h_1 &= (N_{33} - N_{31})M_s^2 \\ h_2 &= (N_{11} - N_{13})M_s^2 \\ h_3 &= (N_{12} - N_{13})M_s^2 \\ h_4 &= (N_{11} - N_{12})M_s^2 \\ h_5 &= 2N_{44}M_s^2 \\ h_6 &= (N_{31} - N_{13})M_s^2 \end{aligned} \tag{1.5.9.15}$$

Table 1.5.9.1. *Correspondence between matrix indices α, A and tensor indices of the tensors describing spontaneous magnetostriction*

α	ij	A	$k\ell mn$
1	11	01	1111
2	22	02	2222
3	33	03	3333
4	23, 32	04	2233, 2323, 2332, 3223, 3232, 3322
5	31, 13	05	3311, 3131, 3113, 1331, 1313, 1133
6	12, 21	06	1122, 1212, 1221, 2112, 2121, 2211
		07	1123, 1132, 1213, 1231, 1312, 1321, 2113, 2131, 2311, 3112, 3121, 3211
		08	2231, 2213, 2321, 2312, 2123, 2132, 3221, 3212, 3122, 1223, 1232, 1322
		09	3312, 3321, 3132, 3123, 3231, 3213, 1332, 1323, 1233, 2331, 2313, 2133
		10	2223, 2232, 2322, 3222
		11	3331, 3313, 3133, 1333
		12	1112, 1121, 1211, 2111
		13	3332, 3323, 3233, 2333
		14	1113, 1131, 1311, 3111
		15	2221, 2212, 2122, 1222

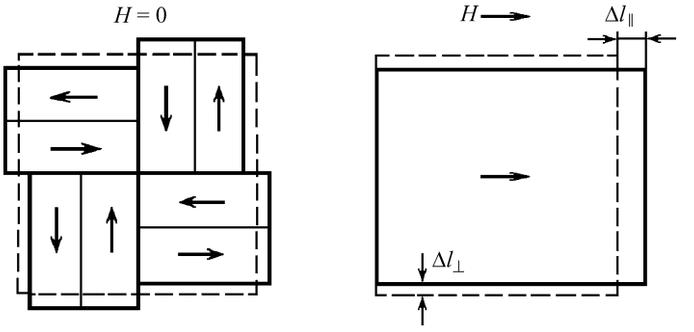

Fig. 1.5.9.1. Diagram explaining the occurrence of magnetostrictive strains in the demagnetized and saturated states of a cube-shaped crystal with a cubic prototype.

As mentioned above, the values of the magnetostrictive coefficients h_i and the spontaneous magnetostriction λ^0_β may be obtained from measurements of magnetostriction in a magnetic field. The latter will be discussed in the next section.

Notice that there is some disagreement between our results (1.5.9.12)–(1.5.9.13) and the corresponding results of Mason (1951), and similarly between (1.5.9.14)–(1.5.9.15) and the results of Mason (1954).

1.5.9.2. *Magnetostriction in an external magnetic field*

There are three reasons for the magnetostriction arising in a magnetic field: (*a*) the transfer of the crystal into a single-domain state if the magnetic field is directed along one of the easy axes; (*b*) the deflection of the magnetization (or antiferromagnetic vector) by the magnetic field from the easy axis in a single-domain crystal; (*c*) the change of the magnetization in a sufficiently strong magnetic field.

Let us begin with case (*a*) and consider a crystal with cubic symmetry in the paramagnetic state (*i.e.* with a cubic prototype). We calculate the magnetostriction that occurs when the applied magnetic field transforms the crystal from the demagnetized multidomain state into the saturated single-domain state. This transformation is shown schematically in Fig. 1.5.9.1.

Each domain in the demagnetized state is distorted by spontaneous magnetostriction. The number of domains in the sample is usually much larger than shown in the figure. Thus a sample of a crystal with a cubic prototype which in the paramagnetic state has the form of a cube will retain this form in the ordered state. Its linear dimension will be changed as a result of magnetostriction. Averaging these strains over all the domains, one gets the spontaneous magnetostrictive change of the linear dimension of the sample, which is equal for any direction x, y or z:

$$(\delta l)_{\rm dem}/l_0 = \lambda^{\rm dem} = \overline{\lambda^0_\beta(n_k)}, \tag{1.5.9.16}$$

where n_k defines the directions parallel to all the easy axes of the crystal. For crystals with a cubic prototype, there are two principal ordered states: with the easy axis along the ⟨111⟩ directions as in nickel or along the ⟨100⟩ directions as in iron. Averaging the strains of all eight possible easy-axis directions of the domains in the ⟨111⟩-type ferromagnet we obtain from (1.5.9.12) the following expression for the spontaneous magnetostriction of the demagnetized crystal:

$$\lambda^{\rm dem} = h_0 + \tfrac{1}{3}(h_1 + h_3 + h_4). \tag{1.5.9.17}$$

In the case of the ⟨100⟩-type ferromagnet, the averaging over the six groups of domains leads to

$$\lambda^{\rm dem} = h_0 + \tfrac{1}{3}(h_1 + h_4). \tag{1.5.9.18}$$

In the saturated state, the sample loses its cubic form. It becomes longer parallel to the magnetic field and thinner perpendicular to it. By definition, the demagnetized state is taken as a reference state for the magnetostriction in the magnetic field. Subtracting from the general relation for spontaneous magnetostriction (1.5.9.12) the expressions (1.5.9.17) and (1.5.9.18) for the demagnetized sample, Becker & Döring (1939) obtained the equations that describe the anisotropy of the magnetostriction caused by saturation magnetization of the ⟨111⟩ and ⟨100⟩ types of magnetic crystals:

⟨111⟩ type:

$$\lambda_\beta^{\rm sat} = h_1[S(n_1^2\beta_1^2) - \tfrac{1}{3}] + 2h_2 S(n_1 n_2 \beta_1 \beta_2) + h_3[S(n_1^2 n_2^2) - \tfrac{1}{3}] + h_4[S(n_1^4\beta_1^2 + \tfrac{2}{3}n_1^2 n_2^2) - \tfrac{1}{3}] + 2h_5 S(n_1^2 n_2 n_3 \beta_2 \beta_3); \quad (1.5.9.19)$$

⟨100⟩ type:

$$\lambda_\beta^{\rm sat} = h_1[S(n_1^2\beta_1^2) - \tfrac{1}{3}] + 2h_2 S(n_1 n_2 \beta_1 \beta_2) + h_3 S(n_1^2 n_2^2) + h_4[S(n_1^4\beta_1^2 + \tfrac{2}{3}n_1^2 n_2^2) - \tfrac{1}{3}] + 2h_5 S(n_1^2 n_2 n_3 \beta_2 \beta_3). \quad (1.5.9.20)$$

Both types of magnetics with a cubic prototype are described by a two-constant equation if the terms of fourth power are neglected. This equation was obtained by Akulov (1928) in the form

$$\lambda_\beta^{\rm sat} = \tfrac{3}{2}\lambda_{100}(n_1^2\beta_1^2 + n_2^2\beta_2^2 + n_3^2\beta_3^2 - \tfrac{1}{3}) + 3\lambda_{111}(n_1 n_2 \beta_1 \beta_2 + n_2 n_3 \beta_2 \beta_3 + n_3 n_1 \beta_3 \beta_1), \quad (1.5.9.21)$$

where the constants λ_{100} and λ_{111} correspond to the magnetostrictive deformation of a 'cubic' ferromagnet along the direction of the magnetic field that is applied along the directions ⟨100⟩ and ⟨111⟩, respectively. Let us denote by Q_1 and Q_2 the following equal coefficients in the equation for the magnetoelastic energy (1.5.9.3):

$$Q_1 = Q_{xxxx} = Q_{yyyy} = Q_{zzzz}; \quad Q_2 = Q_{xyxy} = Q_{yzyz} = Q_{zxzx}. \quad (1.5.9.22)$$

According to (1.5.9.9), the coefficients λ_{100} and λ_{111} may be written as the following fractions of Q_i and the elastic stiffnesses $c_{\alpha\beta}$:

$$\lambda_{100} = \frac{Q_1}{c_{12} - c_{11}}, \quad \lambda_{111} = -\frac{1}{3}\frac{Q_2}{c_{44}}. \quad (1.5.9.23)$$

If the magnetic field transforms the crystal from the demagnetized to the saturated state and if the linear dimension of the sample along the magnetic field increases, then its dimension perpendicular to the field will decrease (see Fig. 1.5.9.1). It follows from relation (1.5.9.21) that the magnetostriction perpendicular to the magnetic field is

$$\lambda_{100}^{\perp} = -\tfrac{1}{2}\lambda_{100} \ \text{ and } \ \lambda_{111}^{\perp} = -\tfrac{1}{2}\lambda_{111}. \quad (1.5.9.24)$$

Some data for magnetostriction of ferromagnets with prototype symmetry $m\bar{3}m1'$ are presented in Table 1.5.9.2.

In a uniaxial crystal, the magnetostriction in the magnetic field arises mainly as a result of the rotation of the magnetization vector from the direction of the easy axis to the direction of the applied field. The magnetostriction in the magnetic field of an easy-axis hexagonal ferromagnet can be obtained from the relation for the spontaneous magnetostriction (1.5.9.14). In the demagnetized state, such a ferromagnet possesses only two types of antiparallel domains, in which the magnetization is aligned parallel or antiparallel to the hexagonal axis ($n_z = \pm 1$, $n_x = n_y = 0$).

Table 1.5.9.2. *Magnetostriction data for ferromagnets with prototype symmetry* $m\bar{3}m1'$

Compound	$\lambda_{100} \times 10^6$	$\lambda_{111} \times 10^6$	References†
Fe	20.7	−21.2	(1)
Ni	−45.9	−24.3	(1)
Fe_3O_4	−20	78	(2)
YIG ($T = 300$ K)	−1.4	−2.4	(3)
DyIG ($T = 300$ K)	−12.5	−5.9	(3)
DyIG ($T = 4.2$ K)	−1400	−550	(4)

† References: (1) Lee (1955); (2) Bickford *et al.* (1955); (3) Iida (1967); (4) Clark *et al.* (1966).

Thus the magnetostriction of the demagnetized state is described by

$$\lambda_\beta^{\rm dem} = h_0 + (h_1 + h_6)\beta_3^2. \quad (1.5.9.25)$$

The saturation magnetostriction can be calculated for different directions of the applied magnetic field using the equations (1.5.9.14), (1.5.9.15) and (1.5.9.25). If the magnetic field is applied along the x axis ($n_x = 1$, $n_y = n_z = 0$), the saturation magnetostrictions for three directions of the vector $\boldsymbol{\beta}$: $\lambda_\beta^{\rm sat} = \lambda_A, \lambda_B, \lambda_C$ are

$$\begin{aligned} \boldsymbol{\beta} \parallel Ox \quad & \lambda_A = h_2, \\ \boldsymbol{\beta} \parallel Oy \quad & \lambda_B = h_3, \\ \boldsymbol{\beta} \parallel Oz \quad & \lambda_C = -h_1. \end{aligned} \quad (1.5.9.26)$$

If the magnetic field is applied at an angle of 45° to the hexagonal axis along the [101] direction, the saturation magnetostriction along the magnetic field is described by

$$\lambda_D = \lambda_{101}^{\rm sat} = \tfrac{1}{4}(h_2 - h_1 + 2h_5). \quad (1.5.9.27)$$

Using the constants λ_A, λ_B, λ_C and λ_D introduced above, the general relation for the magnetostriction caused by magnetization to saturation can be presented in the form

$$\begin{aligned} \lambda_\beta^{\rm sat} = {} & \lambda_A[(n_1\beta_1 + n_2\beta_2)^2 - (n_1\beta_1 + n_2\beta_2)n_3\beta_3] \\ & + \lambda_B[(1 - n_3^2)(1 - \beta_3^2) - (n_1\beta_1 + n_2\beta_2)^2] \\ & + \lambda_C[(1 - n_3^2)\beta_3^2 - (n_1\beta_1 + n_2\beta_2)n_3\beta_3] \\ & + 4\lambda_D(n_1\beta_1 + n_2\beta_2)n_3\beta_3. \end{aligned} \quad (1.5.9.28)$$

A typical hexagonal ferromagnet is cobalt. The magnetostriction constants introduced above have the following values for Co at room temperature:

$$\begin{aligned} \lambda_A &= -45 \times 10^{-6} \quad \lambda_C = +110 \times 10^{-6} \\ \lambda_B &= -95 \times 10^{-6} \quad \lambda_D = -100 \times 10^{-6} \end{aligned}$$

A more sophisticated treatment of the symmetry of the magnetostriction constants is given in the monograph of Birss (1964) and in Zalessky (1981).

1.5.9.3. *The difference between the magnetic anisotropies at zero strain and zero stress*

The spontaneous magnetostriction makes a contribution to the magnetic anisotropy (especially in magnetics with a cubic prototype). Therefore, to find the full expression for the anisotropy energy one has to sum up the magnetic U_a^0 [see (1.5.9.5)], the magnetoelastic $U_{\rm me}$ [see (1.5.9.3)] and the elastic $U_{\rm el}$ [see (1.5.9.6)] energies. At zero strain ($S_{ij}^* = 0$), only $U_a^0 \neq 0$. At zero stress

$$\begin{aligned} U_a^0 + U_{\rm me} + U_{\rm el} &= U_a^0 + V_{ij}^0 S_{ij}^* + \tfrac{1}{2}c_{ijk\ell}S_{ij}^* S_{k\ell}^* \\ &= U_a^0 + \tfrac{1}{2}V_{ij}^0 S_{ij}^*. \end{aligned} \quad (1.5.9.29)$$

Table 1.5.10.1. *Conversion of Gaussian to SI units*

Symbol	Quantity	Gaussian unit and its SI equivalent
B	Magnetic induction	1 gauss (G) = 10^{-4} tesla (T)
H	Magnetic field	1 oersted (Oe) = $10^3/(4\pi)$ A m^{-1}
M	Magnetization (= magnetic moment per unit volume)	1 emu cm^{-3} = 10^3 A m^{-1}
α	Linear magnetoelectric tensor (rationalized units)	1 (dimensionless units) = $4\pi \times 10^{-8}/3$ s m^{-1}
Λ	Piezomagnetic tensor	1 Oe^{-1} = $4\pi \times 10^{-3}$ m A^{-1} = $4\pi \times 10^{-3}$ T Pa^{-1}
χ	Magnetic volume susceptibility	1 (dimensionless units) = 4π (dimensionless units)
χ_g	Magnetic mass susceptibility	1 cm^3 g^{-1} = $4\pi \times 10^{-6}$ m^3 g^{-1}
$\chi_{\rm mol}$	Magnetic molar susceptibility	1 cm^3 mol^{-1} = $4\pi \times 10^{-6}$ m^3 mol^{-1}

We used here the modified equation (1.5.9.7):

$$\tfrac{1}{2}c_{ijk\ell}S^*_{ij}S^*_{k\ell} = -\tfrac{1}{2}V^0_{ij}S^*_{ij}. \qquad (1.5.9.30)$$

Substituting the values for the spontaneous magnetostriction, the final equation for the anisotropy energy measured at atmospheric pressure may be written as

$$\begin{aligned} U_a &= U^0_a + \tfrac{1}{2}V^0_{ij}S^*_{ij} \\ &= (K^0_{ij} + K'_{ij})n_in_j + (K^0_{ijk\ell} + K'_{ijk\ell})n_in_jn_kn_\ell \\ &\quad + (K^0_{ijk\ell mn} + K'_{ijk\ell mn})n_in_jn_kn_\ell n_mn_n + \ldots . \end{aligned} \qquad (1.5.9.31)$$

As an example, for the ferromagnets with a cubic prototype this equation may be written as

$$U_a = (K^0_1 + K'_1)S(n^2_1n^2_2) + (K^0_2 + K'_2)n^2_1n^2_2n^2_3. \qquad (1.5.9.32)$$

The coefficients K'_1 and K'_2 may be expressed in terms of the saturation magnetostriction constants $h_0, \ldots, h_5$ [see (1.5.9.12)] and the elastic stiffnesses $c_{\alpha\beta}$:

$$\begin{aligned} K'_1 &= c_{11}[h_0(2h_4 - 3h_3) + h_1(h_1 - h_3 + 3h_4) - h_4(h_3 - 2h_4)] \\ &\quad + c_{12}[2h_0(2h_4 - 3h_3) - (h_1 + h_4)(h_1 + 2h_3)] - \tfrac{1}{2}c_{44}h^2_2, \end{aligned} \qquad (1.5.9.33)$$

$$\begin{aligned} K'_2 &= -c_{11}[3h_4(h_1 + h_3) + (h_4 - h_3)(4h_4 - 3h_3)] \\ &\quad + c_{12}[3h_4(h_1 + h_3) + h_3(5h_4 - 6h_3)] \\ &\quad - \tfrac{1}{2}c_{44}(6h_2 + h_5)h_5. \end{aligned} \qquad (1.5.9.34)$$

For cubic crystals, K^0_i and K'_i are of the same magnitude. As an example, for Ni one has $K^0_1 = 80\,000$ erg cm^{-3} = 8000 J m^{-3} and $K'_1 = -139\,000$ erg cm^{-3} = $-13\,900$ J m^{-3}.

1.5.10. Transformation from Gaussian to SI units

Numerical values of magnetic quantities are given in Gaussian units in this chapter. For each quantity that appears in a table or figure, Table 1.5.10.1 gives the corresponding Gaussian unit and its value expressed in SI units. More details on the transformation between Gaussian and SI units are given *e.g.* in the Appendix of Jackson (1999).

1.5.11. Glossary

α_{ij}	(linear) magnetoelectric tensor
β_{ijk}	nonlinear magnetoelectric tensor *EHH*
γ_{ijk}	nonlinear magnetoelectric tensor *HEE*
Δ	Weiss constant
Δn	magnetic birefringence
ε_{ij}	dielectric permittivity
λ	constant describing magnetostriction
Λ_{ijk}	tensor describing the piezomagnetic effect
$\Lambda_{i\alpha}$	matrix describing the piezomagnetic effect
μ_{ij}	magnetic permeability
$\boldsymbol{\mu}$	magnetic moment
μ_B	Bohr magneton
$\pi_{ijk\ell}$	piezomagnetoelectric tensor
$\rho(\mathbf{r})$	charge density
Φ	thermodynamic potential
χ^e_{ij}	dielectric susceptibility
χ_{ij}, χ^m_{ij}	magnetic susceptibility
B	magnetic induction
c	speed of light
$c_{ijk\ell}$	elastic stiffness
$\mathrm{d}\tau$	volume element
e	charge of the electron
E	electric field
g	Landé g-factor
H	magnetic field
j(**r**)	current density
J	total angular momentum
k	position vector in reciprocal space
k_B	Boltzmann factor
$\mathbf{l}_i$	sum of the magnetic moments in a unit cell, in which some of the moments are taken with opposite sign
$\mathbf{L}_i$	antiferromagnetic vector
L	orbital angular momentum (Section 1.5.1.1), antiferromagnetic vector (remainder of this chapter)
m(**r**)	magnetic moment density
m	sum of the magnetic moments in a unit cell
M	magnetization (= magnetic moment per unit volume = ferromagnetic vector)
N	No. of atoms per unit volume
p	effective number of Bohr magnetons (Section 1.5.1), pressure (remainder of this chapter)
P	electric polarization
r	position vector in space
S(**r**)	spin density
S	spin angular momentum (of an atom or ion)
$s_{ijk\ell}$	elastic compliance
S_{ij}	strain tensor
T_{ij}	stress tensor
T	temperature
T_c	transition temperature, in particular Curie temperature
T_N	Néel temperature
U	energy
U_a	anisotropy energy
$U_{\rm el}$	elastic energy
$U_{\rm me}$	magnetoelastic energy
v	velocity
Z	atomic number (= number of electrons per atom)

The authors express their gratitude to Dr Elena Zhdanova for her great support in the preparation of the figures, and to Professor Stephen Lovesey, Dr Jean-Pierre Rivera and Professor

Hans Schmid for suggesting numerous improvements to the manuscript.

References

Aizu, K. (1970). *Possible species of ferromagnetic, ferroelectric and ferroelastic crystals. Phys. Rev. B*, **2**, 754–772.

Akulov, N. (1928). *Über die Magnetostriktion der Eisenkristalle. Z. Phys.* **52**, 389–405.

Alcantara Bonfim, O. F. de & Gehring, G. A. (1980). *Magnetoelectric effect in antiferromagnetic crystals. Adv. Phys.* **29**, 731–769.

Anderson, J. C., Birss, R. R. & Scott, R. A. M. (1964). *Linear magnetostriction in hematite.* In *Proc. Int. Conf. Magnetism*, Nottingham, pp. 597–599. London: Institute of Physics and the Physical Society.

Andratskii, V. P. & Borovik-Romanov, A. S. (1966). *Piezomagnetic effect in α-Fe_2O_3.* (In Russian.) *Zh. Eksp. Teor. Fiz.* **51**, 1030–1036. [English translation: *Sov. Phys. JETP*, **24** (1967), 687–691.]

Andreev, A. F. & Marchenko, V. I. (1976). *Macroscopic theory of spin waves.* (In Russian.) *Zh. Eksp. Teor. Fiz.* **70**, 1522–1538. (English translation: *Sov. Phys. JETP*, **43**, 794–803.)

Andreev, A. F. & Marchenko, V. I. (1980). *Symmetry and the macroscopic dynamics of magnetic materials.* (In Russian.) *Usp. Fiz. Nauk*, **130**, 39–63. (English translation: *Sov. Phys. Usp.* **23**, 21–34.)

Ascher, E. (1966). *Some properties of spontaneous currents. Helv. Phys. Acta*, **39**, 40–48.

Ascher, E. (1968). *Higher-order magneto-electric effects. Philos. Mag.* **17**, 149–157.

Ascher, E. (1970). *The interactions between magnetization and polarization: phenomenological symmetry considerations on boracites. J. Phys. Soc. Jpn*, **28** Suppl., 7–14.

Ascher, E., Rieder, H., Schmid, H. & Stössel, H. (1966). *Some properties of ferromagnetoelectric nickel–iodine boracite, $Ni_3B_7O_{13}I$. J. Appl. Phys.* **37**, 1404–1405.

Astrov, D. N. (1960). *The magnetoelectric effect in antiferromagnetics.* (In Russian.) *Zh. Eksp. Teor. Fiz.* **38**, 984–985. (English translation: *Sov. Phys. JETP*, **11**, 708–709.)

Astrov, D. N. (1961). *Magnetoelectric effect in chromium oxide.* (In Russian.) *Zh. Eksp. Teor. Fiz.* **40**, 1035–1041. (English translation: *Sov. Phys. JETP*, **13**, 729–733.)

Astrov, D. N., Al'shin, B. I., Zorin, R. V. & Drobyshev, L. A. (1968). *Spontaneous magnetoelectric effect.* (In Russian.) *Zh. Eksp. Teor. Fiz.* **55**, 2122–2127. [English translation: *Sov. Phys. JETP*, **28** (1969), 1123–1125.]

Barbara, B., Gignoux, D. & Vettier, C. (1988). *Lectures on modern magnetism.* Beijing: Science Press.

Bazhan, A. N. & Bazan, Ch. (1975). *Weak ferromagnetism in CoF_2 and NiF_2.* (In Russian.) *Zh. Eksp. Teor. Fiz.* **69**, 1768–1781. (English translation: *Sov. Phys. JETP*, **42**, 898–904.)

Becker, R. & Döring, W. (1939). *Ferromagnetismus.* Berlin: Springer.

Belov, N. V., Belova, E. N. & Tarkhova, T. N. (1964). *Polychromatic plane groups*. In Shubnikov & Belov (1964). *Colored symmetry*, edited by W. T. Holser, pp. 228–237. Oxford: Pergamon.

Belov, N. V., Neronova, N. N. & Smirnova, T. S. (1957). *Shubnikov groups.* (In Russian.) *Kristallografiya*, **2**, 315–325. (English translation: *Sov. Phys. Crystallogr.* **2**, 311–322.)

Bertaut, E. F. (1963). *Spin configurations of ionic structures: theory and practice.* In *Magnetism*, Vol. III, edited by G. T. Rado & H. Suhl, pp. 149–209. New York: Academic Press.

Bertaut, E. F., Mercier, M. & Pauthenet, R. (1964). *Ordre magnétique et propriétés magnétiques de $MnYO_3$. J. Phys.* **25**, 550–557.

Bichurin, M. (1997). Editor. *Proceedings of the 3rd international conference on magnetoelectric interaction phenomena in crystals (MEIPIC-3). Ferroelectrics*, **204**.

Bichurin, M. (2002). Editor. *Proceedings of the 4th international conference on magnetoelectric interaction phenomena in crystals (MEIPIC-4). Ferroelectrics*, **279–280**.

Bickford, L. R. Jr, Pappis, J. & Stull, J. L. (1955). *Magnetostriction and permeability of magnetite and cobalt-substituted magnetite. Phys. Rev.* **99**, 1210–1214.

Birss, R. R. (1964). *Symmetry and magnetism.* Amsterdam: North-Holland.

Birss, R. R. & Anderson, J. C. (1963). *Linear magnetostriction in antiferromagnetics. Proc. Phys. Soc.* **81**, 1139–1140.

Bloembergen, N. (1962). In *Proc. Int. Conf. High Magnetic Fields*, edited by B. Lax, p. 454. New York: John Wiley.

Borovik-Romanov, A. S. (1959*a*). *Investigation of weak ferromagnetism in the $MnCO_3$ single crystal.* (In Russian.) *Zh. Eksp. Teor. Fiz.* **36**, 766–781. (English translation: *Sov. Phys. JETP*, **9**, 539–549.)

Borovik-Romanov, A. S. (1959*b*). *Piezomagnetism in the antiferromagnetic fluorides of cobalt and manganese.* (In Russian.) *Zh. Eksp. Teor. Fiz.* **36**, 1954–1955. (English translation: *Sov. Phys. JETP*, **9**, 1390–1391.)

Borovik-Romanov, A. S. (1960). *Piezomagnetism in the antiferromagnetic fluorides of cobalt and manganese.* (In Russian.) *Zh. Eksp. Teor. Fiz.* **38**, 1088–1098. (English translation: *Sov. Phys. JETP*, **11**, 786–793.)

Borovik-Romanov, A. S. & Orlova, M. P. (1956). *Magnetic properties of cobalt and manganese carbonates.* (In Russian.) *Zh. Eksp. Teor. Fiz.* **31**, 579–582. [English translation: *Sov. Phys. JETP*, **4** (1957), 531–534.]

Borovik-Romanov, A. S. & Ozhogin, V. I. (1960). *Weak ferromagnetism in an antiferromagnetic $CoCO_3$ single crystal.* (In Russian.) *Zh. Eksp. Teor. Fiz.* **39**, 27–36. (English translation: *Sov. Phys. JETP*, **12**, 18–24.)

Borovik-Romanov, A. S. & Yavelov, B. E. (1963). *Linear magnetostriction in antiferromagnetic CoF_2.* In *Proc. 3rd Regional Conf. Prague*, 81–83.

Burzo, E. (1993). *Magnetic properties of non-metallic inorganic compounds based on transition elements. Boron containing oxides.* Landolt-Börnstein **III** 27 h, Berlin: Springer.

Cardwell, M. J. (1969). *Measurements of the magnetic field dependent electric susceptibility of yttrium iron garnet. Phil. Mag.* **20**, 1087–1089.

Chappert, J. (1965). *Etude par effet Mössbauer de la substitution partielle par le fer du manganèse dans les manganites de terres rares. Phys. Lett.* **18**, 229–230.

Clark, A. E., DeSavage, B. F., Tsuya, N. & Kawakami, S. (1966). *Magnetostriction of dysprosium, holmium, and erbium iron garnets. J. Appl. Phys.* **37**, 1324–1326.

Cox, D. E. (1974). *Spin ordering in magnetoelectrics. Int. J. Magn.* **6**, 67–75. [Reprinted in Freeman & Schmid (1975), pp. 111–119.]

Cracknell, A. P. (1975). *Magnetism in crystalline materials.* Oxford: Pergamon.

Curie, P. (1894). *Sur la symétrie dans les phénomènes physiques, symétrie d'un champ électrique et d'un champ magnétique. J. Phys.*, 3rd series **III**, 393–415.

Dzyaloshinskii, I. E. (1957*a*). *Thermodynamic theory of 'weak' ferromagnetism in antiferromagnetic substances.* (In Russian.) *Zh. Eksp. Teor. Fiz.* **32**, 1547–1562. (English translation: *Sov. Phys. JETP*, **5**, 1259–1272.)

Dzyaloshinskii, I. E. (1957*b*). *The problem of piezomagnetism.* (In Russian.) *Zh. Eksp. Teor. Fiz.* **33**, 807–808. [English translation: *Sov. Phys. JETP*, **6** (1958), 621–622.]

Dzyaloshinskii, I. E. (1957*c*). *The magnetic structure of fluorides of the transition metals.* (In Russian.) *Zh. Eksp. Teor. Fiz.* **33**, 1454–1456. [English translation: *Sov. Phys. JETP*, **6** (1958), 1120–1122.]

Dzyaloshinskii, I. E. (1959). *On the magneto-electrical effect in antiferromagnets.* (In Russian.) *Zh. Eksp. Teor. Fiz.* **37**, 881–882. [English translation: *Sov. Phys. JETP*, **10** (1960), 628–629.]

Dzyaloshinskii, I. E. (1964). *Theory of helicoidal structures in antiferromagnets.* (In Russian.) *Zh. Eksp. Teor. Fiz.* **46**, 1420–1437, **47**, 336–348 and 992–1002. [English translation: *Sov. Phys. JETP*, **19**, 960–971, **20** (1965), 223–231 and 665–671.]

Dzyaloshinskii, I. E. & Man'ko, V. I. (1964). *Nonlinear effects in antiferromagnets. 'Latent' antiferromagnetism.* (In Russian.) *Zh. Eksp. Teor. Fiz.* **46**, 1352–1359. (English translation: *Sov. Phys. JETP*, **19**, 915–919.)

Eremenko, V. V., Kharchenko, N. F., Litvinenko, Yu. G. & Naumenko, V. M. (1989). *Magneto-optics and spectroscopy of antiferromagnets.* (In Russian.) Kiev: Naukova Dumka. [English translation (1992): New York: Springer.]

Faber, J., Lander, G. H. & Cooper, B. R. (1975). *Neutron-diffraction study of UO_2: observation of an internal distortion. Phys. Rev. Lett.* **35**, 1770–1773.

Ferré, J. & Gehring, G. A. (1984). *Linear optical birefringence of magnetic crystals. Rep. Prog. Phys.* **47**, 513–611.

Folen, V. J., Rado, G. T. & Stalder, E. W. (1961). *Anisotropy of the magnetoelectric effect in Cr_2O_3. Phys. Rev. Lett.* **6**, 607–608.

Foner, S. (1963). *Antiferromagnetic and ferrimagnetic resonance.* In *Magnetism*, Vol. I, edited by G. T. Rado & H. Suhl, pp. 383–447. New York: Academic Press.

Freeman, A. J. & Schmid, H. (1975). *Magnetoelectric interaction phenomena in crystals.* London: Gordon and Breach.

Gijsman, H. M., Poulis, N. J. & Van den Handel, J. (1959). *Magnetic susceptibilities and phase transitions of two antiferromagnetic manganese salts. Physica*, **25**, 954–968.

Gorbatsevich, A. A. & Kopaev, Yu. V. (1994). *Toroidal order in crystals. Ferroelectrics*, **161**, 321–334.

Grimmer, H. (1991). *General connections for the form of the property tensors in the 122 Shubnikov point groups. Acta Cryst.* A**47**, 226–232.

Grimmer, H. (1992). *The piezomagnetoelectric effect. Acta Cryst.* A**48**, 266–271.

Heesch, H. (1930). *Über die vierdimensionalen Gruppen des dreidimensionalen Raumes. Z. Kristallogr.* **73**, 325–345.

Hou, S. L. & Bloembergen, N. (1965). *Paramagnetoelectric effects in $NiSO_4{\cdot}6H_2O$. Phys. Rev. A*, **138**, 1218–1226.

Iida, S. (1967). *Magnetostriction constants of rare earth iron garnets. J. Phys. Soc. Jpn*, **22**, 1201–1209.

Indenbom, V. L. (1959). *Relation of the antisymmetry and color symmetry groups to one-dimensional representations of the ordinary symmetry groups. Isomorphism of the Shubnikov and space groups.* (In Russian.) *Kristallografiya*, **4**, 619–621. [English translation: *Sov. Phys. Cryst.* **4** (1960), 578–580.]

International Tables for Crystallography (2002). Vol. A. *Space-group symmetry*, edited by Th. Hahn. Dordrecht: Kluwer Academic Publishers.

Izyumov, Yu. A. & Naish, V. E. (1979). *Symmetry analysis in neutron diffraction studies of magnetic structures. J. Magn. Magn. Mater.* **12**, 239–248.

Izyumov, Yu. A., Naish, V. E. & Petrov, S. B. (1979). *Symmetry analysis in neutron diffraction studies of magnetic structures. J. Magn. Magn. Mater.* **13**, 267–274, 275–282.

Izyumov, Yu. A., Naish, V. E. & Syromiatnikov, V. N. (1979). *Symmetry analysis in neutron diffraction studies of magnetic structures. J. Magn. Magn. Mater.* **12**, 249–261.

Jackson, J. D. (1999). *Classical electrodynamics*, 3rd ed. New York: Wiley.

Joshua, S. J. (1991). *Symmetry principles and magnetic symmetry in solid state physics.* Graduate Student Series in Physics. Bristol: Hilger.

Kadomtseva, A. M., Agafonov, A. P., Lukina, M. M., Milov, V. N., Moskvin, A. S. & Semenov, V. A. (1981). *Characteristic magnetoelastic properties of yttrium orthochromite.* (In Russian.) *Fiz. Tverd. Tela*, **23**, 3554–3557. (English translation: *Sov. Phys. Solid State*, **23**, 2065–2067.)

Kadomtseva, A. M., Agafonov, A. P., Milov, V. N., Moskvin, A. S. & Semenov, V. A. (1981). *Direct observation of symmetry change induced in orthoferrite crystals by an external magnetic field.* (In Russian.) *Pis'ma Zh. Eksp. Teor. Fiz.* **33**, 400–403. (English translation: *JETP Lett.* **33**, 383–386.)

Kharchenko, N. F., Eremenko, V. V. & Belyi, L. I. (1979). *Visual observation of 180-degree antiferromagnetic domains.* (In Russian.) *Pis'ma Zh. Eksp. Teor. Fiz.* **29**, 432–435. (English translation: *JETP Lett.* **29**, 392–395.)

Kharchenko, N. F. & Gnatchenko, S. L. (1981). *Linear magnetooptic effect and visual observation of antiferromagnetic domains in an orthorhombic crystal of $DyFeO_3$.* (In Russian.) *Fiz. Nizk. Temp.* **7**, 475–493. (English translation: *Sov. J. Low Temp. Phys.* **7**, 234–243.)

Kiselev, S. V., Ozerov, R. P. & Zhdanov, G. S. (1962). *Detection of magnetic order in ferroelectric $BiFeO_3$ by neutron diffraction.* (In Russian.) *Dokl. Akad. Nauk SSSR*, **145**, 1255–1258. [English translation: *Sov. Phys. Dokl.* **7** (1963), 742–744.]

Kopský, V. (1979*a*). *Tensorial covariants for the 32 crystal point groups. Acta Cryst.* A**35**, 83–95.

Kopský, V. (1979*b*). *A simplified calculation and tabulation of tensorial covariants for magnetic point groups belonging to the same Laue class. Acta Cryst.* A**35**, 95–101.

Koptsik, V. A. (1966). *Shubnikov groups.* (In Russian.) Moscow: Izd. MGU.

Koptsik, J. N. & Kuzhukeev, Zh.-N. M. (1972). *Derivation of the three-, four- and six-color Belov space groups from tables of irreducible representations.* (In Russian.) *Kristallografiya*, **17**, 705–711. [English translation: *Sov. Phys. Crystallogr.* **17** (1973), 622–627.]

Kouvel, J. S. & Fisher, M. E. (1964). *Detailed magnetic behavior of nickel near its Curie point. Phys. Rev. A*, **136**, 1626–1632.

Kovalev, O. V. (1987). *Representations of the crystallographic space groups*, 2nd ed. (In Russian.) Moscow: Nauka. [English translation (1993): New York: Gordon and Breach.]

Landau, L. D. (1933). *Eine mögliche Erklärung der Feldabhängigkeit der Suszeptibilität bei niedrigen Temperaturen. Phys. Z. Sowjet.* **4**, 675–679.

Landau, L. D. (1937). *Zur Theorie der Phasenumwandlungen. I. Phys. Z. Sowjet.* **11**, 26–47.

Landau, L. D. & Lifshitz, E. M. (1951). *Statistical physics.* (In Russian.) Moscow: Gostekhizdat. [English translation (1958): London: Pergamon.]

Landau, L. D. & Lifshitz, E. M. (1957). *Electrodynamics of continuous media.* (In Russian.) Moscow: Gostekhizdat. [English translation (1960): London: Pergamon.]

Le Gall, H., Leycuras, C., Minella, D., Rudashevskii, E. G. & Merkulov, V. S. (1977). *Anomalous evolution of the magnetic and magnetooptical properties of hematite at temperature near and lower than the Morin phase transition. Physica B*, **86–88**, 1223–1225.

Lee, E. W. (1955). *Magnetostriction and magnetomechanical effects. Rep. Prog. Phys.* **18**, 184–229.

Lee, G., Mercier, M. & Bauer, P. (1970). *Mesures magnétoélectriques sur les grenats de Y, de Gd et de Dy aux basses températures*. In *Les éléments des terres rares*, Vol. II, pp. 389–399. Paris: Editions du CNRS.

Levitin, R. Z. & Shchurov, V. A. (1973). In *Physics and chemistry of ferrites*, pp. 162–194. (In Russian.) Moscow: Izd. Mosk. Gos. Univ.

Lifshitz, E. M. (1942). *On the theory of phase transitions of the second order. J. Phys. (Moscow)*, **6**, 61–74.

Lyubimov, V. N. (1965). *The interaction of polarization and magnetization in crystals.* (In Russian.) *Kristallografiya*, **10**, 520–524. [English translation: *Sov. Phys. Crystallogr.* **10** (1966), 433–436.]

Mason, W. P. (1951). *A phenomenological derivation of the first- and second-order magnetostriction and morphic effects for a nickel crystal. Phys. Rev.* **82**, 715–723; erratum (1952), **85**, 1065.

Mason, W. P. (1954). *Derivation of magnetostriction and anisotropic energies for hexagonal, tetragonal, and orthorhombic crystals. Phys. Rev.* **96**, 302–310.

Matarrese, L. M. & Stout, J. W. (1954). *Magnetic anisotropy of NiF_2. Phys. Rev.* **94**, 1792–1793.

Mercier, R. (1974). *Magnetoelectric behaviour in garnets. Int. J. Magn.* **6**, 77–88. [Reprinted in Freeman & Schmid (1975), pp. 99–110.]

Merkulov, V. S., Rudashevskii, E. G., Le Gall, H. & Leycuras, C. (1981). *Linear magnetic birefringence of hematite in the vicinity of the Morin temperature.* (In Russian.) *Zh. Eksp. Teor. Fiz.* **80**, 161–170. (English translation: *Sov. Phys. JETP*, **53**, 81–85.)

Michel, Ch., Moreau, J.-M., Achenbach, G. D., Gerson, R. & James, W. J. (1969). *The atomic structure of $BiFeO_3$. Solid State Commun.* **7**, 701–704.

Morin, F. J. (1950). *Magnetic susceptibility of α-Fe_2O_3 and α-Fe_2O_3 with added titanium. Phys. Rev.* **78**, 819–820.

Moriya, T. (1960*a*). *Theory of magnetism of NiF_2. Phys. Rev.* **117**, 635–647.

Moriya, T. (1960*b*). *Anisotropic superexchange interaction and weak ferromagnetism. Phys. Rev.* **120**, 91–98.

Moriya, T. (1963). *Weak ferromagnetism.* In *Magnetism*, Vol. I, edited by G. T. Rado & H. Suhl, pp. 85–125. New York: Academic Press.

Néel, L. & Pauthenet, R. (1952). *Étude thermomagnétique d'un monocristal de $Fe_2O_3\alpha$. C. R. Acad. Sci.* **234**, 2172–2174.

Neronova, N. N. & Belov, N. V. (1959). *Ferromagnetic and ferroelectric space groups.* (In Russian.) *Kristallografiya*, **4**, 807–812. (English translation: *Sov. Phys. Crystallogr.* **4**, 769–774.)

O'Dell, T. H. (1967). *An induced magneto-electric effect in yttrium iron garnet. Philos. Mag.* **16**, 487–494.

O'Dell, T. H. (1970). *The electrodynamics of magneto-electric media.* Amsterdam: North-Holland.

Opechowski, W. & Guccione, R. (1965). *Magnetic symmetry.* In *Magnetism*, Vol. IIA, edited by G. T. Rado & H. Suhl, pp. 105–165. New York: Academic Press.

Popov, Yu. F., Kazei, Z. A. & Kadomtseva, A. M. (1992). *Linear magnetoelectric effect in Cr_2O_3 in strong magnetic fields.* (In Russian.) *Pis'ma Zh. Eksp. Teor. Fiz.* **55**, 238–241. (English translation: *JETP Lett.* **55**, 234–238.)

Prokhorov, A. S. & Rudashevskii, E. G. (1969). *Magnetostriction of antiferromagnetic cobalt fluoride.* (In Russian.) *Pis'ma Zh. Eksp. Teor. Fiz.* **10**, 175–179. (English translation: *JETP Lett.* **10**, 110–113.)

Prokhorov, A. S. & Rudashevskii, E. G. (1975). *Magnetoelastic interactions and the single-domain antiferromagnetic state in cobalt fluoride.* (In Russian.) *Kratk. Soobshch. Fiz.* **11**, 3–6. (English translation: *Sov. Phys. Lebedev Inst. Rep.* **11**, 1–4.)

Rado, G. T. (1961). *Mechanism of the magnetoelectric effect in an antiferromagnet. Phys. Rev. Lett.* **6**, 609–610.

Rado, G. T. (1962). *Statistical theory of magnetoelectric effects in antiferromagnets. Phys. Rev.* **128**, 2546–2556.

Rado, G. T. (1964). *Observation and possible mechanisms of magnetoelectric effects in a ferromagnet. Phys. Rev. Lett.* **13**, 335–337.

Rado, G. T. (1969). *Magnetoelectric evidence for the attainability of time-reversed antiferromagnetic configurations by metamagnetic transitions in $DyPO_4$. Phys. Rev. Lett.* **23**, 644–647, 946.

Rado, G. T. & Ferrari, J. M. (1973). *Magnetoelectric effects in $TbPO_4$. AIP Conf. Proc.* **10**, 1417.

Rado, G. T., Ferrari, J. M. & Maisch, W. G. (1984). *Magnetoelectric susceptibility and magnetic symmetry of magnetoelectrically annealed $TbPO_4$. Phys. Rev. B*, **29**, 4041–4048.

Rado, G. T. & Folen, V. J. (1961). *Observation of the magnetically induced magnetoelectric effect and evidence for antiferromagnetic domains. Phys. Rev. Lett.* **7**, 310–311.

Rado, G. T. & Folen, V. J. (1962). *Magnetoelectric effects in antiferromagnetics. J. Appl. Phys.* **33** Suppl., 1126–1132.

Rivera, J.-P. (1994). *On definitions, units, measurements, tensor forms of the linear magnetoelectric effect and on a new dynamic method applied to Cr–Cl boracite. Ferroelectrics*, **161**, 165–180.

Rivera, J.-P. & Schmid, H. (1994). *Search for the piezomagnetoelectric effect in $LiCoPO_4$. Ferroelectrics*, **161**, 91–97.

Schlenker, M. & Baruchel, J. (1978). *Neutron techniques for the observation of ferro- and antiferromagnetic domains. J. Appl. Phys.* **49**, 1996–2001.

Schmid, H. (1965). *Die Synthese von Boraziten mit Hilfe chemischer Transportreaktionen. J. Phys. Chem. Solids*, **26**, 973–988.

Schmid, H. (1967). *Twinning and sector growth in nickel boracites grown by transport reactions.* (In Russian.) *Rost Krist.* **7**, 32–65. (English translation: *Growth Cryst. USSR*, **7**, 25–52.)

Schmid, H. (1973). *On a magnetoelectric classification of materials. Int. J. Magn.* **4**, 337–361. [Reprinted in Freeman & Schmid (1975) pp. 121–146.]

Schmid, H. (1994*a*). *Introduction to the proceedings of the 2nd international conference on magnetoelectric interaction phenomena in crystals, MEIPIC-2. Ferroelectrics*, **161**, 1–28.

Schmid, H. (1994*b*). *Multi-ferroic magnetoelectrics. Ferroelectrics*, **162**, 317–338.

Schmid, H., Janner, A., Grimmer, H., Rivera, J.-P. & Ye, Z.-G. (1994). Editors. *Proceedings of the 2nd international conference on magnetoelectric interaction phenomena in crystals (MEIPIC-2). Ferroelectrics*, **161–162**.

Schwarzenberger, R. L. E. (1984). *Colour symmetry. Bull. London Math. Soc.* **16**, 209–240.

Scott, R. A. M. & Anderson, J. C. (1966). *Indirect observation of antiferromagnetic domains by linear magnetostriction. J. Appl. Phys.* **37**, 234–237.

Shubnikov, A. V. (1951). *Symmetry and antisymmetry of finite figures.* (In Russian.) Moscow: Acad. Sci. USSR. [English translation in Shubnikov & Belov (1964) pp. 3–172 and 249–252.]

Shubnikov, A. V. & Belov, N. V. (1964). *Colored symmetry*, edited by W. T. Holser. Oxford: Pergamon.

Shubnikov, A. V. & Koptsik, V. A. (1972). *Symmetry in science and art.* (In Russian.) Moscow: Nauka. [English translation (1974): New York: Plenum.]

Shuvalov, L. A. & Belov, N. V. (1962). *The symmetry of crystals in which ferromagnetic and ferroelectric properties appear simultaneously.* (In Russian.) *Kristallografiya*, **7**, 192–194. (English translation: *Sov. Phys. Crystallogr.* **7**, 150–151.)

Sirotin, Y. I. & Shaskol'skaya, M. P. (1979). *Fundamentals of crystal physics.* (In Russian.) Moscow: Nauka. [English translation (1982): Moscow: Mir.]

Smolenskii, G. A., Agranovskaia, A. I., Popov, S. N. & Isupov, V. A. (1958). *New ferroelectrics of complex composition.* (In Russian.) *Zh. Tekh. Fiz.* **28**, 2152–2153. (English translation: *Sov. Phys. Tech. Phys.* **3**, 1981–1982.)

Smolenskii, G. A., Yudin, V. M., Sher, E. S. & Stolypin, Yu. E. (1962). *Antiferromagnetic properties of some perovskites.* (In Russian.) *Zh. Eksp. Teor. Fiz.* **43**, 877–880. [English translation: *Sov. Phys. JETP*, **16** (1963), 622–624.]

Sosnovska, I., Peterlin-Neumaier, T. & Steichele, E. (1982). *Spiral magnetic ordering in bismuth ferrite. J. Phys. C*, **15**, 4835–4846.

Tavger, B. A. (1958). *The symmetry of ferromagnetics and antiferromagnetics.* (In Russian.) *Kristallografiya*, **3**, 339–341. (English translation: *Sov. Phys. Crystallogr.* **3**, 341–343.)

Tavger, B. A. & Zaitsev, V. M. (1956). *Magnetic symmetry of crystals*. (In Russian.) *Zh. Eksp. Teor. Fiz.* **30**, 564–568. (English translation: *Sov. Phys. JETP*, **3**, 430–436.)

Townsend Smith, T. (1916). *The magnetic properties of hematite. Phys. Rev.* **8**, 721–737.

Turov, E. A. (1963). *Physical properties of magnetically ordered crystals.* (In Russian.) Moscow: Akad. Nauk SSSR. [English translation (1965): New York: Academic Press.]

Venevtsev, Yu. N., Gagulin, V. V. & Zhitomirsky, I. D. (1987). *Material science aspects of seignette-magnetism problem. Ferroelectrics*, **73**, 221–248.

Voigt, W. (1928). *Lehrbuch der Kristallphysik.* Leipzig: Teubner.

Waerden, B. L. van der & Burckhardt, J. J. (1961). *Farbgruppen. Z. Kristallogr.* **115**, 231–234.

White, R. L. (1974). *Microscopic origins of piezomagnetism and magnetoelectricity. Int. J. Magn.* **6**, 243–245. [Reprinted in Freeman & Schmid (1975), pp. 41–43.]

Wijn, H. P. J. (1994). *Magnetic properties of non-metallic inorganic compounds based on transition elements. Perovskites. II. Oxides with corundum, ilmenite and amorphous structures.* Landolt-Börnstein **III**, 27, f3, Berlin: Springer.

Zalessky, A. V. (1981). *Magnetic properties of crystals.* In *Modern crystallography*, Vol. IV, edited by L. A. Shuvalov. (In Russian.) Moscow: Nauka. [English translation (1988): Berlin: Springer.]

Zamorzaev, A. M. (1957). *Generalization of Fedorov groups.* (In Russian.) *Kristallografiya*, **2**, 15–20. (English translation: *Sov. Phys. Crystallogr.* **2**, 10–15.)

Zvezdin, A. K., Zorin, I. A., Kadomtseva, A. M., Krynetskii, I. B., Moskvin, A. S. & Mukhin, A. A. (1985). *Linear magnetostriction and antiferromagnetic domain structure in dysprosium orthoferrite.* (In Russian.) *Zh. Eksp. Teor. Fiz.* **88**, 1098–1102. (English translation: *Sov. Phys. JETP*, **61**, 645–647.)